A mathematical and algorithmic study of the Lambertian SFS problem for orthographic and pinhole cameras

Emmanuel Prados, Olivier Faugeras

INRIA

INSTITUT NATIONAL DE RECHERCHE EN INFORMATIQUE ET EN AUTOMATIQUE

A mathematical and algorithmic study of the Lambertian SFS problem for orthographic and pinhole cameras

Emmanuel Prados — Olivier Faugeras

N° 5005

November 2003

THÈME 3

ISSN 0249-6399 ISRN INRIA/RR--5005--FR+ENG

INRIA
SOPHIA ANTIPOLIS

A mathematical and algorithmic study of the Lambertian SFS problem for orthographic and pinhole cameras

Emmanuel Prados * , Olivier Faugeras †

Thème 3 — Interaction homme-machine,
images, données, connaissances
Projet Odyssee

Rapport de recherche n° 5005 — November 2003 — 129 pages

Abstract: This report proposes a *mathematical and algorithmic study* of the Lambertian SFS problem for *orthographic and pinhole cameras*. Our approach is based upon the notion of *viscosity solutions* of Hamilton-Jacobi equations. This approach provides a mathematical framework in which we can prove the well-posedness of the problem (proof of the existence of a solution and characterization of all solutions). This mathematical approach allows also to prove the correctness of our methods. In particular, we describe a simple monotonous *stability* condition for the studied decentered schemes and we prove the *convergence* of their solutions toward the viscosity solution of the associated Hamilton-Jacobi-Bellman equation. Also, we show that this theory naturally applies to the SFS problems.

Our work extends previous work in the SFS area in three directions. First, it models the camera both as orthographic and as perspective (*pinhole*), i.e whereas most authors assume an orthographic projection (see [20] for a panorama of the SFS problem up to 1989 and [43, 28] for more recent surveys); thus we extend the applicability of shape from shading methods to more realistic acquisition models. In particular it extends the work of [37, 38] and [39]. Also, by introducing a *"generic" Hamiltonian*, we work in a general framework allowing to deal with both models, thereby simplifying the formalization of the problem. Second, it gives some novel mathematical formulations of this problem yielding *new partial differential equations*. Results about the *existence and uniqueness* of their solution are also obtained. Third, it allows us to come up with two *new generic algorithms* for computing numerical approximations of the "continuous" solution (of the "generic SFS problem") as well as a proof of their convergence toward that solution. Moreover, our two generic algorithms are able to deal with *discontinuous images* as well as images containing *black shadows*. Also,

* http://www-sop.inria.fr/odyssee/team/Emmanuel.Prados/
† http://www-sop.inria.fr/odyssee/team/Olivier.Faugeras/

Unité de recherche INRIA Sophia Antipolis
2004, route des Lucioles, BP 93, 06902 Sophia Antipolis Cedex (France)
Téléphone : +33 4 92 38 77 77 — Télécopie : +33 4 92 38 77 65

one of the algorithms we propose in this report, seems to be *the most effective iterative algorithm* of the SFS literature.

From a more general viewpoint, our numerical results follow from a new method for solving *Hamilton-Jacobi-Bellman* equations. We propose two *decentered finite difference schemes*. We detail the proofs of the stability and the consistency of these schemes, and the proof of the convergence of their associated algorithms.

Key-words: Shape from Shading, Lambertian reflectance, pinhole camera, orthographic and perspective projection, unification of various modelizations, black shadows, discontiuous images, noise robustness, fast SFS algorithm, viscosity solutions, existence and uniqueness of a solution, characterization of the solutions, Hamilton-Jacobi-Bellman equations, monotonous approximation schemes, decentered schemes for HJB equations, finite difference schemes, stability and convergence of schemes, iterative numerical algorithms.

Une étude mathématique et algorithmique du problème de "Shape-From-Shading" avec des projections orthographiques et des projections en perpective

Résumé : Ce rapport de recherche propose une étude mathématique et algorithmique du problème de "Shape-From-Shading" Lambertien avec des projections orthographiques et des projections en perpective. Notre approche est basée sur la notion de *solutions de viscosité* des équations de Hamilton-Jacobi. Cette approche fournit un cadre mathématique permettant de bien poser le problème (preuve d'existence de solutions et caractérisation des solutions). Ce cadre permet aussi de prouver la pertinence de nos algorithmes. En particulier, nous décrivons une condition de stabilité adaptée à nos schémas décentrés (cette condition est simple et est basée sur la "monotonie" du schéma) et nous prouvons la convergence de ses solutions vers la solution de viscosité de l'équation de Hamilton-Jacobi-Bellman associée. De plus, nous montrons que cette théorie s'applique aisément aux problèmes de SFS.

Dans le domaine du SFS, nos travaux étendent les précédents travaux, sous trois aspects: premièrement, nous modélisons le processus d'acquisition de l'image par une projection orthographique mais aussi par une *projection en perspective.* La plupart des autres auteurs considèrent une projection orthographique (pour un panorama complet jusqu'en 1989, voir [20]; pour un état de l'art plus récent, voir [43, 28]). Le SFS devient ainsi applicable à des scènes plus réalistes. De plus, en introduisant un *Hamiltonien "générique"*, nous nous travaillons dans un cadre général permettant de traiter en même temps les deux modélisations. Nous simplifions ainsi la formalisation du problème.
Deuxièmement, ils proposent des nouvelles formulations mathématiques de ce problème et aboutissent à de nouvelles équations aux dérivées partielles. Aussi, nous traitons alors les questions d'*existence et d'unicité* des solutions de viscosité de ces nouvelles équations.
Troisièmement, nos travaux aboutissent à la création de deux *nouveaux algorithmes génériques* permettant de calculer des approximations numériques des solutions du SFS générique (unification algorithmique du "SFS perspectif" et du "SFS orthographique"); nous prouvons la convergence de ces approximations numériques vers la solution de viscosité de l'équation aux dérivées partielles associée. Par ailleurs, ces algorithmes permettent de traiter les *images comportant des discontinuités* ainsi que des *ombres portées.* De plus, un des algorithmes que nous proposons (l'algorithme "implicite") semble être l'algorithme itératif le plus efficace (en rapidité et précision) parmi ceux présents dans la littérature du SFS.

Enfin, dans ce rapport, nous proposons une méthode numérique permettant de résoudre les équations de Hamilton-Jacobi-Bellman. Nous proposons deux *schémas décentrés aux différences finies.* Nous détaillons les preuves de stabilité et de cohérence de ces schémas, ainsi que les preuves de convergence des algorithmes associés.

Mots-clés : Shape from Shading, réflectance Lambertienne, modèle de caméra Sténopé, projection orthographique et perspective, unification des différentes modélisations, ombres portées, images discontinues, solutions de viscosité, existence et unicité de solutions, équa-

tions de Hamilton-Jacobi-Bellman, schémas aux différences finies, stabilité et convergence de schémas monotones, algorithmes numeriques itératifs.

Chapter 1

Introduction

Shape From Shading (SFS) has been a central problem in the field of computer vision since the early days. The problem is to compute the three-dimensional shape of a surface from the brightness variations in a black and white image of that surface (see figure 1.1). The

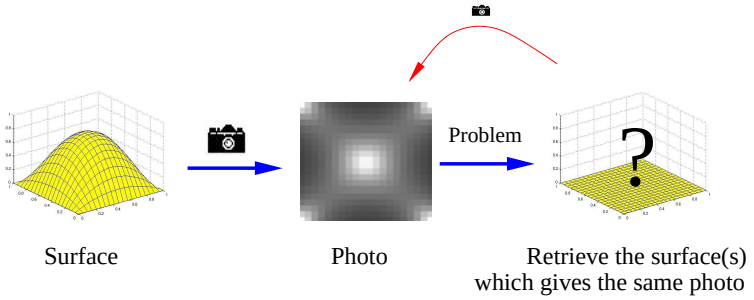

Figure 1.1: The "Shape-from-Shading" problem.

work in our field was pioneered by Horn who was the first to pose the problem as that of finding the solution of a nonlinear first-order partial differential equation (PDE) called the brightness equation [21]. Later on, various approaches have been proposed: the book [20] contains a very nice panorama of the research in SFS up to 1989; for a more recent overview, see [43, 28]. Despite the richness of the literature in this area, all approaches are based on very restrictive conditions. For example, most SFS algorithms have been developed under the assumption of orthographic projection. Few SFS approaches consider the perspective projection problem (i.e consider a pinhole camera model as opposed to a simple affine model). Penna [34, 33] proposes a local method using geometrical properties. His formulation of the problem leads him to solve a system of algebric equations. Lee and Kuo [29] present a variational approach. They minimize a cost functional based on a local

linear approximation of the reflectance map. Hasegawa and Tozzi [19] suggest to combine SFS technique with photogrammetric technique to reconstruct the surface and to calibrate the camera. Their method consists in solving large systems of linear equations and seems to be suitable only for small images. Finally, Weiss [41] proposes a physical formalism which can exploit invariants of the imaging processes and geometric knowledges about the surface. Penna [34, 33] and Weiss [41] do not present numerical results; they only describe a theoretical method.
By the perspective projection hypothesis, these four approaches extend the applicability of SFS methods to more realistic images: we can recover the shapes of objects which are located near the camera (see [42] for an example of application).
In this research report, we deal with camera which performs a perspective projection of the scene. In the previous four approaches, the authors use a 3D coordinate system attached to the scene. We find it a lot simpler to use the camera coodinate system. In sections 2.2 and 2.3, this choice of coordinates allows us to formulate the problem as new PDEs.
Let us note that we deal with the perspective case, for scenes illuminated by different light sources: First we consider a single point source located at infinity; second, we consider a single point source located at optical center.
In this research report, we also deal with the classical modelization which suppose that the camera performs an orthographic projection. This work generalizes the work of Rouy and Tourin [39] and our previous work [37, 38].
Let us emphasize that we propose a global nonlinear method and we do not need to linearize the reflectance map.

A very important aspect of the SFS problem are the questions of the existence and uniqueness of a solution. These questions as well as those related to the convergence of numerical schemes for computing the solutions became central in the last decade of the 20th century. For example, the papers of Bruss [5], Brooks [4], Horn [22], and Durou [13, 14], show the difficulty of the questions of existence and uniqueness. The first results related to the convergence of the numerical approximations have been presented by Dupuis and Oliensis [12] and P.-L. Lions, Rouy and Tourin [39, 31]. These results have been generalized by the recent papers of Falcone [16, 17] and of Prados, Faugeras and Rouy [38, 37]. Let us mention here that all of these works only deal with the simplest version of the SFS problem (with orthographic projection). In this article, we deal with the same questions in the framework of "perspective SFS" problem. Let us also remark that the papers of Penna [34, 33], Lee and Kuo [29], Hasegawa and Tozzi [19], and Weiss [41] do not deal at all with these questions.

Chapter 2

Mathematical formulations of the Lambertian SFS problem

The SFS problem is to retrieve the three-dimensional shape of a scene from the brightness variations in a black and white image of that scene.
The scene is represented by a surface $\mathcal{S}$. Let Ω be an open set of $\mathbb{R}^2$ representing the domain of definition of the image; for example, Ω is the rectangular domain $]0, X[\times]0, Y[$. We assume that $\mathcal{S}$ can be explicitly parameterized by a function S from the closure $\overline{\Omega}$ of the set Ω into $\mathbb{R}^3$ by $x \mapsto S(x)$;

$$\mathcal{S} = \left\{ S(x); \quad x \in \overline{\Omega} \right\}.$$

The image intensity is modelled as a function I from $\overline{\Omega}$ into the closed interval $[0, 1]$, by

$$I : \overline{\Omega} \longrightarrow [0, 1] : x \mapsto I(x).$$

For all $x \in \overline{\Omega}$ the intensity $I(x)$ is the brightness obtained at the point $S(x)$ of the surface $\mathcal{S}$.
We assume that a *single point light source* illuminates the scene. Thus with each point X in $\mathbb{R}^3$ we associate the unit "light vector" $\mathbf{L}(X)$ pointing to the light source.
Finally, we assume that the scene is *Lambertian*. We suppose that the albedo is constant and equal to 1.

For all x in $\overline{\Omega}$, let us denote $\mathbf{n}(x)$, a normal vector of the surface $\mathcal{S}$ at the point $S(x)$ such that

$$\mathbf{n}(x) \cdot \mathbf{L}(S(x)) \geq 0.$$

With all hypotheses above, the brightness $I(x)$ of the point $S(x)$ of the surface $\mathcal{S}$ is the cosine of the angle $(\mathbf{n}(x), \mathbf{L}(S(x)))$. In other words:

$$I(x) = \frac{\mathbf{n}(x) \cdot \mathbf{L}(S(x))}{|\mathbf{n}(x)|}. \tag{2.1}$$

REMARK 1. Through differential calculus, we can easily obtain an explicit expression for $\mathbf{n}(x)$. In effect, the two columns h_1 and h_2 of the Jacobian $DS(x)$ are two, in general different, tangent vectors to the surface $\mathcal{S}$ at point $S(x)$. Thus their cross product provides in general a normal vector to $\mathcal{S}$.
In the remaining, we study in detail three different modelizations of the SFS problem.
We deal with

1. "orthographic SFS" with a point light source at infinity,
2. "perspective SFS" with a point light source at infinity,
3. and "perspective SFS" with a point light source at the focal center.

For a more realistic modelization, the reader can see [27].

2.1 The "orthographic SFS" problem

In this subsection we revisit one of the simplest versions of the shape from shading problem.

We assume that the *light source is located at infinity*. Thus, all light vectors are parallel and we can represent the light direction by a constant vector $\mathbf{L} = (\alpha, \beta, \gamma)$. We assume that the light source is above the surface, then $\gamma > 0$. We note $\mathbf{l} = (\alpha, \beta)$.

We assume that the camera performs an *orthographic projection* of the scene. With this hypothesis, it is natural to define the surface $\mathcal{S}$ by

$$\mathcal{S} = \left\{(x_1, x_2, u(x_1, x_2)); \quad (x_1, x_2) \in \overline{\Omega}\right\}.$$

So, if the plane $(0, \overrightarrow{x_1}, \overrightarrow{x_2})$ represents the retinal plane then $|u(x)|$ is the distance of the points $S(x)$ in the scene to the camera (see figure 2.1-a)).
For such a surface $\mathcal{S}$, a normal vector $\mathbf{n}(x)$ is given by

$$\mathbf{n}(x) = (-\nabla u(x), 1).$$

Given these hypotheses, the brightness equation (2.1) becomes

$$\forall x \in \Omega, \quad I(x) = \frac{-\nabla u(x) \cdot \mathbf{l} + \gamma}{\sqrt{1 + |\nabla u(x)|^2}}, \tag{2.2}$$

and therefore the shape from shading problem is, given an image I and a light source direction $\mathbf{L}$, find a function $u : \overline{\Omega} \longrightarrow \mathbb{R}$ satisfying the equation:

$$\forall x \in \Omega, \quad I(x)\sqrt{1 + |\nabla u(x)|^2} + \nabla u(x) \cdot \mathbf{l} - \gamma = 0. \tag{2.3}$$

Note that in the case where the light source is in the same direction as the direction of projection (it is the case considered by Rouy and Tourin in [39]), we have $\mathbf{L} = (0, 0, 1)$, and the PDE (2.2) can be rewriten as an Eikonal equation:

$$|\nabla u(x)| - \sqrt{\frac{1}{I(x)^2} - 1} = 0. \tag{2.4}$$

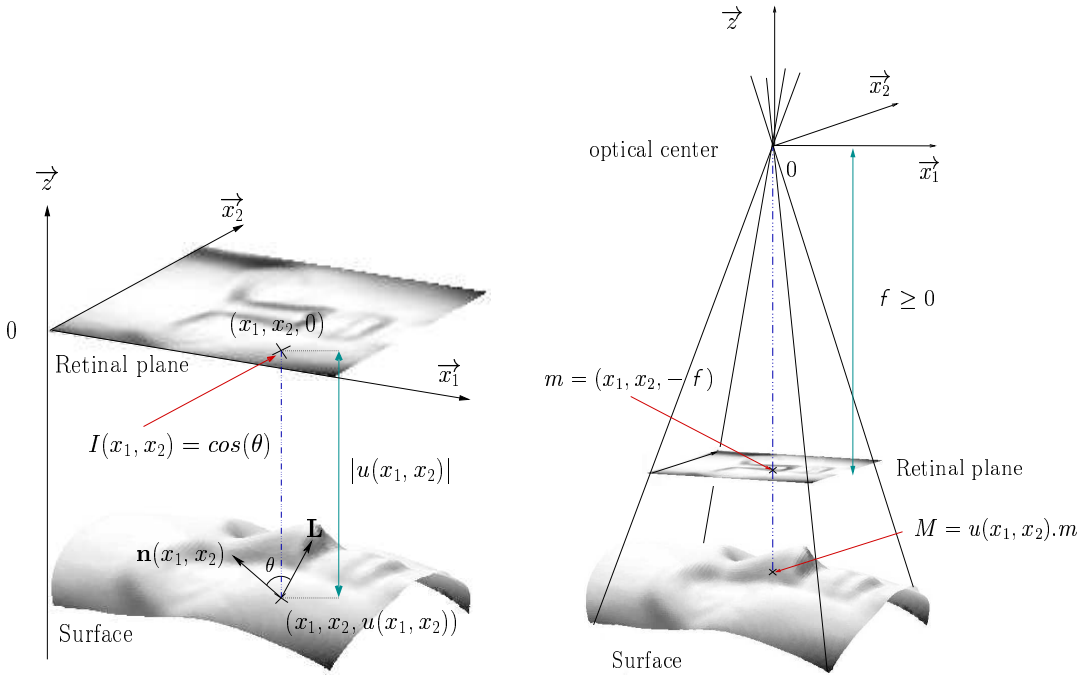

Figure 2.1:
a) Image arising from an orthogonal projection. The intensity of the "pixel"(x_1, x_2) is the intensity of the point $(x_1, x_2, u(x_1, x_2))$ on the surface $\mathcal{S}$;
b) Image arising from a perspective projection. The intensity of the "pixel"(x_1, x_2) is the intensity of the point $u(x_1, x_2)(x_1, x_2, -f)$ on the surface $\mathcal{S}$;
In both cases, we assume that the camera and the light source are above the surface.

2.2 The "perspective SFS" problem

In this section, we assume that the camera performs a *perspective projection* of the scene and that the *light source is located at infinity.*

A "pinhole" camera is represented by its retinal plane and its optical center. It is characterized by its focal length f; see figure 2.1-b.
We assume that the scene can be represented by a surface $\mathcal{S}$ defined by

$$\mathcal{S} = \left\{ u(x_1, x_2)(x_1, x_2, -f); \quad (x_1, x_2) \in \overline{\Omega} \right\}.$$

A normal vector of such a surface is given by:

$$\mathbf{n}(x) = \begin{pmatrix} f \nabla u(x) \\ u(x) + x \cdot \nabla u(x) \end{pmatrix}.$$

As in section 2.1, we represent the light by a constant unit vector $\mathbf{L} = (\alpha, \beta, \gamma)$, with $\gamma > 0$ (we suppose that the light source is above the surface $\mathcal{S}$). We note $\mathbf{l} = (\alpha, \beta)$.
In this context, the irradiance equation becomes:

$$I(x) = \frac{f \quad \mathbf{l} \cdot \nabla u(x) + \gamma \ (x \cdot \nabla u(x) + u(x))}{\sqrt{f^2 |\nabla u(x)|^2 + (x \cdot \nabla u(x) + u(x))^2}}. \tag{2.5}$$

Now, let us suppose that the surface is visible (in front of the retinal plane); i.e. u verifies $\forall x \in \overline{\Omega}, \quad u(x) \geq 1$. Since equation (2.5) is homogeneous in $\nabla u(x)$ and $u(x)$, we can simplify it by the change of variables $v = ln(u)$, $v \geq 0$. Thus the "perspective SFS" problem consists in solving the original PDE[1]:

$$I(x) \sqrt{f^2 |\nabla v|^2 + (x \cdot \nabla v + 1)^2} - (f \, \mathbf{l} + \gamma x) \cdot \nabla v - \gamma = 0. \tag{2.6}$$

2.3 The "Perspective SFS" with a point light source located at the optical center

In this section, we assume that the camera performs a *perspective projection* of the scene and that the scene is illuminated by a single point light source located at the optical center. This modelization corresponds approximately to the real situation encountered when we use a camera equiped with a flash in a dark place. If the scene is relatively far from the camera, this modelization should be relevant.
As in section 2.2, $f \geq 0$ represents the focal length. For mathematical convenience, we change slightly the parameterization of the scene. According to figure 2.2, we suppose that the scene is represented by a surface $\mathcal{S}$ defined by

$$\mathcal{S} = \left\{ \frac{f \ u(x)}{\sqrt{|x|^2 + f^2}} \begin{pmatrix} x \\ -f \end{pmatrix}; \quad x \in \overline{\Omega} \right\}.$$

[1] already formulated in [35]

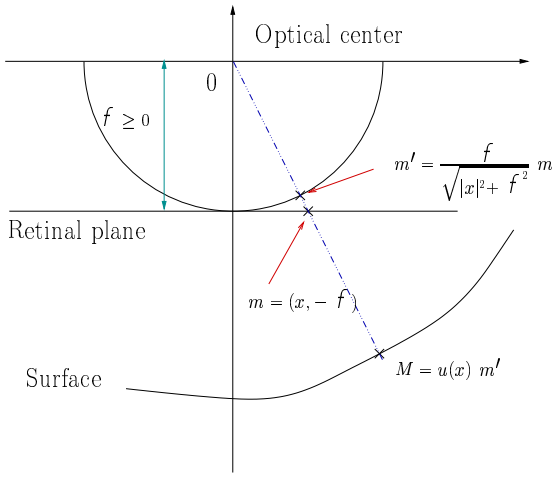

Figure 2.2: Perspective projection with a point light source located at the optical center. The intensity of the "pixel"$(x, -f)$ is the intensity of the point $u(x)(x, -f)\frac{f}{\sqrt{|x|^2 + f^2}}$ on the surface $\mathcal{S}$.

For such a surface $\mathcal{S}$, a normal vector $\mathbf{n}(x)$ at the point $S(x)$ is given by:

$$\mathbf{n}(x) = \begin{pmatrix} f\nabla u - \frac{f\, u(x)}{|x|^2 + f^2}\, x \\ \nabla u \cdot x + \frac{f\, u(x)}{|x|^2 + f^2}\, f \end{pmatrix}.$$

The single point light source is located at the optical center, so the unit light vector $\mathbf{L}$ at point $S(x)$ is the vector

$$\mathbf{L}(S(x)) = \frac{1}{\sqrt{|x|^2 + f^2}} \begin{pmatrix} -x \\ f \end{pmatrix}.$$

The irradiance equation (2.1) then becomes:

$$I(x)\sqrt{\left(\frac{|x|^2 + f^2}{f^2}\right)\left[\, f^2 |\nabla u(x)|^2 + (\nabla u(x) \cdot x)^2\right] + u(x)^2} - u(x) = 0. \tag{2.7}$$

Now, let us suppose that the surface $\mathcal{S}$ is visible (in front of the retinal plane). So u verifies

$$\forall x \in \overline{\Omega}, \quad u(x) \geq \frac{\sqrt{|x|^2 + f^2}}{f} \geq 1.$$

In this case, equation (2.7) being homogeneous, we can rewrite it by using the change of variables $v = ln(u)$, $v \geq 0$:

$$I(x)\sqrt{\left(\frac{|x|^2 + f^2}{f^2}\right)[\, f^2|\nabla v(x)|^2 + (\nabla v(x) \cdot x)^2] + 1} - 1 = 0.$$

It is equivalent to:

$$I(x)\sqrt{f^2|\nabla v(x)|^2 + (\nabla v(x) \cdot x)^2 + \frac{f^2}{|x|^2 + f^2}} - \frac{f}{\sqrt{|x|^2 + f^2}} = 0. \tag{2.8}$$

Chapter 3

Shape from Shading and Viscosity solutions

3.1 Why using viscosity solutions to solve SFS

The SFS PDEs (2.3), (2.4), (2.6) and (2.8) do not depend on u; so they are ill-posed[1] To characterize a solution, we need to impose some constraints. Let us impose Dirichlet boundary conditions[2] (DBC) for insuring uniqueness:

$$\forall x \in \partial\Omega, \quad u(x) = \varphi(x), \tag{3.1}$$

φ being continuous on $\partial\Omega$.
The SFS equations (2.3), (2.4), (2.6), and (2.8) are Hamilton-Jacobi equations. Generally, Hamilton-Jacobi equations with DBC do not have classical solutions. For example, the Rolles' theorem insures that the Eikonal equation

$$|\nabla u(x)| = 1 \text{ for all } x \text{ in }]0,1[\tag{3.2}$$

with the DBC $u(0) = u(1) = 0$, does not have classical solutions. For solving this PDE, we need to consider a notion of weak solutions. It then appears natural to consider the notion of viscosity solutions of Hamilton-Jacobi equations. In effect, the notion of viscosity solutions is a very nice way of making quantitative and operational the intuitive idea of weak solutions of first-order[3] (and for that matter, second-order) PDEs. It has been introduced by Crandall and Lions [9, 30, 11, 10] in the 80s. This theory has reached its maturity (see

[1] For example, the solution is not unique. In effect, if u is a solution, then for all $c \in \mathbb{R}$, $u + c$ is also a solution.

[2] Therefore we assume that the "distance" from the camera to the scene is known on the boundary of the image. Admitedly, this hypothesis may appear a bit restrictive. We are in the process of extending our approach to remove the requirement for boundary conditions. This will be the subject of another report.

[3] In the context of the shape from shading problem we are only concerned with first-order PDEs.

the book of Barles and the book of Bardi and Capuzzo-Dolcetta [2, 1]) and the numerical analysis of Hamilton-Jacobi equations has progressed considerably (see [18]).
Thus, in the Shape from shading area, the first interest of the notion of viscosity solutions of Hamilton-Jacobi equations is theoretical: it allows to characterize the SFS solutions, and makes the problem well-posed. But let us emphasize that this notion does not only have a theoretical interest. In effect, Barles and Souganidis [3] have proved that generally, the numerical solutions obtained by using monotonous schemes are approximations of the viscosity solutions. Thus, thanks to the notion of the viscosity solutions, we understand exactly the numerical properties of our SFS algorithms.

In the following, we recall the definitions of viscosity solutions of Hamilton-Jacobi equations and some fundamental theorems. More details about these definitions and all proofs of these theorems can be found in Barles's, Bardi and Capuzzo Dolcetta's or Lions's books [2, 1, 30].

3.2 Viscosity solutions of Hamilton-Jacobi equations

Let us start with the notion of *continuous* viscosity solutions introduced by Crandall and Lions [9, 30, 11].

3.2.1 Continuous viscosity solutions

Let $\mathbf{u} : \Omega \subset \mathbb{R}^n \to \mathbb{R}$ be a C^1 function (Ω is an open set of $\mathbb{R}^n$).
We consider a Hamilton-Jacobi equation of the form:

$$H(x, \mathbf{u}(x), \nabla \mathbf{u}(x)) = 0, \qquad x \in \Omega, \tag{3.3}$$

where H is a continuous real function defined by

$$\begin{array}{rccc} H: & \Omega \times \mathbb{R} \times \mathbb{R}^n & \longrightarrow & \mathbb{R} \\ & (x, u, p) & \longmapsto & H(x, u, p) \end{array} .$$

H is called the *Hamiltonian*. The variable associated to $\nabla \mathbf{u}(x)$ is often noted p.
Let $BUC(\Omega)$ be the set of bounded and uniformly continuous functions on Ω.

Definition 1 (Continuous viscosity solution) *$u \in BUC(\Omega)$ is a viscosity subsolution (respectively, a viscosity supersolution) of equation (3.3) if:*

$$\forall \phi \in C^1(\Omega) \ , \forall x_0 \in \Omega \text{ local maximum of } (u - \phi), \qquad H(x_0, u(x_0), \nabla \phi(x_0)) \leq 0$$

(respectively, if:

$$\forall \phi \in C^1(\Omega) \ , \forall x_0 \in \Omega \text{ local minimum of } (u - \phi), H(x_0, u(x_0), \nabla \phi(x_0)) \geq 0$$

).
u is a continuous viscosity solution of equation (3.3) if it is both a subsolution and a supersolution of (3.3).

Viscosity solutions are weak solutions. They are not differentiable! Nevertheless, this notion is consistent with the notion of classical solutions, as shown by the next

Theorem 1 *Let u be differentiable on Ω, a classical solution of (3.3). If $u \in BUC(\Omega)$, then u is a continuous viscosity solution.*
Let u be a continuous viscosity solution of equation (3.3). If u is differentiable on Ω, then u is a classical solution.

We specify for the inexperienced reader that the definition of the viscosity solutions is associated to the Hamiltonian and not to the equation. For example, it is well known that the viscosity solutions of the Hamiltonian $H(x,p)$ are different from the viscosity solutions of the Hamiltonian $-H(x,p)$. More precisely, u is a viscosity solution of $-H(x,p)$ iff $-u$ is a viscosity solution of $H(x,-p)$. Clearly, in the classical sense, the PDEs $H(x,\nabla u(x)) = 0$ and $-H(x,\nabla u(x)) = 0$ have the same solutions.

EXAMPLE : When we consider $H(x,p) = |p| - 1$, the opposite two Hamiltonians on $]0,1[$ with the DBC $u(0) = u(1) = 0$ have a unique viscosity solution shown in figure 3.1. Remember that there do not exist solutions in the classical sense. Schematically, the viscosity solutions of the Hamiltonian $H(x,p)$ allow upward kinks whereas the viscosity solutions of the Hamiltonian $-H(x,p)$ allow downward kinks.

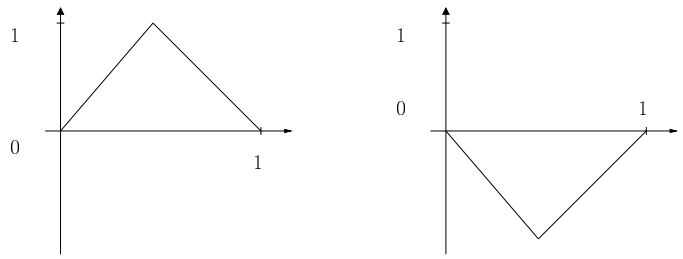

Figure 3.1: a) solution with $H(x,p) = |p| - 1$; b) solution with $H(x,p) = 1 - |p|$

Even if the viscosity solutions of a PDE depend on the Hamiltonian, the notion of viscosity solutions is consistent with strictly increasing changes of unknown (see proposition II.2.5 of [1]):

Proposition 1 (change of unknown) *Let $u \in C(\Omega)$ be a viscosity solution of (3.3) and $\Phi \in C^1(\mathbb{R})$ be such that $\Phi'(t) > 0$. Then $v = \Phi(u)$ is a viscosity solution of*

$$H(x, \Psi(v(x)), \Psi'(v(x))\nabla v(x)) = 0 \qquad x \in \Omega,$$

where $\Psi = \Phi^{-1}$.

Thus, in order to simplify the equations, we can perform (strictly increasing) changes of variables, see sections 2.2 and 2.3.

One of the most important interests of the viscosity solutions theory is that it provides a set of general existence and uniqueness theorems which require very weak hypotheses.

Let us recall that the SFS Hamiltonians do not depend on u. Thus, to have uniqueness we must add boundary conditions. Our choice turns to Dirichlet conditions. Thus for the SFS problems we consider equations (3.4)

$$\begin{cases} H(x, \nabla u(x)) = 0 \text{ on } \Omega \\ u = \varphi \text{ on } \partial\Omega \end{cases} \tag{3.4}$$

with Ω a bounded regular and convex open set of $\mathbb{R}^n$, φ a real function defined on $\partial\Omega$ and H the adequate Hamiltonian.

The following theorem 2 applies in the special case where the Hamiltonian H appearing in equation (3.4) (hence with Dirichlet boundary conditions) is convex with respect to ∇u. It ensures the *existence* of the continuous viscosity solutions of the PDE (3.4).

We note H^* the Legendre transform[4] of H:

$$H^*(x, q) = \sup_{p \in \mathbb{R}^2} \{p.q - H(x, p)\} \ \leq +\infty.$$

Let us define $\forall x, y \in \overline{\Omega}$,

$$L(x, y) = \inf_{\xi \in C_{x,y}, T_0 > 0} \{ \int_0^{T_0} H^*(\xi(s), -\xi'(s)) ds \ \}$$

where $C_{x,y}$ is the set of $\xi : [0, T_0] \to \mathbb{R}^2$ such that

- $\xi(0) = x$,
- $\xi(T_0) = y$,
- $\forall t \in [0, T_0], \xi(t) \in \overline{\Omega}$,
- $\xi' \in L^\infty(0, T_0)$
  (We denote by $L^\infty(0, T_0)$ the set of bounded real measurable functions defined on the interval $(0, T_0)$.)

Theorem 2 (Existence of continuous solutions) *If*

(H1) [**convexity**] *H is convex with respect to p for all x in $\overline{\Omega}$,*

(H2) [**uniform coercivity**]
$H(x, p) \to +\infty$ when $|p| \to +\infty$ uniformly with respect to $x \in \overline{\Omega}$,

[4] see appendix A.

(H3) [**subsolution**] $inf_{p\in\mathbb{R}^2} H(x,p) \leq 0$ *in* $\overline{\Omega}$,

(H4) [**regularity**] $H \in C(\overline{\Omega}\times\mathbb{R}^2)$,

(H5) [**compatibility**] $\forall x,y \in \partial\Omega\ ,\ \varphi(x)-\varphi(y) \leq L(x,y)$;

then the function u *defined in* $\overline{\Omega}$ *by:*

$$\begin{aligned} u(x) &= \inf_{y\in\partial\Omega}\{\varphi(y)+L(x,y)\} \\ &= \inf\{\int_0^{T_0} H^*(\xi(s),-\xi'(s))ds+\varphi(\xi(T_0))\} \end{aligned} \tag{3.5}$$

is a continuous viscosity solution of equation (3.4) (in particular u *verifies* $u(x)=\varphi(x)$ *for all* x *in* $\partial\Omega$*).*

Theorem 2 is a special case of theorem 5.3 in [30]. It can be interpreted as giving compatibility constraints for the boundary conditions.

REMARKS 2.

R2.1 - Under hypotheses (H1)-(H3), we have then the following necessary and sufficient condition:
u defined by (3.5) is a viscosity solution of (3.4) iff the hypothesis (H5) *is true.*
We will say that φ verifies the *compatibility condition* if (H5) is verified.

R2.2 - An other interest of the viscosity theory is its link with control theory. For example, theorem 2 gives the solutions as value functions.

Theorem 2 allows to prove the existence of continuous viscosity solutions of our SFS problems (see section 3.4). Nevertheless, let us point out that the existence of such a solution requires a constraint on the variation of φ (the compatibility condition).

EXAMPLE : Let us consider again the PDE

$$|\nabla u(x)| - 1 = 0.$$

The reader can verify easily that $H^*(x,.)$ is defined on the ball $B(0,1)$ and that for all x in Ω and for all q in $B(0,1)$, $H^*(x,q)=1$. So

$$L(x,y) = \inf_{\xi|\xi(0)=x,\xi(T_0)=y,\forall s\in[0,T_0],|\xi'(s)|\leq 1} T_0 = y-x.$$

Therefore for the Hamiltonian $H(x,p) = |p| - 1$ with DBC on $\{0,1\}$, the compatibility condition is:

$$\begin{cases} \varphi(0) - \varphi(1) & \leq L(0,1) & = 1 - 0, \\ \varphi(1) - \varphi(0) & \leq L(1,0) & = 0 - 1, \end{cases}$$

that is to say

$$|\varphi(0) - \varphi(1)| \ \leq \ 1.$$

Consequently, we can not prove that the PDE

$$\begin{cases} |\nabla u| - 1 = 0, \\ u(0) = 0 \text{ and } u(1) = 1.5, \end{cases}$$

has a continuous viscosity solution. Also, remark that it is possible to prove that this PDE does not have continuous viscosity solutions.

Come back to the SFS problem. Let us suppose that we make a large error on the function φ[5] when we compute a numerical solution of the SFS problems. If this error is too large then there do not exist continuous viscosity solutions. So what do the numerical algorithms compute? In other words, how do interpret the numerical results obtained by the algorithms?
So as soon as there do not exist continuous viscosity solutions, we need to introduce a notion of solution weaker than this notion. Also, the notion of discontinuous viscosity solutions provides an answer to these problems. The notion of discontinuous viscosity solutions is due mostly to Ishii [25, 24] and is covered in detail in the book of Barles [2]. The recent book of Bardi and Capuzzo Dolcetta [1] synthesizes some recent results.

3.2.2 Discontinuous viscosity solutions

Let us consider the following equation on the closed subset $\overline{\Omega}$:

$$F(x, u(x), \nabla u(x)) = 0, \text{ for } x \in \overline{\Omega}, \tag{3.6}$$

where F, defined on $\overline{\Omega} \times \mathbb{R} \times \mathbb{R}^N$, is only locally bounded (F is not supposed to be continuous). The idea is to consider both the equation and the boundary condition.
Generally F is defined by:

$$F(x,u,p) = \begin{cases} H(x,u,p) & \text{for x in } \Omega, \\ G(x,u,p) & \text{for x in } \partial\Omega, \end{cases} \tag{3.7}$$

where H is a continuous function on $\overline{\Omega} \times \mathbb{R} \times \mathbb{R}^N$ and G is a continuous function on $\partial\Omega \times \mathbb{R} \times \mathbb{R}^N$. For example, in the case of the Dirichlet condition, we can take:

$$F(x,u,p) = \begin{cases} H(x,u,p) & \text{for x in } \Omega, \\ u - \varphi(x) & \text{for x in } \partial\Omega, \end{cases} \tag{3.8}$$

[5] Let us remember that we assume that we know this function φ, but in practice we only can have an approximation of it.

with φ continuous on $\partial\Omega$.

Definition 2 *Let u be a locally bounded function on a set E.*
$\forall x \in E$, let us note:

$$u^*(x) = \limsup_{y \to x} u(y)$$

$$u_*(x) = \liminf_{y \to x} u(y)$$

u^* et u_* are respectively call the upper semicontinuous envelope and lower semicontinuous envelope of u.

We recall also that $u : E \to \mathbb{R}$ is upper (respectively, lower) semicontinuous (u.s.c, resp. l.s.c) if for any $x \in E$ and $\varepsilon > 0$ there exists a δ such that for all $y \in E \cap B(x, \delta)$ $u(y) < u(x) + \varepsilon$ (respectively, $u(y) > u(x) - \varepsilon$). To familiarize oneself with these notions, the reader can refer to the sections V-1 and V-2.1 of [1].

Definition 3 (Discontinuous viscosity solutions) *A locally bounded function, u.s.c (respectively, l.s.c) on $\overline{\Omega}$, v is a discontinuous viscosity subsolution (respectively, supersolution) of equation (3.6) if:*

$$\forall \phi \in C^1(\overline{\Omega}) \ , \forall x_0 \in \overline{\Omega} \text{ local maximum of } (v - \phi), \quad F_*(x_0, v(x_0), \nabla\phi(x_0)) \leq 0.$$

(respectively, if:

$$\forall \phi \in C^1(\overline{\Omega}) \ , \forall x_0 \in \overline{\Omega} \text{ local minimum of } (v - \phi), \quad F^*(x_0, v(x_0), \nabla\phi(x_0)) \geq 0.$$

).
A locally bounded function, u is a discontinuous viscosity solution of (3.6) if u^* is a subsolution and u_* is a supersolution of (3.6).

For the Dirichlet problem (3.8) with H and φ continuous, it is easy to calculate the functions F^* and F_*. We have:

$$\begin{array}{ll} F^*(x) = F_*(x) = H(x) & \text{if } x \in \Omega, \\ F^*(x) = max(H(x, u, \nabla u), u(x) - \varphi(x)) & \text{if } x \in \partial\Omega, \\ F_*(x) = min(H(x, u, \nabla u), u(x) - \varphi(x)) & \text{if } x \in \partial\Omega. \end{array}$$

For more details, we advise the reader to read chapter 4 of Barles's book [2].

Let us emphasize that the notion of discontinuous viscosity solutions extends the notion of continuous viscosity solutions. In particular a continuous viscosity solution is a discontinuous viscosity solution. Also, the notion of discontinuous viscosity solutions allows to define solutions when there do not exist continuous viscosity solutions. For example, the reader will verify easily that the function represented in figure 3.2 is a discontinuous viscosity solution of

$$\left\{ \begin{array}{l} |\nabla u| - 1 = 0, \\ u(0) = 0 \text{ and } u(1) = 1.5. \end{array} \right. \tag{3.9}$$

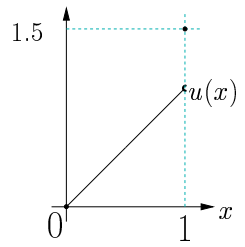

Figure 3.2: Example of a discontinuous viscosity solution of (3.9).

There exist many existence theorems for discontinuous viscosity solutions.We only give here the one we need for our applications. The reader can find the following theorem in Bardi and Capuzzo Dolcetta's book [1] (theorem V.4.13), it deals with Hamilton-Jacobi-Bellman equations.

Definition 4 *Let Ω be an open set of $\mathbb{R}^N$. We call Hamilton-Jacobi-Bellman (HJB) the PDE defined as follows:*

$$\lambda u(x) + \sup_{a \in A}\{-f(x,a) \cdot \nabla u(x) - l(x,a)\} = 0 \quad \forall x \in \Omega. \tag{3.10}$$

where f is a function from $\Omega \times A$ into $\mathbb{R}^N$ and l is a function defined from $\Omega \times A$ into $\mathbb{R}$. According to the optimal control theory (see theorem 3 and more generally the book [1]), a is called the control, *l is called* the running cost, *f is called* the dynamics *and $\lambda \geq 0$ is called* the interest rate.

We associate with the HJB equations (3.10), the convex Hamiltonian

$$H(x,u,p) = \lambda u + \sup_{a \in A}\{-f(x,a) \cdot p - l(x,a)\},$$

which we call "HJB Hamiltonian".

Before giving the theorem, let us state the assumptions we need:

(H6) *A is a compact topological space and Ω is a bounded open subset of $\mathbb{R}^N$;*

(H7) *$f : \overline{\Omega} \times A \to \mathbb{R}^N$ is continuous;*
$l : \overline{\Omega} \times A \to \mathbb{R}$ is continuous and bounded.

(H8) *f and l are Lipschitz continuous in $x \in \overline{\Omega}$ uniformly in $a \in A$.*

Theorem 3 *Let $H(x,p) = \sup_{a \in A}\{-f(x,a) \cdot p - l(x,a)\}$; assume the hypotheses* (H6)-(H8) *are satisfied and let $\varphi \in BC(\partial\Omega)$, then u defined by*

$$u(x) = \inf_{\xi : \mathbb{R}^+ \to A} \int_0^{t_x(\xi)} l(y_x(s), \xi(s)) e^{-\lambda s} ds + e^{-\lambda t_x(\xi)} \varphi(y_x(t_x(\xi))),$$

(where y_x is the solution of the differential equation

$$\begin{cases} y'(t) = f(y(t), \xi(t)), & t > 0, \\ y(0) = x, \end{cases}$$

and $t_x(\xi)$ is the first time the trajectory $y_x(., \xi)$ goes out of $\overline{\Omega}$)
is a viscosity solution in the discontinuous sense of

$$\begin{cases} \lambda u + H(x, \nabla u) = 0 & \text{in } \Omega, \\ u = \varphi & \text{on } \partial\Omega. \end{cases} \tag{3.11}$$

REMARKS 3.

R3.1 - In other words, this theorem states that the value function of the classical optimal control problem is the viscosity solution of the adequate HJB equation.

R3.2 - We emphasize the fact that the theorem is true even if $\lambda = 0$.

The HJB equations are useful for the SFS problems. As we will see below, we can rewrite the SFS equations as HJB equations. The reader unfamiliar with control theory can read appendix A in which we detail the tools allowing to make this transformation.

3.3 Hamiltonians for the SFS problems and unification of the "perspective" and "orthographic SFS"

3.3.1 Basic Hamiltonians for SFS

In chapter 2, we have presented several PDEs arising from various mathematical formulations of the SFS problem. Let us recall that the definition of the viscosity solutions is associated with the Hamiltonians and not with the equations. So for each SFS equation we have to specify an Hamiltonian.

1. In the case where $\mathbf{L} = \begin{pmatrix} 0 \\ 0 \\ 1 \end{pmatrix}$, we associate the "Eikonal" Hamiltonian H^{orth}_{Eiko} with the Eikonal equation (2.4):

$$H^{orth}_{Eiko}(x, p) = |p| - \sqrt{\frac{1}{I(x)^2} - 1}. \tag{3.12}$$

In the case where $\mathbf{L} = \begin{pmatrix} 0 \\ 0 \\ 1 \end{pmatrix}$, we can also consider the Hamiltonian $H^{orth}_{(0,0,1)}$:

$$H^{orth}_{(0,0,1)}(x,p) = I(x)\sqrt{1+|p|^2} - 1; \tag{3.13}$$

$H^{orth}_{(0,0,1)}$ is a particular case of $H^{orth}_{R/T}$, see below.

2. With equation (2.3) of the general "orthographic SFS" ($\mathbf{L} = (\mathbf{l}, \gamma)$), we associate the Hamiltonian[6] $H^{orth}_{R/T}$:

$$H^{orth}_{R/T}(x,p) = I(x)\sqrt{1+|p|^2} + p\cdot\mathbf{l} - \gamma; \tag{3.14}$$

3. With equation (2.6) of the "perspective SFS" with a constant light source vector $\mathbf{L} = (\mathbf{l}$ $\gamma)$, we associate the Hamiltonian H^{pers}_1:

$$H^{pers}_1(x,p) = I(x)\sqrt{f^2|p|^2 + (x\cdot p + 1)^2} - (f\,\mathbf{l} + \gamma x)\cdot p - \gamma; \tag{3.15}$$

4. With the "perspective SFS" with $\mathbf{L} = (0,0,1)$ (the light direction corresponds to the optical axis of the camera) we associate

$$H^{pers}_{(0,0,1)}(x,p) = I(x)\sqrt{f^2|p|^2 + (x\cdot p + 1)^2} - x\cdot p - 1; \tag{3.16}$$

5. And with the "perspective SFS" with a single point light source located at the optical center, we associate the Hamiltonian H^{pers}_F;

$$H^{pers}_F(x,p) = I(x)\sqrt{f^2|p|^2 + (p\cdot x)^2 + \frac{f^2}{|x|^2 + f^2}} - \frac{f}{\sqrt{|x|^2 + f^2}} \tag{3.17}$$

Let us remind the reader that we assume $\gamma > 0$.

3.3.2 A "generic" Hamiltonian for SFS

As we have seen in the previous section, the SFS problem leads to several Hamiltonians; nevertheless we show that all these SFS Hamiltonians are special cases of a general one, thereby simplifying the formalization of the problem.

[6] This Hamiltonian has been introduced by Rouy and Tourin [39].

Explicit formulation of H_g

In appendix B.1, we show that all the Hamiltonians H_*^{orth} and H_*^{pers} are special cases of the following "generic" Hamiltonian H_g

$$H_g(x,p) = \tilde{H}_g(x, A_x p + \overrightarrow{v_x}) + \overrightarrow{w_x} \cdot p + c_x,$$

with $\tilde{H}_g(x,q) = \kappa_x \sqrt{|q|^2 + K_x^2}$,

- $\kappa_x > 0$ and $K_x \geq 0$,
- $A_x = D_x\ R_x$, where
  - $D_x = \begin{pmatrix} \mu_x & 0 \\ 0 & \nu_x \end{pmatrix}$, $\mu_x, \nu_x \neq 0$,
  - if $x \neq 0$, R_x is the rotation matrix $R_x = \begin{pmatrix} \cos\theta & \sin\theta \\ -\sin\theta & \cos\theta \end{pmatrix}$; where $\cos\theta = \frac{x_2}{|x|}$ and $\sin\theta = -\frac{x_1}{|x|}$,
  - if $x = 0$, $R_x = Id_{2\times 2}$;
- $\overrightarrow{v_x}, \overrightarrow{w_x} \in \mathbb{R}^2$,
- $c_x \in \mathbb{R}$.

In appendix B.1, we detail the associated functions $\overrightarrow{v_x}, \overrightarrow{w_x}, c_x, \mu_x, \nu_x, \kappa_x$ and K_x, for all the Hamiltonians H_*^{orth} and H_*^{pers}.

Control formulation of H_g

Let us remind the reader that we call "HJB Hamiltonian", a Hamiltonian which has the following form (see definition 4):

$$H(x,u,p) = \lambda u + \sup_{a \in A} \{ -f(x,a) \cdot p - l(x,a) \}$$

From a theoretical point of view as well as from a practical one, it is very interesting to formulate the SFS Hamiltonians as HJB Hamiltonians. For example, such a formulation allows to apply the existence theorem 3. Also, in chapter 4, we show that the HJB formulation allows to design approximations schemes and numerical algorithms. Therefore it allows to compute numerical approximations of the viscosity solutions of SFS PDEs.

We now give a HJB formulation of the "generic" Hamiltonian H_g.
By using the Legendre transform[7] of $\tilde{H}_g$, we can rewrite the Hamiltonian H_g as a supremum[8]:

$$H_g(x,p) = \sup_{a \in Dom\tilde{H}_g{}^*(x,.)} \{\ [{}^t A_x a + \overrightarrow{w_x}] \cdot p\ -\ [\tilde{H}_g{}^*(x,a) - \overrightarrow{v_x} \cdot a - c_x]\ \}.$$

[7] See appendix A.
[8] See appendix B.2.

Now, let us write

$$Dil_x = \kappa_x \, {}^tR_x D_x R_x. \tag{3.18}$$

By using the change of variables $b = \kappa_x^{-1} \, {}^tR_x a \quad (a = \kappa_x R_x b)$, we have:

$$H_g(x,p) = \sup_{a \in \overline{B}(0,1)} \{ \, [\, Dil_x a + \overrightarrow{w_x} \,] \cdot p \; - \; [\tilde{H_g}^*(x, \kappa_x R_x a) - \kappa_x ({}^tR_x \overrightarrow{v_x}) \cdot a - c_x] \, \}.$$

Through differential calculus[9], we obtain

$$\tilde{H_g}^*(x,a) = -K_x \sqrt{\kappa_x^2 - |a|^2},$$

so that

$$\tilde{H_g}^*(x, \kappa_x R_x a) = -\kappa_x K_x \sqrt{1 - |a|^2}.$$

Then we have

$$H_g(x,p) = \sup_{a \in \overline{B}_2(0,1)} \{ -f_g(x,a) \cdot p - l_g(x,a) \}, \tag{3.19}$$

with

$$\begin{aligned} f_g(x,a) &= - \, [\, Dil_x a + \overrightarrow{w_x} \,], \\ l_g(x,a) &= - \, [\, K_x \kappa_x \sqrt{1 - |a|^2} + \kappa_x ({}^tR_x \overrightarrow{v_x}) \cdot a + c_x]. \end{aligned}$$

In order to apply the theory of the viscosity solutions on HJB equations, it is important that the supremum is on a set which does not depend on x. In the control formulation (3.19) of H_g, the supremum is on the closed ball $\overline{B}_2(0,1)$.

REMARK 4. This formulation is still valid at the points x such that $\kappa_x = 0$. For most of the SFS Hamiltonians, these points correspond to pixels in *shadows*.
At these points we have

$$H_g(x,p) = \overrightarrow{w_x} \cdot p + c_x = \sup_{a \in \overline{B}_2(0,1)} \{ \, \overrightarrow{w_x} \cdot p + c_x \, \},$$

So

$$\begin{aligned} f_g(x,a) &= - \, \overrightarrow{w_x}, \\ l_g(x,a) &= - \, c_x. \end{aligned}$$

Thus, the approximation schemes based on this formulation and presented in section 4.2 provide numerical algorithms allowing to compute solutions of SFS for images including shadows.

[9] Using the method described in appendix A.

3.3.3 SFS Hamiltonians such that $H(x,0) \leq 0$

The SFS Hamiltonians are convex with respect to p, so the property $H(x,0) \leq 0$ can be rewritten as $H^*(x,q) \geq 0$ (where H^* is the Legendre transform of H, see appendix A).

PROOF.

$$\begin{array}{rcl} H(x,0) \leq 0 & \Longleftrightarrow & \sup_{q \in Dom H^*(x,.)} \{\ 0 \cdot q\ -\ H^*(x,q)\ \} \leq 0 \\ & \Longleftrightarrow & -\inf_{q \in Dom H^*(x,.)} \{\ H^*(x,q)\ \} \leq 0 \\ & \Longleftrightarrow & \inf_{q \in Dom H^*(x,.)} \{\ H^*(x,q)\ \} \geq 0 \\ & \Longleftrightarrow & \forall q \in Dom H^*(x,.), \qquad H^*(x,q) \geq 0. \end{array}$$

□

Moreover, the running cost l_g (associated to the generic Hamiltonian H_g) is equal to $H_g^*(x,q) = l_g(x, Dil_x^{-1}(q - \overrightarrow{w_x}))$. Therefore H_g verifies $H_g(x,0) \leq 0$ iff the running cost l_g is positive. Therefore this is also true for all SFS Hamiltonians.

Essentially, there are four (theoretical) reasons for dealing with such Hamiltonians:

1. It allows to apply the theory developed by Camilli which can deal with degenerate PDEs. For obtaining uniqueness, Camilli proposes to choose the "maximal" solution [8, 7]. In [18][10], Camilli deals with HJB equations with positive running cost.

2. The work of Dupuis and Oliensis [12] can be extended to such Hamiltonians.

3. The proofs of the existence and uniqueness of the viscosity solutions are easier with these Hamiltonians than with other Hamiltonians. For example, hypothesis (H3) becomes obvious. This is also true when we consider schemes. The proof of the stability of the schemes and the proof of the convergence of their solutions toward the viscosity solution (of the associated equations) are simpler; see for example proposition 5.

4. The work of Ostrov [26, 32] can be related to such Hamiltonians. See section 3.7.

Since the intensity image I verifies $I(x) \leq 1$, the SFS Hamiltonians H_{Eiko}^{orth}, $H_{(0,0,1)}^{orth}$, H_F^{pers} and $H_{(0,0,1)}^{pers}$ verify $H(x,0) \leq 0$. For the Hamiltonians $H_{R/T}^{orth}$ and H_1^{pers}, the associated running costs are not positive. Nevertheless, by performing some changes of variables, we can design other Hamiltonians which verify this property.

"Orthographic Hamiltonian" such that $H(x,0) \leq 0$

By using the change of variables[11]

$$v(x) = 1 \cdot x + \gamma u(x), \tag{3.20}$$

[10] "A Characterization of the Value Function for a Class of Degenerate Control Problems" (F. Camilli) - p.47 of [18].

[11] Proposed by Dupuis and Oliensis [12].

the PDE (2.3) can be rewriten as

$$\forall x \in \Omega, \quad I(x)\sqrt{|\nabla u(x) - 1|^2 + \gamma^2} + \nabla u(x) \cdot 1 - 1 = 0. \tag{3.21}$$

Let us note that the "change of unknown" proposition 1 does not apply to the change of variables (3.20).

With equation (3.21), we associate the Hamiltonian $H^{orth}_{D/O}$:

$$H^{orth}_{D/O}(x,p) = I(x)\sqrt{|p - 1|^2 + \gamma^2} + p \cdot 1 - 1. \tag{3.22}$$

Since $H^{orth}_{D/O}(x,0) = I(x) - 1$ and $I(x) \leq 1$, $H^{orth}_{D/O}$ verifies:

$$\forall x \in \overline{\Omega}, \qquad H^{orth}_{D/O}(x,0) \leq 0.$$

"Perspective Hamiltonian" such that $H(x,0) \leq 0$

By using the change of variable

$$v(x) = \frac{\gamma}{f}[\ \gamma\ f - 1 \cdot x\ ]\ u(x), \tag{3.23}$$

before the change of variables $v = ln(u)$, the PDE (2.5) can be rewritten as a PDE which the associated Hamiltonian H^{pers}_2 verifies

$$\forall x \in \overline{\Omega}, \qquad H^{pers}_2(x,0) \leq 0.$$

Since the interest of this formulation is essentially theoretic, we do not give more details about this Hamiltonian.

Remark:

Let us note that the two Hamiltonians $H^{orth}_{D/O}$ and H^{pers}_2 are some particular cases of the generic SFS Hamiltonian H_g described above.

3.4 Existence of viscosity solutions of the SFS problems

3.4.1 Existence of continuous viscosity solutions of the SFS problems

In this section, we apply theorem 2 for proving the existence of continuous viscosity solutions of the SFS Hamiltonians.

Let us remind the reader that the SFS Hamiltonians are special cases of the generic Hamiltonian H_g. Therefore all the properties proved for the generic Hamiltonian are also available for all the SFS Hamiltonians.

- At first, the generic Hamiltonian H_g is convex with respect to p: (H1) is true.
- About the uniform coercivity, we have the following proposition:

Proposition 2 *Let us consider a Hamiltonian H_g defined as in section 3.3.2. such that the functions κ_x, c_x, A_x^{-1}, $\overrightarrow{w_x}$, $\overrightarrow{v_x}$ are continuous and bounded on the compact set $\overline{\Omega}$. We assume that $\overrightarrow{w_x} \neq 0$ for all x in $\overline{\Omega}$.*
If $\forall x \in \overline{\Omega}$, $|{}^t A_x^{-1} \overrightarrow{w_x}| < \kappa_x$ then $H_g(x,.)$ is coercive uniformly with respect to x in $\overline{\Omega}$.

The proof of proposition 2 is based on the following lemma:

Lemma 1 *Let Q be a function defined by:*

$$\begin{array}{rccl} Q: & E \times \mathbb{R}^N & \longrightarrow & \mathbb{R} \\ & (x,q) & \longmapsto & Q(x,q) := |q| + W(x) \cdot q + C(x), \end{array}$$

where E is any set, $C : E \to \mathbb{R} : x \mapsto C(x)$ is a function bounded below by $c \in \mathbb{R}$, and W is a function defined by: $W : E \to \mathbb{R}^N : x \mapsto W(x)$.
If there exists $\varepsilon > 0$ such that $\forall x \in E$, $|W(x)| \leq 1 - \varepsilon$ then $Q(x,.) : q \mapsto Q(x,q)$ is coercive uniformly with respect to x in E.

Proof of lemma 1. By the Cauchy-Schwarz's inequality we have:

$$W(x) \cdot q \geq -|W(x)||q|.$$

Therefore, $\forall x \in E$, $\forall q \in \mathbb{R}^N$,

$$|q| + W(x) \cdot q \geq |q|(1 - |W(x)|) \geq |q|\varepsilon.$$

Hence $Q(x,q) \geq |q|\varepsilon + c$, and the conclusion follows. □

PROOF OF PROPOSITION 2.

- Let us define
$$\hat{H}(x,p) := \kappa_x |A_x p + \overrightarrow{v_x}| + \overrightarrow{w_x} \cdot p + c_x.$$
We have
$$\forall x \in \overline{\Omega}, \forall p \in \mathbb{R}^2, \qquad H_g(x,p) \geq \hat{H}(x,p),$$
So if $\hat{H}(x,.) : p \mapsto \hat{H}(x,p)$ is coercive uniformly with respect to x then $H_g(x,.)$ is also coercive uniformly with respect to x.

- We now consider
$$\begin{array}{rccl} Q: & \overline{\Omega} \times \mathbb{R}^2 & \longrightarrow & \mathbb{R} \\ & (x,q) & \longmapsto & |q| + \underbrace{\frac{1}{\kappa_x}[{}^t A_x^{-1} \overrightarrow{w_x}]}_{W(x)} \cdot q + \underbrace{c_x - [{}^t A_x^{-1} \overrightarrow{w_x}] \cdot \overrightarrow{v_x}}_{C(x)}. \end{array}$$
Since we have assumed that
i) c_x, A_x^{-1}, $\overrightarrow{w_x}$, $\overrightarrow{v_x}$ were bounded
and that
ii) $|{}^t A_x^{-1} \overrightarrow{w_x}| < \kappa_x$, (so that, by continuity, there exists $\varepsilon > 0$ such that for
all x in the compact set $\overline{\Omega}$, $\frac{1}{\kappa_x}|{}^t A_x^{-1} \overrightarrow{w_x}| \leq 1 - \varepsilon$).
Therefore by lemma 1, $Q(x,.)$ is coercive uniformly with respect to x in $\overline{\Omega}$.

- Now, let us rewrite the uniform coercivity of $Q(x,.)$ as follows:
$$\forall A \in \mathbb{R}, \ \exists M \in \mathbb{R} \ / \ \forall q \in \mathbb{R}^2, \forall x \in \overline{\Omega}, \qquad |q| \geq M \text{ implies } Q(x,q) \geq A.$$
Let us fix A and $M_1 \in \mathbb{R}$ such that the above implication is true (with $M = M_1$).
We can consider $M_2 \in \mathbb{R}$ such that for all x on $\overline{\Omega}$,
$$M_2 \geq \frac{1}{\kappa_x} |A_x^{-1}| (|M_1| + \kappa_x |\overrightarrow{v_x}|)$$
(we have assumed that $\overrightarrow{v_x}$ and A_x^{-1} were bounded; moreover, since $|{}^t A_x^{-1} \overrightarrow{w_x}| > 0$ and $|{}^t A_x^{-1} \overrightarrow{w_x}|$ is continuous on the compact set $\overline{\Omega}$, κ_x^{-1} is also bounded).
Then for all p in $\mathbb{R}^2$, $|p| \geq M_2$ implies:
$$\begin{array}{rcl} \kappa_x |A_x p + \overrightarrow{v_x}| & \geq & \kappa_x (|A_x p| - |\overrightarrow{v_x}|) \\ & \geq & \kappa_x \left(\frac{1}{|A_x^{-1}|} |p| - |\overrightarrow{v_x}| \right) \\ & \geq & \kappa_x \left(\frac{1}{|A_x^{-1}|} |M_2| - |\overrightarrow{v_x}| \right) \\ & \geq & \kappa_x \left(\frac{1}{\kappa_x} (|M_1| + \kappa_x |\overrightarrow{v_x}|) - |\overrightarrow{v_x}| \right) \\ & \geq & M_1. \end{array}$$

Then:
$\forall A \in \mathbb{R},\ \exists M_2 \in \mathbb{R}\ /\ \forall p \in \mathbb{R}^2, \forall x \in \overline{\Omega},$

$$|p| \geq M_2 \qquad \text{implies} \qquad \hat{H}(x,p) = Q(x, \kappa_x(A_x p + \overrightarrow{v_x})) \geq A.$$

In other words, $\hat{H}(x,.)$ is coercive uniformly with respect to x in $\overline{\Omega}$.
The conclusion follows.

□

Using the results of the appendix B.1 and applying proposition 2 to the corresponding SFS Hamiltonians, we obtain the following statements:

- H^{orth}_{Eiko}, $H^{orth}_{(0,0,1)}$, H^{pers}_{F} are uniformly coercive as soon as $I(x) > 0$.
- $H^{orth}_{R/T}$, $H^{orth}_{D/O}$ are uniformly coercive as soon as $I(x) > |\mathbf{l}|$.
- $H^{pers}_{(0,0,1)}$ is uniformly coercive if $I(x) > \frac{|x|}{\sqrt{f^2+|x|^2}}$.
- H^{pers}_{1}, H^{pers}_{2} are coercive as soon as

$$I(x)^2 > \frac{1}{f^2+|x|^2}\ \left[\ |\gamma x + f\mathbf{l}|^2 + \left(\ |x|^2|\mathbf{l}|^2 - (x\cdot\mathbf{l})^2\ \right)\ \right].$$

Hence, subject toy the adequate conditions, all SFS Hamiltonians verify hypothesis (H2).

- Concerning hypothesis (H3), we verify that:
  - for the Hamiltonians H^{orth}_{Eiko}, $H^{orth}_{(0,0,1)}$, H^{pers}_{F}, $H^{orth}_{D/O}$, $H^{pers}_{(0,0,1)}$ and H^{pers}_{2} we have

$$\inf_{p\in\mathbb{R}^2} H(x,p) \leq H(x,0) \leq 0.$$

  - for the Hamiltonian $H^{orth}_{R/T}$ (taking the derivative):

$$\inf_{p\in\mathbb{R}^2} H(x,p) = \begin{cases} \sqrt{I^2(x) - |\mathbf{l}|^2} - \gamma & \text{if } I(x) \geq |\mathbf{l}|. \\ -\infty & \text{otherwise.} \end{cases}$$

    Since $I^2 \leq \alpha^2 + \beta^2 + \gamma^2 = 1$, we have $\inf_{p\in\mathbb{R}^2} H(x,p) \leq 0$.
  - for the Hamiltonian H^{pers}_{1}, we can consider the subsolution $\tilde{u}$ described at the page 33. We have

$$\inf_{p\in\mathbb{R}^2} H^{pers}_{1}(x,p) \leq H^{pers}_{1}(x, \nabla\tilde{u}(x)) \leq 0.$$

- If $\kappa_x,\ K_x,\ A_x,\ \overrightarrow{v_x},\ \overrightarrow{w_x},\ c_x$ are continuous then H_g is continuous in $\overline{\Omega} \times \mathbb{R}^2$. Therefore as soon as the intensity image I is continuous, all SFS Hamiltonians H_*^{pers} and H_*^{orth} are continuous in $\overline{\Omega} \times \mathbb{R}^2$ (for the Hamiltonian H_{Eiko}^{orth}, I must also verify $I > 0$ on $\overline{\Omega}$).

Therefore, if the *compatibility condition* (H5) is satisfied on $\partial\Omega$ (and if the above conditions are verified), *then all the SFS problems* (PDEs with DBC) *have continuous viscosity solutions.*

3.4.2 Existence of discontinuous viscosity solutions of the SFS problems

In section 3.3.2 we have shown that the "generic" Hamiltonian H_g is a HJB Hamiltonian. Precisely we have shown that:

$$H_g(x,p) = \sup_{a \in \overline{B}_2(0,1)} \{-f_g(x,a) \cdot p - l_g(x,a)\},$$

with

$$\begin{aligned} f_g(x,a) &= -\ [\ Dil_x a + \overrightarrow{w_x}\ ], \\ l_g(x,a) &= -\ [\ K_x \kappa_x \sqrt{1-|a|^2} + \kappa_x ({}^t R_x \overrightarrow{v_x}) \cdot a + c_x]. \end{aligned} \tag{3.24}$$

Also we have:

- If κ_x, μ_x and ν_x are continuous on $\overline{\Omega}$, then Dil_x is continuous on $\overline{\Omega}$. If furthermore $\overrightarrow{w_x}$ is continuous then f_g is continuous on $\overline{\Omega} \times \overline{B}_2(0,1)$.
- If μ_x and ν_x are bounded (which is true as soon as $\overline{\Omega}$ is bounded and μ_x and ν_x are continuous on $\overline{\Omega}$) and if κ_x is Lipschitz continuous, then Dil_x is Lipschitz continuous. If furthermore $\overrightarrow{w_x}$ is Lipschitz continuous then f_g is Lipschitz continuous with respect to x with a Lipschitz constant which does not depend on $a \in \overline{B}_2(0,1)$.
- If K_x and $\overrightarrow{v_x}$ are bounded and if κ_x and c_x are Lipschitz continuous then l_g is Lipschitz continuous with respect to x (with a Lipschitz constant which does not depend on $a \in \overline{B}_2(0,1)$) and continuous on $\overline{\Omega} \times \overline{B}_2(0,1)$.
- If κ_x, μ_x, ν_x, $\overrightarrow{w_x}$, $\overrightarrow{v_x}$, μ_x, K_x and c_x are bounded on $\overline{\Omega}$ then f_g and l_g are bounded on $\overline{\Omega} \times \overline{B}_2(0,1)$.

Therefore,

- if $\overline{\Omega}$ is bounded,
- if μ_x and ν_x are continuous on $\overline{\Omega}$,
- if K_x and $\overrightarrow{v_x}$ are bounded and

- if κ_x, $\overrightarrow{w_x}$ and c_x are Lipschitz continuous

then all hypotheses (H6)-(H8) of theorem 3 are verified for the "generic" Hamiltonian H_g.

Consequently, using appendix B.1, we verify easily that as soon as the *intensity image I is Lipschitz continuous*, the hypotheses (H6)-(H8) hold for *all SFS Hamiltonians*[12]. Therefore, theorem 3 (described at page 21) applies for each modelisation of the SFS problem.

Thus, if $\varphi \in BC(\partial\Omega)$[13] then for all our SFS problems (PDEs with DBC), *there exists a discontinuous viscosity solution.*

3.5 Characterization of viscosity solutions of the SFS problems

In the previous section we have proved the existence of viscosity solutions of the Lambertian SFS problems. Nevertheless, as we will show in this section, the Lambertian SFS problems with DBC (on the boundary of the image) do not have a unique viscosity solution. For computing a numerical solution of the SFS problems, we need to choose one solution among all. To make this choice, we must characterize the solutions. Also, as Rouy and Tourin have proposed in [39], we satisfy this requirement by enlarging the DBC to the set $\partial\Omega \cup \{\, x \mid I(x) = 1 \,\}$.

3.5.1 Uniqueness results for continuous viscosity solutions

Let us recall the following standard definition:

Definition 5 *We say that there is a* maximum principle *for the Hamilton-Jacobi equation*

$$H(x, u(x), \nabla u(x)) = 0 \text{ in an open set } \Omega, \tag{3.25}$$

when we have:
"for all subsolution u and supersolution v defined on $\overline{\Omega}$, $u \leq v$ on $\partial\Omega$ involves $u \leq v$ on $\overline{\Omega}$".

Let $\varphi : \partial\Omega \to \mathbb{R}$ be a continuous function.
In the case of the *continuous* viscosity solutions, the maximum principle involves the uniqueness of the solution of the Dirichlet problem

$$\begin{cases} H(x, u(x), \nabla u(x)) = 0 \text{ on } \Omega \\ \qquad\qquad\qquad u = \varphi \text{ on } \partial\Omega. \end{cases} \tag{3.26}$$

In other words, the maximum principle ensures that there exists at most one continuous viscosity solution of equation (3.25) verifying $u = \varphi$ in $\partial\Omega$.

[12] For the Hamiltonian H^{orth}_{Eiko}, we also need to impose $I > 0$ on $\overline{\Omega}$.
[13] The compatibility conditions are no more required!

PROOF. Let u, v be two continuous viscosity solutions to the Dirichlet problem. Since for all x in $\partial\Omega$, $u(x) = v(x)$ (Dirichlet condition) and u, v are both subsolution and supersolution, the maximum principle implies that $u \leq v$ and $v \leq u$ on $\overline{\Omega}$. The conclusion follows. □

Essentially, there exists two classical uniqueness theorems for the *continuous* viscosity solutions. The first deals with the PDE(s) of the form $\lambda u(x) + H(x, \nabla u(x)) = 0$ with $\lambda > 0$. The second deals with equations of the form $H(x, \nabla u(x)) = 0$ with $H(x, p)$ convex with respect to p. The first theorem is proved in [1] (theorem II.3.1 and remark II.3.3).

Theorem 4 (uniqueness result (1)) *Let Ω be a bounded open subset of $\mathbb{R}^N$. Let us consider the Hamilton-Jacobi equation*

$$\lambda u(x) + H(x, \nabla u(x)) = 0, \qquad x \in \Omega; \qquad (\lambda > 0).$$

We assume that H satisfies

(H9) [**space variable regularity**]
There exists a nondecreasing function ω which goes to zero at zero, such that $\forall x, y \in \Omega,\ \forall p \in \mathbb{R}^N, \qquad |H(x,p) - H(y,p)| \leq \omega(|x-y|(1+|p|))$.

Then there is a maximum principle for this equation.

The second uniqueness result is due to Ishii [23] and has been proved later in a different manner by Lions [30]. For the SFS problems, this theorem is important. In effect as we have seen above, the equations provided by our formulations of the SFS problems, involve Hamiltonians which do not depend on u.

Theorem 5 (uniqueness result (2)) *Let Ω be a bounded open subset of $\mathbb{R}^N$. Let us consider the Hamilton-Jacobi equation*

$$H(x, \nabla u(x)) = 0 \qquad \forall x \in \Omega. \tag{3.27}$$

If the hypothesis (H9) *and the following hypotheses are verified:*

(H10) [p **- convexity**]
For all x in Ω, $H(x, p)$ is convex with respect to p.

(H11) [**strict subsolution**]
there exists a strict viscosity subsolution $\underline{u} \in C^1(\Omega) \cap C(\overline{\Omega})$ of (3.27) (i.e. such that $H(x, \nabla \underline{u}(x)) < 0$ for all x in Ω);

then there is a maximum principle for this equation.

For more general conditions, see [31]. A proof can be found in section II.5.3 of Bardi and Capuzzo-Dolcetta 's book [1].

These theorems apply to the SFS. In particular, by theorem 5, we can characterize the continuous viscosity solutions of the SFS problems.

Let us consider the generic Hamiltonian H_g defined in section 3.3.2. We have:

1. If we assume that κ_x, $\overrightarrow{w_x}$ and c_x are Lipschitz continuous and that K_x, D_x and $\overrightarrow{v_x}$ are bounded, then the Hamiltonian H_g verifies the regularity hypothesis (H9).
   In particular, for all the SFS Hamiltonians H_*^{orth} and H_*^{pers}, these conditions are true as soon as the intensity image I is Lipschitz continuous[14] (see appendix B).

2. H_g is convex with respect to p and therefore the hypothesis (H10) is verified for all our SFS Hamiltonians.

3. About the existence of strict viscosity subsolutions:

   - The generic Hamiltonian H_g does not have a generic strict viscosity subsolution. Nevertheless, all SFS Hamiltonians H_*^{orth} and H_*^{pers} have one.
   - Let us assume that
     $$\text{for all } x \text{ in } \Omega, \qquad I(x) < 1.$$
     Then, we have:
     - all constant functions are strict viscosity subsolutions of the Hamiltonians H_{Eiko}^{orth}, $H_{D/O}^{orth}$, H_F^{pers} and H_2^{pers}.
       In effect, all these Hamiltonians verify $H(x,0) < 0$.
     - it is easy to verify that the function
       $$\tilde{u} : \overline{\Omega} \longrightarrow \mathbb{R} : \; x \longmapsto -\frac{1}{\gamma}\, \mathbf{l} \cdot x$$
       is a strict viscosity subsolution of the Rouy-Tourin Hamiltonian $H_{R/T}^{orth}$.
     - the reader can verify that the function
       $$\tilde{u} : \overline{\Omega} \longrightarrow \mathbb{R} : \; x \longmapsto -\ln \frac{\gamma}{f} - \ln\left(\gamma\, f - \mathbf{l} \cdot x\right)$$
       is a strict viscosity subsolution of the perspective Hamiltonian H_1^{pers}
       (we need to impose $\gamma\, f - \mathbf{l} \cdot x > 0$, ie. $\mathbf{L} \cdot (x, -f) < 0$).

Thus, for all SFS Hamiltonians, as soon as the intensity image I is Lipschitz continuous and verifies
$$\forall x \in \Omega, \quad I(x) < 1,$$
all the hypotheses of theorem 5 are verified. Therefore, under these conditions, the SFS Hamiltonians H_*^{orth} and H_*^{pers} have a unique continuous viscosity solution.

[14] for the Eikonal Hamiltonian H_{Eiko}^{orth}, we also need to impose $\forall x \in \overline{\Omega},\ I(x) > 0$.

REMARK 5. To apply theorem 5, a difficulty lies in the search of a strict viscosity subsolution. To get around this difficulty, we can make a change of variables for obtaining a new Hamiltonian (with $\lambda \neq 0$) and we can try to apply theorem 4.
For example, we can consider the Eikonal equation (3.28) with f strictly positive and Lipschitz. By using the Kruzkov change of variable $v(x) = 1 - e^{-u(x)}$ (therefore $\nabla u(x) = \frac{1}{1-v(x)} \nabla v(x)$, $v(x) \geq 1$), we rewrite the Eikonal equation

$$|\nabla u(x)| = f(x) \tag{3.28}$$

as

$$v(x) + \frac{1}{f(x)} |\nabla v(x)| - 1 = 0, \tag{3.29}$$

and theorem 4 applies to (3.29).

3.5.2 uniqueness results for discontinuous viscosity solutions

The uniqueness results for the discontinuous viscosity solutions are almost the same as the uniqueness results for the continuous viscosity solutions. Nevertheless, they need stronger hypotheses; which is reasonable because discontinuous viscosity solutions are weaker solutions than continuous viscosity solutions (the set of the discontinuous viscosity solutions of a HJB equation contains the set of the continuous viscosity solutions).
Also, the consequences on the SFS problem are almost the same.

In the continuous case, the maximum principle involves the uniqueness of the solution of the Dirichlet problem. Nevertheless in the discontinuous case, to have uniqueness we need a stronger property (see section 2.2.3 of [38]):

Definition 6 *Let Ω be an open subset of $\mathbb{R}^N$, let $E \subset \overline{\Omega}$ and let F be a real function defined on $\overline{\Omega} \times \mathbb{R} \times \mathbb{R}^N$.*
We say that the strong uniqueness property holds on the set E for the equation

$$F(x, u(x), \nabla u(x)) = 0 \tag{3.30}$$

when we have:
"for all subsolution u, for all supersolution v and for all x in E, $u(x) \leq v(x)$".

We have the following strong uniqueness result:

Theorem 6 *Let Ω be an open subset of $\mathbb{R}^N$ verifying* (H12). *Let H be a continuous real function defined on $\overline{\Omega} \times \mathbb{R}^N$ and let φ be a real continuous function defined on $\partial\Omega$.*
If *H satisfies the hypotheses* (H9) *and* (H10) *of the uniqueness theorems 4 and 5, if H*

satisfies the hypothesis[15] (H11') *and if* H *satisfies the boundary hypotheses* (H13), (H14) *and* (H15) *(described below) which impose properties of* H *on* $\partial\Omega$
then *the strong uniqueness property holds on the set* Ω *for the equation*

$$F(x, u(x), \nabla u(x)) = 0 \qquad \text{for } x \in \overline{\Omega}, \tag{3.31}$$

which defines the following Dirichlet problem (in the discontinuous sense)

$$F(x, u, p) = \begin{cases} H(x,p) & \text{for } x \text{ in } \Omega, \\ u - \varphi(x) & \text{for } x \text{ in } \partial\Omega. \end{cases} \tag{3.32}$$

The hypothesis (H11') is a hypothesis slightly stronger than hypothesis (H11) of the theorem 5:

(H11') [**strict subsolution**]
there exist $\underline{u} \in C^1(\Omega) \cap C(\overline{\Omega})$ *and* $\delta < 0$ *such that for all* x *in* Ω,

$$H(x, \nabla \underline{u}(x)) < \delta.$$

The hypothesis (H12) deals with the regularity of the set Ω:

(H12) [**regularity of** Ω]
Ω *is a bounded open subset of* $\mathbb{R}^N$ *of class* $W^{2,\infty}$.

The hypotheses (H13), (H14) and (H15) are the following:
There exist a constant $C > 0$ and a neighborhood Γ of $\partial\Omega$ (ie. Γ is an open subset of $\mathbb{R}^N$ such that $\partial\Omega \subset \Gamma$) such that

(H13) [p **- regularity on** $\partial\Omega$]
There exists a function ω *which goes to zero at zero, such that*

$$\forall x \in \Gamma,\ \forall p, q \in \mathbb{R}^N,\ |H(x,p) - H(x,q)| \leq \omega(|p-q|);$$

(H14) $\forall x \in \Gamma,\ \forall p \in \mathbb{R}^N, \qquad H(x, p + \lambda\eta(x)) \leq 0 \implies \lambda \leq C(1 + |p|);$

(H15) [**directional coercivity on** $\partial\Omega$]
$\forall p \in \mathbb{R}^N, \qquad H(x, p - \lambda\eta(x)) \to +\infty$ *uniformly with respect to* x *in* Γ,
when $\lambda \to +\infty$;

(where $\eta(x)$ is the unit outward pointing normal vector to $\partial\Omega$).

PROOF OF THEOREM 6. See theorem 4.5 and more exactly of its corollary 4.1, of Barles'book [2] in the particular case where the Hamiltonian H does not depend on u. □

[15] a hypothesis slightly stronger than hypothesis (H11) of the theorem 5;

REMARKS 6.

R6.1 - Clearly, the strong uniqueness property involves the uniqueness of the discontinuous viscosity solution. Therefore, thanks to theorem 6, we can prove the uniqueness of discontinuous viscosity solutions of (3.31) in Ω. Nevertheless, generally we do not have the uniqueness in $\overline{\Omega}$! So if u and v are two solutions, then for all x in Ω, $u(x) = v(x)$; but for all x in $\partial\Omega$, $u(x)$ can be different from $v(x)$.

R6.2 - The strong uniqueness property involves the continuity of the solution (see proposition 2 of [38]).

R6.3 - Theorem 6 deals with a Hamiltonian H which does not depend of u; More general results can be found in [2].

Proposition 3 *A sufficient condition for the hypotheses* (H14) *and* (H15) *to be satisfied is:* $H(x,p)$ *coerciv in* p *uniformly with respect to* x *in* Γ, *a neighborhood of* $\partial\Omega$.

PROOF. See proposition 3 of [38]. □

As theorem 5 (uniqueness of the continuous viscosity solution), theorem 6 applies to the SFS problem. The three hypotheses (H9), (H10) and (H11') are (almost) the hypotheses of theorem 5. As in the previous section, we prove that they are verified for the SFS Hamiltonians H_*^{orth} and H_*^{pers} as soon as the intensity image is Lipschitz continuous and verifies $I < 1$ on $\overline{\Omega}$. Concerning the hypothesis (H13), we can easily prove (by computing the gradient of $H_g(x,.) : p \mapsto H_g(x,p)$) that if κ_x and $\overrightarrow{w_x}$ are bounded then $H_g(x,.)$ is Lipschitz continuous (with a Lipschitz constant which does not depend on x). Therefore (H13) is true for all SFS Hamiltonians H_*^{orth} and H_*^{pers}.
Then, thanks to proposition 3, the strong uniqueness theorem applies as soon as the considered Hamiltonian $H(x,p)$ is coercive with respect to p uniformly with respect to x *in a neighborhood of* $\partial\Omega$. In section 3.4.1 (when we apply the existence theorem 2 to the Hamiltonian H_g and later to the SFS Hamiltonians), we have described in detail the conditions for the coercivity property for the SFS Hamiltonians H_*^{pers} and H_*^{orth}.

Conclusion: If the intensity image I is Lipschitz continuous, if I verifies $I < 1$ on $\overline{\Omega}$ and if the values of I on the *boundary of the image* are such that the coercivity hypothesis holds, then there exists at most one discontinuous viscosity solution on Ω.

3.5.3 Characterization of the viscosity solutions of the SFS problem when the set $\{x \mid I(x) = 1\}$ is not empty

In practice, I can reach the value 1 in an arbitrary compact set in $\overline{\Omega}$. This implies that there does not exist a strict viscosity subsolution and *we lose uniqueness.* In [39], Rouy and Tourin characterize the loss of uniqueness of the continuous viscosity solution of the equation (3.4)

$$\begin{cases} H(x, \nabla u(x)) = 0 & \forall x \in \Omega \\ u = \varphi & \forall x \in \partial\Omega, \end{cases}$$

in the case where H is the Hamiltonian $H^{orth}_{R/T}$ and where the set $\{x \mid I(x) = 1\}$ is a set of isolated points. In their paper [31], Lions, Rouy and Tourin characterize completely the continuous viscosity solutions, in the case where the set $\{x \mid I(x) = 1\}$ is a finite union $\cup_{i=1}^{n} K_i$ of disjoint connected compact sets. Nevertheless, they only consider the particular case of the Eikonal Hamiltonian H^{orth}_{Eiko}. We generalize their result: we characterize the continuous viscosity solutions of all our SFS Hamiltonians (H^{orth}_{*} and H^{pers}_{*}); in particular we extend their work to the "perspective SFS" problem. Also, we consider the case where the set $\{ x \mid I(x) = 1 \}$ is a union of compact sets and we deal with the characterization of the discontinuous viscosity solutions of all SFS Hamiltonians.

Case of the continuous viscosity solutions

To begin with, we generalize [39, 31] (concerning the continuous viscosity solutions) to all the SFS Hamiltonians H^{orth}_{*} and H^{pers}_{*}.
First, we assume that $\{x \mid I(x) = 1\} = \{x_1, ..., x_n\}$. Let us fix n real constants $(C_i)_{i=1..n}$. For all SFS equations with Dirichlet boundary conditions,

$$\begin{cases} H(x, \nabla u(x)) = 0 & \forall x \in \Omega \\ u = \varphi & \forall x \in \partial\Omega, \end{cases}$$

there exists at most one continuous viscosity solution u such that for all $i = 1..n$, $u(x_i) = C_i$ (the various constants C_i have just to verify the compatibility conditions[16]). To prove this last assertion, we just have to enlarge the DBC to the set $\partial\Omega \cup \{ x \mid I(x) = 1 \}$ and to apply theorems 2 and 5, and the results presented in section 3.5.1. Thus, in the case where $\{x \mid I(x) = 1\} = \{x_1, ..., x_n\}$, we just have to fix the constants C_i, for characterizing a viscosity solution of the SFS problems.
Now, let us assume that $\{x \mid I(x) = 1\} = \cup_{i=1}^{n} K_i$; $(K_i)_i$ being a finite collection of disjoint connected compact sets. The main point is that, over the K_i's, the viscosity solutions are equal, up to an additive constant C_i (distinct for each K_i), to the "strict viscosity subsolution" associated with the considered Hamiltonian[17] (the strict viscosity subsolutions associated with the SFS Hamiltonians are described page 33). Therefore, if for all K_i's we fix $C_i \in \mathbb{R}$, then by section 3.5.1, there exists at most one viscosity solution u of (3.4) such

[16] See page 17
[17] An idea of the proof can be found in [31].

that $\forall x \in K_i$, $u(x) = \tilde{u}(x) + C_i$ ($\tilde{u}$ is the adequate "strict viscosity subsolution"). Thus, for characterizing a solution, we only need to specify the values of these constants for each K_i.

In other words, globally, for characterizing a SFS (viscosity) solution, we can ignore the set $\{x \mid I(x) = 1\}$ and work in the open set $\Omega' = \Omega - \{x \mid I(x) = 1\}$. Therefore, we consider the problem

$$\begin{cases} H(x, \nabla u(x)) = 0 & \forall x \in \Omega' \\ u(x) = \varphi(x) & \forall x \in \partial\Omega', \end{cases} \tag{3.33}$$

rather than (3.4). Thus, as soon as the intensity image I is Lipschitz continuous, the problem (3.33) associated to any SFS Hamiltonian has at most one continuous viscosity solution. All the continuous viscosity solutions of (3.4) are then obtained from these by choosing almost arbitrarily[18] the constants C_i.

REMARKS 7.

R7.1 - In practice, for computing a numerical solution of the SFS problem, we must characterize the solution we want to compute, first. The characterization we propose here is somewhat disappointing. In effect, it assumes that we know the values of the solution at all the critical points and on the boundary of the image. But the input data to a SFS problem consists only in general of an image. We do not have at our disposal the values of the solution at the critical points or on the boundary of the image. Nevertheless, although this may appear a bit restrictive, in this paper we will assume that we know these "boundary" data. In a forthcoming paper, we will describe how to remove this constraint.

R7.2 - Another possibility is to choose among all solutions one which possesses an extra property, as in the work of M. Falcone et al. [6, 16, 17] where the uniqueness is obtained by choosing the maximal solution. This method has been developed by F. Camilli et al. in [8, 7]. Let us emphasize that M. Falcone assumes (as we do) that the solution is known on the boundary $\partial\Omega$. Also, note that the theory used by Falcone applies only to the Eikonal equation [6, 16] and that the theory developed by Camilli in [18] applies only to Hamilton-Jacobi-Bellman equations with positive running cost[19].

Case of the discontinuous viscosity solutions

The above result does not apply directly to the discontinuous viscosity solutions of the SFS problem. The reason of this difficulty lies on the difference between the hypotheses (H11) and (H11') (hypotheses dealing with the strict subsolutions) we recall them here:

[18] Let us recall that for ensuring the existence of a continuous viscosity solution, the compatibility condition must be verified.

[19] See the definition 4 of "HJB equations".

(H11) *there exists* $\underline{u} \in C^1(\Omega) \cap C(\overline{\Omega})$ *such that for all* x *in* Ω, $H(x, \nabla \underline{u}(x)) < 0$;

(H11') *there exist* $\underline{u} \in C^1(\Omega) \cap C(\overline{\Omega})$ *and* $\delta < 0$ *such that for all* x *in* Ω, $H(x, \nabla \underline{u}(x)) < \delta$.

The uniqueness of the continuous viscosity solution only requires the hypothesis (H11) (theorem 5), when the uniqueness of the discontinuous viscosity solution requires the stronger hypothesis (H11') (theorem 6). In the first case, the hypothesis (H11) holds even if there are critical points on the boundary of Ω, whereas in the second case, the hypothesis (H11') imposes that $\forall x \in \overline{\Omega},\ I(x) < 1$; and so there are not critical points on $\partial\Omega$.

REMARK 8. It is important to notice that the hypothesis (H11') is optimal for obtaining the uniqueness of the *discontinuous* viscosity solution (the hypothesis (H11) is not sufficient). In effect, for example, although the following SFS equation verifies the hypothesis (H11) (therefore it has a unique continuous viscosity solution), it has several discontinuous viscosity solutions.

EXAMPLE : Let us consider the orthographic SFS problem, in dimension 1, with a vertical light direction. Let I be the intensity image obtained from the C^1 surface v represented in figure 3.3. Let us note that v and I are defined on $[0,1]$, that for all x in $]0,1]$, we have

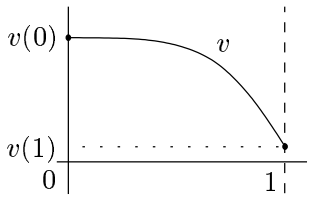

Figure 3.3: A surface with a critical point at the boundary.

$0 < I(x) < 1$, and that 0 is a critical point ($I(0) = 1$). Clearly, v is the unique continuous viscosity solution of

$$\begin{cases} H^{orth}_{Eiko}(x, \nabla u) = 0, & \forall x \in]0,1[, \\ u(0) = v(0) \quad \text{and} \quad & u(1) = v(1); \end{cases} \tag{3.34}$$

but there exist several discontinuous viscosity solutions. In effect, the continuous viscosity solutions of all the equations

$$\begin{cases} H^{orth}_{Eiko}(x, \nabla u) = 0, & \forall x \in]0,1[, \\ u(0) = u_0 \quad \text{and} \quad & u(1) = v(1), \end{cases}$$

where $u_0 \leq v(0)$, are discontinous viscosity solutions of (3.34). Some examples of discontinuous viscosity solutions of (3.34) are shown in figure 3.4.

PROOF.
For all x in $]0,1]$, there are not difficulties.
For $x = 0$:

- $u(0)$ is always inferior to $v(0)$ then the subsolution property[20] always holds;
- since $I(0) = 1$, then for all test functions ϕ, we have $H^{orth}_{Eiko}(0, \nabla\phi(0)) \geq 0$. Therefore the supersolution property holds at the point 0.

□

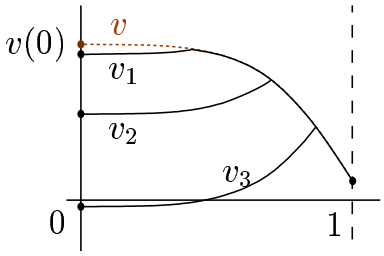

Figure 3.4: Examples of some discontinous viscosity solutions when there exists a critical point on the boundary.

As a matter of fact, this limitation is not really a problem. In effect, before we have assumed that we know the values of the solution at all the critical points of the image. Also it is not more absurd to assume that we know the values of the solution on an extremely small neighbourhood of the set the critical points. Thus for characterizing a discontinuous viscosity solution, we can specify the values of this solution on the boundary of the image and in a neighbourhood of its critical points.

[20] In the discontinuous sense, the subsolution property at a point x_0 in $\partial\Omega$ is:
- $H(x_0, \nabla\phi(x_0)) \leq 0$, where ϕ is an adequate test function;

or
- $u(x_0) \leq \varphi(x_0)$, where φ is the boundary condition.

3.6 Noise robustness of the viscosity solutions of SFS

Viscosity solutions also enjoy important stability properties.
Let $(v_\varepsilon)_{\varepsilon>0}$ be a sequence of uniformly locally bounded functions defined on $\overline{\Omega}$. Let us define the two functions $\overline{v}$ and $\underline{v}$:

Definition 7 $\forall x \in \overline{\Omega}$,

$$\overline{v}(x) = \limsup_{\substack{\varepsilon \to 0,\\ y \to x}} v_\varepsilon(y)$$

$$\underline{v}(x) = \liminf_{\substack{\varepsilon \to 0,\\ y \to x}} v_\varepsilon(y)$$

We have the theorem (see Barles' book [2]):

Theorem 7 (Stability of viscosity solutions) *Let F_ε be a sequence of uniformly locally bounded functions on $\overline{\Omega} \times \mathbb{R} \times \mathbb{R}^N$ (Ω being a open set of $\mathbb{R}^N$). Let us suppose that for all $\varepsilon > 0$, u_ε is a subsolution (respectively a supersolution) of F_ε on $\overline{\Omega}$ and that the functions u_ε are uniformly locally bounded on $\overline{\Omega}$.*
Then

$$\overline{v}(x) = \limsup_{\substack{\varepsilon \to 0,\\ y \to x}} v_\varepsilon(y) \qquad \textit{(respectively } \underline{v}(x) = \liminf_{\substack{\varepsilon \to 0,\\ y \to x}} v_\varepsilon(y)\textit{)}$$

is a subsolution (a supersolution, respectively) of the equation

$$\underline{F}(x, u(x), \nabla u(x)) = 0 \text{ on } \overline{\Omega} \qquad \textit{(respectively } \overline{F}(x, u(x), \nabla u(x)) = 0 \text{ on } \overline{\Omega}\textit{)};$$

where $\underline{F}(X) = \liminf_{\substack{\varepsilon \to 0,\\ Y \to X}} F_\varepsilon(Y)$ *($X, Y \in \overline{\Omega} \times \mathbb{R} \times \mathbb{R}^N$)*
($\overline{F}(X) = \limsup_{\substack{\varepsilon \to 0,\\ Y \to X}} F_\varepsilon(Y)$, respectively).

When the strong uniqueness property is true the previous result yields:

Corollary 1 *Let $F : \overline{\Omega} \times \mathbb{R} \times \mathbb{R}^N \to \mathbb{R}$ be a locally bounded function verifying the strong uniqueness property on Ω (see definition 6). Let $(F_\varepsilon)_{\varepsilon>0}$ be a sequence of functions such that*

$$F_\varepsilon \underset{\varepsilon \to 0}{\longrightarrow} F$$

locally uniformly with respect to the other variables. Let u_ε be uniformly locally bounded functions such that for all $\varepsilon > 0$, u_ε is a solution *(in the discontinuous sense) of*

$$F_\varepsilon(x, u, \nabla u) = 0 \text{ on } \overline{\Omega}.$$

Then, when ε vanishes to zero, the sequence u_ε converges on Ω toward a function u which is equal to the discontinuous viscosity solution of $F(x, u, \nabla u) = 0$ on Ω.

In computer vision or more generally in image processing, the images are always corrupted by noise. It is therefore very important to design schemes and algorithms *robust* to noise. That is to say we would like that the result obtained by the algorithm from a noisy image be close to the ideal result obtained from the perfect image. This property is often difficult to guarantee.

For the "SFS" problem, the robustness is mathematically expressed by the continuity of the application which, given an image I, returns the associated surface u. In other words, we would like that, for all sequences of noisy images I_ε uniformly converging toward an image I, the sequence of recovered solutions u_ε uniformly converges toward the solution u associated to I.

In the research report [38], section 4.1.3, we have applied corollary 1 to the Hamiltonian $H^{orth}_{R/T}$ associated to the orthographic SFS problem. Thus, we have proved that if the intensity image I verifies $I(x) < 1$ for all x in $\overline{\Omega}$, then the viscosity solutions (of this SFS problem) are robust to noise.
This also applies to the other SFS Hamiltonians H^{orth}_* and H^{pers}_*. In effect, the reader will verify that the proof proposed for the orthographic case can be easily adapted to the generic Hamiltonian.

3.7 SFS with discontinuous images; shadows

The reader has most probably noticed that the existence theorems 2 and 3, and the uniqueness theorems 4 and 5 require regularity of the Hamiltonians with respect to the space variable x. For the SFS Hamiltonians, these regularity hypotheses impose to take intensity functions I which are *Lipschitz continuous*.
Let us emphasize that this limitation is very constraining; in effect, generally, edges, black shadows and occluding boundaries involve discontinuities. Therefore the *theoretical part* of our method (based on the notion of the viscosity solutions) cannot deal with such singularities, yet[21].

Nevertheless, as we will see in the following chapters, the *numerical method* we propose does not require such a regularity of the intensity function I. In effect, we prove that our schemes are stable (see remark R16.4 page 53 and the remark at the end of section 5.1) and that our algorithms converge even when the image I is discontinuous (see section 6.2.3). Also, in practice, our algorithms produce suitable numerical solutions even when the input image has some black shadows and some edges (see section 7).

[21] Most probably, ongoing work will shortly allow to extend the theory to discontinuous Hamiltonians in the space variables. See the work of Ostrov [26, 32], the work of Soravia [40] or the work of A. Siconolfi and F. Camilli (Talk at the TMR conference entitled "Eikonal equations with measurable dependence on the state variable" [6th-8th march 2002, in Tours, France]; article to appear.) which only deals with the Eikonal case.

Chapter 4

Monotonous approximation schemes of the form $S(\rho, x, u^\rho(x), u^\rho) = 0$; Two examples for HJB equations

In the previous chapters, we have shown that the Lambertian SFS problems lead to solving HJB equations with Dirichlet boundary conditions. In this chapter, we present some schemes for approximating the viscosity solutions of the HJB equations, thereby allowing to solve numerically the SFS equations. Despite the fact that for SFS problems we only need the two-dimensional case, we consider the general case.

4.1 Approximation schemes

In this section, we remind the reader of the definition of an approximation scheme. An approximation scheme is a functional equation of the form

$$T(\rho, x, u^\rho) = 0 \qquad \forall x \in \overline{\Omega};$$

where $T : \mathcal{M} \times \overline{\Omega} \times B(\overline{\Omega}) \to \mathbb{R}$, $\mathcal{M} = (\mathbb{R}^+)^N$, $N \in \mathbb{N}^*$ and $B(D)$ is the space of bounded functions defined on a set D.
$\rho \in \mathcal{M}$ defines the size of the mesh that is used in the corresponding numerical algorithms, see chapter 6, u^ρ is a solution of the scheme T. When $N > 1$, we write $\rho = (h_1, .., h_N)$; $(h_i \in \mathbb{R}^+)$. If $h_1 = h_2 = ... = h_N$, we let $\rho = h_i \in \mathbb{R}^+$. Also, we (mis)use the notation "$\forall \rho > 0$" which stands for "$\forall \rho \in \mathcal{M}$ such that $\forall i \in 1, .., N,\ h_i > 0$".

Following [3], we introduce the representations S of a scheme T as as

$$S(\rho, x, u^\rho(x), u^\rho) = 0 \qquad \forall x \in \overline{\Omega},$$

where

$$\begin{array}{rccc} S: & \mathcal{M} \times \overline{\Omega} \times \mathbb{R} \times B(\overline{\Omega}) & \longrightarrow & \mathbb{R} \\ & (\rho, x, t, u) & \longmapsto & S(\rho, x, t, u). \end{array}$$

Note that a representation of a scheme is also a scheme. It is in effect a way to simplify computations, see below. For example, suppose we want to approximate a function u such that its directional derivative in the direction $\overrightarrow{v}$ at point x is equal to $\lambda(x)$. We can use the following scheme $S(\rho, x, u(x), u) = 0$ in $\mathbb{R}^N$:

$$S(\rho, x, t, u) = \frac{u(x + \rho\overrightarrow{v}) - t}{\rho} - \lambda(x).$$

REMARK 9. For a scheme $T(\rho, x, u^\rho) = 0$, we can come up with various representations $S : \mathcal{M} \times \overline{\Omega} \times \mathbb{R} \times B(\overline{\Omega}) \to \mathbb{R}$ such that $S(\rho, x, u(x), u) = T(\rho, x, u)$.
For example, we can take

$$S_1(\rho, x, t, u) = T(\rho, x, u),$$

or

$$S_2(\rho, x, t, u) = u(x) + T(\rho, x, u) \ - t \ , \text{ etc.}$$

In the sequel, we will see that the choice of the representation S implies some important differences in the corresponding numerical algorithm. It also influences greatly the complexity of the proofs of stability and convergence, see sections 4.3 and 4.4.
In the SFS problem, the open set Ω is bounded. In practice, we generally consider the rectangular domain $]0, X[\times]0, Y[$ of $\mathbb{R}^2$. Since we are considering HJB equations with Dirichlet boundary conditions, we consider "schemes with Dirichlet conditions"; these schemes are defined by $S(\rho, x, u^\rho(x), u^\rho) = 0$, where S is defined by

$$S(\rho, x, t, u) = \begin{cases} \tilde{S}(\rho, x, t, u) & \text{if } x \in \Omega^\rho, \\ t - \varphi(x) & \text{if } x \in \flat\Omega^\rho, \end{cases} \tag{4.1}$$

where

$$\Omega^\rho = \{x \in \Omega \mid \forall i = 1..N, \ x \pm h_i\overrightarrow{e_i} \in \overline{\Omega}\},$$

and $\flat\Omega^\rho = \overline{\Omega} - \Omega^\rho$. Since φ is defined only on $\partial\Omega$, we assume in (4.1) that we have extended it continuously to $\flat\Omega^\rho$. We now introduce the

Definition 8 (monotonicity) *The scheme $S(\rho, x, u^\rho(x), u^\rho) = 0$ defined on $\overline{\Omega}$, is monotonous if*
$\forall \rho \in \mathcal{M}, \forall x \in \overline{\Omega}, \forall t \in \mathbb{R}$ *and* $\forall u, v \in B(\overline{\Omega})$,

$$u \leq v \quad \Longrightarrow \quad S(\rho, x, t, u) \geq S(\rho, x, t, v)$$

(that is to say: the scheme is nonincreasing with respect to u)

There exists essentially only one method for proving the convergence of the solutions of schemes toward viscosity solutions, i.e. the one presented by Barles and Souganidis in [3]. This method requires the monotonicity of the scheme; this is why we design monotonous schemes in the sequel.

REMARK 10. The representation of a scheme $T(\rho, x, u^\rho) = 0$ by a scheme of the form $S(\rho, x, u^\rho(x), u^\rho) = 0$ is not innocent. In particular, this formulation suggests an iterative algorithm for computing a numerical approximation of the solution of the scheme. Given u^n (the approximation of u^ρ at step n), and a point x of Ω^ρ, the associated algorithm consists in solving the equation

$$S(\rho, x_n, t, u^n) = 0 \tag{4.2}$$

with respect to t. A solution of (4.2) is the updated value of u^n at x (see chapter 6). When this solution can be obtained explicitely we talk about explicit schemes, when it cannot, we talk about implicit schemes, see next section.

4.2 Decentered schemes for HJB equations

4.2.1 An "implicit" decentered scheme

We first introduce the following notations:

NOTATION. Given a function $g : B \to \mathbb{R}$, we denote

$$g_+ : \begin{array}{ccc} B & \to & \mathbb{R} \\ x & \mapsto & \left\{ \begin{array}{ll} g(x) & \text{if } g(x) > 0, \\ 0 & \text{otherwise;} \end{array} \right. \end{array} \qquad g_- : \begin{array}{ccc} B & \to & \mathbb{R} \\ x & \mapsto & \left\{ \begin{array}{ll} -g(x) & \text{if } g(x) < 0, \\ 0 & \text{otherwise;} \end{array} \right. \end{array}$$

REMARK 11. The functions g_+ and g_- are positive.
We consider the HJB equation (3.10)

$$\lambda u(x) + \sup_{a \in A} \{-f(x,a) \cdot \nabla u(x) - l(x,a)\} = 0 \quad \forall x \in \Omega.$$

In this section, we want to design an approximation scheme of (3.10) by using only the backward and forward approximations of the partial derivatives. Thus in order to guarantee the monotonicity of the scheme, it appears natural to substitute $\partial_{\vec{e_i}} u(x)$ with $\left(\frac{t - u(x - h_i \vec{e_i})}{h_i}\right)$ when $-f_i(x,a) \geq 0$ and by $\left(\frac{u(x + h_i \vec{e_i}) - t}{h_i}\right)$ when $-f_i(x,a) \leq 0$.

We therefore consider the scheme S with $\tilde{S}$ (see equation (4.1)) defined as

$$\tilde{S}(\rho,x,t,u) = \lambda t \; + \\ \sup_{a\in A}\left\{\sum_{i=1}^{N}(f_i(x,a))_- \frac{t-u(x-h_i\overrightarrow{e_i})}{h_i} + \sum_{i=1}^{N}(f_i(x,a))_+ \frac{t-u(x+h_i\overrightarrow{e_i})}{h_i} - l(x,a)\right\}, \quad (4.3)$$

which can be rewritten as

$$\tilde{S}(\rho,x,t,u) = \lambda t \; + \\ \sup_{a\in A}\left\{t\sum_{i=1}^{N}\frac{|f_i(x,a)|}{h_i} - \sum_{i=1}^{N}\left(\frac{(f_i(x,a))_-}{h_i}u(x-h_i\overrightarrow{e_i}) + \frac{(f_i(x,a))_+}{h_i}u(x+h_i\overrightarrow{e_i})\right) - l(x,a)\right\}. \quad (4.4)$$

We note $s_i(x,a)$ the sign of $f_i(x,a)$ and obtain

$$\begin{aligned}\tilde{S}(\rho,x,t,u) = \lambda t \; + \; & \sup_{a\in A}\left\{\sum_{i=1}^{N} f_i(x,a)\frac{t-u(x+s_i(x,a)h_i\overrightarrow{e_i})}{s_i(x,a)h_i} - l(x,a)\right\} \\ = \lambda t \; + \; & \sup_{a\in A}\left\{\sum_{i=1}^{N}(-f_i(x,a))\frac{t-u(x+s_i(x,a)h_i\overrightarrow{e_i})}{-s_i(x,a)h_i} - l(x,a)\right\}. \quad (4.5)\end{aligned}$$

The scheme (4.3) is clearly nondecreasing with respect to t and nonincreasing with respect to u. Let us emphasize the fact that the scheme S with $\tilde{S}$ defined by (4.3) is monotonous. Also in section 4.3.2, we prove that this scheme is stable under some mild conditions. Since the variable t appears inside the sup operator, the scheme is implicit (see remark 4.1).

4.2.2 A "Semi implicit" decentered scheme

A classical method to deal with the implicit scheme (4.3) consists in transforming the scheme into a fixed point problem. We multiply $\tilde{S}$ by a fictitious time increment $-\Delta\tau$ (with $\Delta\tau > 0$) and we add $u^\rho(x)$ to both sides of the equation $\tilde{S} = 0$.
In other words, instead of considering the scheme defined by $\tilde{S}(\rho,x,t,u)$, we consider the one defined by the function

$$\hat{S}(\rho,x,t,u) = t - u(x) + \Delta\tau\tilde{S}(\rho,x,u(x),u).$$

For the sake of simplicity, we write s_i for $s_i(x,a)$ in the sequel. Thus we obtain a new formulation of the scheme $S(\rho,x,u^\rho(x),u^\rho) = 0$ by defining

$$\tilde{S}_2(\rho,x,t,u) = t(1+\lambda\Delta\tau) - u(x) \\ + \; \Delta\tau\sup_{a\in A}\left\{\sum_{i=1}^{N} -f_i(x,a)\frac{u(x)-u(x+s_ih_i\overrightarrow{e_i})}{-s_ih_i} - l(x,a)\right\}, \quad (4.6)$$

or, equivalently,

$$\tilde{S}_3(\rho,x,t,u) = t \; + \; \frac{1}{1+\lambda\Delta\tau} \sup_{a\in A}\left\{ -\left(1-\Delta\tau\sum_{i=1}^{N}\frac{|f_i(x,a)|}{h_i}\right)u(x) - \Delta\tau\sum_{i=1}^{N}\frac{|f_i(x,a)|}{h_i}u(x+s_ih_i\overrightarrow{e_i}) - \Delta\tau l(x,a)\right\}. \tag{4.7}$$

Note that $\hat{S}(\rho,x,t,u)$ is nondecreasing with respect to t and nonincreasing with respect to u as soon as the function $t \mapsto -t + \Delta\tau\tilde{S}(\rho,x,t,u)$ is nonincreasing. Also, we can verify easily that the scheme associated to (4.6) and (4.7) is monotonous iff $\Delta\tau$ is small enought ($\Delta\tau \leq \left(\sum_{i=1}^{N}\frac{|f_i(x,a)|}{h_i}\right)^{-1}$, for all a in A and for all x such that $f(x,a)\neq 0$; if $f(x,a)=0$, then no constraints are required). In other words, this formulation of the decentered schemes requires that some conditions be satisfied in order to be monotonous. Despite this disadvantage, the formulation (4.6) or (4.7) is interesting because it yields *semi implicit* algorithms whereas the formulation (4.3) provides *totally implicit* algorithms. We use the expression "semi implicit" because the value of the sup has to be evaluated at each point x, but it does not involve t. Nevertheless in SFS problems, we will see that the algorithms resulting from the formulation (4.3) can be made explicit through the use of calculus.

REMARKS 12.

R12.1 - Let us mention that the larger the "parameter" $\Delta\tau$, the faster the convergence. Therefore, if $f(x,a_0)\neq 0$ (where a_0 is the optimal control of (4.6)), we can choose an optimal $\Delta\tau$:

$$\Delta\tau_{opt} = \left(\sum_{i=1}^{N}\frac{|f_i(x,a_0)|}{h_i}\right)^{-1},$$

where a_0 is the optimal control of (4.6).

Let us remark that a_0 and the optimal $\Delta\tau_{opt}$ depend on x, but that a_0 does not depend on $\Delta\tau$.

Thus, for all x such that $f(x,a_0)\neq 0$, if we choose $\Delta\tau=\Delta\tau_{opt}$, the scheme (4.6) becomes:

$$\tilde{S}_2^{opt}(\rho,x,t,u) = \; (1+\frac{\lambda}{\sum_{j=1}^{N}|f_j(x,a_0)|/h_j})\; t - \sum_{i=1}^{N}\frac{|f_i(x,a_0)|/h_i}{\sum_{j=1}^{N}|f_j(x,a_0)|/h_j}\; u(x+s_ih_i\overrightarrow{e_i}) - \; \frac{1}{\sum_{j=1}^{N}|f_j(x,a_0)|/h_j}\; l(x,a_0),$$

where a_0 is the optimal control of (4.6).

For x such that $f(x, a_0) = 0$,

$$\tilde{S}_2(\rho, x, t, u) = t - \frac{u(x)}{1 + \lambda\Delta\tau} - \frac{\Delta\tau}{1 + \lambda\Delta\tau} l(x, a_0).$$

Therefore, for such an x, if $\lambda \neq 0$ then the optimal (semi-implicit) scheme is

$$\tilde{S}_2^{opt}(\rho, x, t, u) = t - \frac{1}{\lambda} l(x, a_0).$$

If $\lambda = 0$ and $f(x, a_0) = 0$, there no exist optimal $\Delta\tau$. In this case the scheme is

$$\tilde{S}_2(\rho, x, t, u) = t - u(x) - \Delta\tau l(x, a_0).$$

R12.2 - Let us emphasize that the schemes defined with (4.6) have exactly the same solutions as the schemes defined with (4.3).

4.3 Stability of the approximation schemes

Definition 9 (stability) *The scheme $T(\rho, x, u^\rho) = 0$ defined on $\overline{\Omega}$, is stable if $\forall \rho > 0$, it has a solution $u^\rho \in B(\overline{\Omega})$.*

REMARK 13. The stability of a scheme requires the existence of a solution but not its uniqueness.

Definition 10 (uniform stability) *The scheme $T(\rho, x, u^\rho) = 0$ defined on $\overline{\Omega}$, is uniformly stable if it is stable and if its solutions u^ρ are bounded independently of ρ.*

In this section, we consider finite difference schemes. Thus for all schemes $S(\rho, x, u^\rho(x), u^\rho) = 0$, we suppose:

(H16) *For all x fixed in $\overline{\Omega}$ and for all fixed $\rho > 0$, there exists a* finite *"neighbourhood" noted $\mathcal{V}_x^\rho$ of x such that $S_{\rho,x,t}(u) := S(\rho, x, t, u)$ does not depend on all the values of the function u but only on the values it takes at points $y \in \mathcal{V}_x^\rho$.*
In other words, we can rewrite $S(\rho, x, t, u)$ as $\breve{S}(\rho, x, t, (u(y))_{y \in \mathcal{V}_x^\rho})$.

Let us emphasize the fact that in the previous definition, $\mathcal{V}_x^\rho$ is a finite set.

REMARK 14. Note that *a scheme (4.6) is (uniformly) stable iff the associated scheme*

(4.3) is (uniformly) stable.

REMARK 15. The hypothesis (H16) applies to finite difference schemes based on regular meshes as well as to finite difference schemes based on unstructured meshes.
There exists only two main methods for proving the stability of a scheme, they use

1. the monotonicity,
2. fixed point theorems.

4.3.1 Stability of monotonous schemes

We need the definition of a subsolution of a scheme.

Definition 11 (subsolution of an approximation scheme)
For a fixed $\rho > 0$, $v^\rho : \overline{\Omega} \to \mathbb{R}$ is a subsolution of the scheme $S(\rho, x, u^\rho(x), u^\rho) = 0$ if $\forall x \in \overline{\Omega}$, $S(\rho, x, v^\rho(x), v^\rho) \leq 0$.

The stability theorem 8 is based on the monotonicity.

Theorem 8 (Stability of monotonous schemes) *Let us consider a finite difference scheme*

$$S(\rho, x, u^\rho(x), u^\rho) = 0, \qquad \forall x \in \overline{\Omega}. \tag{4.8}$$

We suppose that the scheme (4.8) verifies (H16) *and the following hypotheses:*

(H17) $\forall \rho > 0, x \in \overline{\Omega}, u \in B(\overline{\Omega})$, *the function $S_{\rho,x,u} : t \mapsto S(\rho, x, t, u)$ is continuous, nondecreasing and $lim_{t\to+\infty} S_{\rho,x,u}(t) \geq 0$.*

(H18) *The scheme is monotonous (see definition 8).*

(H19) $\forall \rho > 0$, $x \in \overline{\Omega}$, *the function $\breve{S}_{\rho,x}$ is continuous with respect to $\left(t, (u(y))_{y\in\mathcal{V}_x^\rho}\right)$ (we denote $\breve{S}_{\rho,x}(.,.) := \breve{S}(\rho, x, ., .)$ where $\breve{S}$ is defined in the hypothesis* (H16)*).*

(H20) $\forall \rho > 0$, *there exists a subsolution of the scheme (4.8).*

(H21) $\forall \rho > 0$, *there exists $M^\rho \in \mathbb{R}$ such that for all subsolutions v^ρ of (4.8), $\forall x \in \overline{\Omega}$, $v^\rho(x) \leq M^\rho$.*

Then the scheme (4.8) is stable.

PROOF OF THEOREM 8. The idea of the proof is the following:
ρ being fixed, we construct a nondecreasing sequence of functions u_n such that for all x of $\overline{\Omega}$,

$$S(\rho, x, u_n(x), u_n) \leq 0.$$

In other words, we construct a nondecreasing sequence of subsolutions of the scheme (4.8). By the hypothesis (H21), this sequence is upper bounded therefore convergent. We note u^ρ its limit. For all x in $\overline{\Omega}$, the sequence u_n is constructed such that $S(\rho, x, u_n(x), u_{n-1})$ is zero. Thus by an argument of continuity, we prove that the limit u^ρ of the sequence u_n is a solution of the scheme (4.8).

Let us now fix $\rho > 0$.

1. Recursive construction of the sequence of functions $(u_n)_{n\in\mathbb{N}}$:

   (a) Let u_0 be a subsolution of the scheme (4.8) (see hypothesis (H20)).

   (b) Let us suppose that we have constructed the first n elements $(u_k)_{k=0..n-1}$ of our sequence such that:

   $$\forall k \in [0..n-2], \quad u_{k+1} \geq u_k,$$

   and $\forall k \in [0..n-1]$,

   $$\forall x \in \overline{\Omega}, \quad S(\rho, x, u_k(x), u_k) \leq 0.$$

   - We now construct u_n:
     $\forall x \in \overline{\Omega}$, $u_n(x)$ is chosen in such a way that

     $$S(\rho, x, u_n(x), u_{n-1}) = 0. \tag{4.9}$$

     Note that this is always possible, by hypothesis (H17). In effect, we know that

     $$S(\rho, x, u_{n-1}(x), u_{n-1}) \leq 0;$$

     and

     $$\lim_{t\to+\infty} S(\rho, x, t, u_{n-1}) \geq 0.$$

     So the "intermediate values" theorem applied to the continuous function $t \mapsto S(\rho, x, t, u_{n-1})$ allows us to conclude.
   - By (H17), the function $t \mapsto S(\rho, x, t, u_{n-1})$ is nondecreasing. Then $\forall x \in \overline{\Omega}$, $u_n(x) \geq u_{n-1}(x)$. Therefore

     $$u_n \geq u_{n-1} \text{ on } \overline{\Omega}.$$

   - Finally, u_n is a subsolution of the scheme (4.8):
     By the monotonicity of the scheme (hypothesis (H18)), we have $S(\rho, x, u_n(x), u_n) \leq S(\rho, x, u_n(x), u_{n-1})$. The property (4.9) allows to conlude that

     $$\forall x \in \overline{\Omega}, \quad S(\rho, x, u_n(x), u_n) \leq 0.$$

   Thus we have constructed a nondecreasing sequence $(u_n)_{n\geq 0}$ of subsolutions of the scheme (4.8).

2. Convergence and properties of the limit:
   The functions u_n are subsolutions of the scheme; then the hypothesis (H21) implies that they are upper bounded. Being nondecreasing and upper bounded, the sequence $(u_n)_{n\geq 0}$ converges toward a limit. We note this limit u^ρ.
   Let us fix x in $\overline{\Omega}$. Obviously, $\forall y \in \mathcal{V}_x^\rho$, $u_n(y) \xrightarrow[n\to+\infty]{} u^\rho(y)$. Since $\mathcal{V}_x^\rho$ is finite, then we have clearly by hypothesis (H19):

$$\lim_{n\to+\infty} S(\rho, x, u_n(x), u_{n-1}) = S(\rho, x, u^\rho(x), u^\rho).$$

   Moreover, for all $n > 0$, we have $S(\rho, x, u_n(x), u_{n-1}) = 0$. Therefore, $S(\rho, x, u^\rho(x), u^\rho) = 0$. u^ρ is a solution of the scheme (4.8). Also, we have clearly $u^\rho \leq M^\rho$.

□

REMARKS 16.

R16.1 - By replacing the hypothesis (H21) by (H22)

(H22) *There exists $M \in \mathbb{R}$ such that for all $\rho > 0$, all subsolutions of (4.8) are upper bounded by M,*

we have the uniform stability of the scheme.

R16.2 - *Jacobi and Gauss-Seidel methods*:
In the proof of theorem 8, we construct a sequence $(u_n)_{n\geq 0}$ of subsolutions by using an *update at all points x of $\overline{\Omega}$*: i.e., $\forall x \in \overline{\Omega}$, $u_n(x)$ is chosen in such a way that $S(\rho, x, u_n(x), u_{n-1}) = 0$. As an alternative, we can update the sequence only on part of $\overline{\Omega}$.

For example, suppose that $\overline{\Omega}$ is a bounded set and let us pave the set $\overline{\Omega}$ with $h_1 \times \cdots \times h_N$ boxes (or subsets thereof), see figure 4.1. We order the boxes lexicographically as $P^1, ..., P^q$; since $\overline{\Omega}$ is bounded this is possible with a finite number of boxes. We impose that the subsets $P^1, ..., P^q$ form a partition of $\overline{\Omega}$ (the partition is non unique). We define the infinite periodic sequence $(P_n)_{n\in\mathbb{N}}$ by $P_n = P^i$, where $i \equiv n\ [q]$.
For updating the sequel $(u_n)_{n\geq 0}$, we can use the box P_n:

$$\begin{cases} \forall x \in \overline{\Omega} - P_n, & \text{let } u_n(x) = u_{n-1}(x) \\ \forall x \in P_n, & u_n(x) \text{ is chosen in such a way that } S(\rho, x, u_n(x), u_{n-1}) = 0. \end{cases}$$

As above, we prove that the sequence $(u_n)_{n\geq 0}$ is a nondecreasing sequence of subsolutions of the scheme (4.8). Let us fix $x \in \overline{\Omega}$ and denote n_x the integer such that $n_x \in [1..q]$ and $x \in P^{n_x}$. For all n in $\mathbb{N}$ such that $n \equiv n_x\ (q)$, we have $S(\rho, x, u_n(x), u_{n-1}) = 0$. Thus,

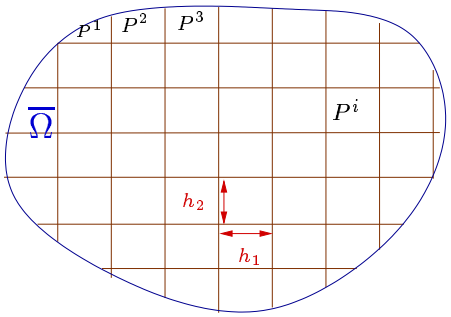

Figure 4.1: Partition of $\overline{\Omega}$ in dimension 2.

as above, by (H19), the sequence $(u_n)_{n\geq 0}$ converges toward a solution of the considered scheme.

From a theoretical point of view we gain nothing. Nevertheless, from an algorithmic point of view, this remark is very interesting. In effect, numerically, for approximating the solution of the scheme (4.8), we compute the sequence u_n. More precisely, for a fixed ρ, we consider a mesh $\mathcal{Z}_\rho$

$$\mathcal{Z}_\rho := \overline{\Omega} \cap \left\{ x_k = \sum_{i=1..N} k_i h_i \overrightarrow{e_i}; k \in \mathbb{Z}^N \right\}$$

and we approximate $u^\rho(x_k)$ by $u_n(x_k)$.

Thus, the sequence u_n designed in the proof of theorem 8 yields *Jacobi*-type algorithms. The sequence u_n constructed in this remark yields *Gauss-Seidel*-type algorithms. In both cases, we prove the convergence of the algorithms. Finally, let us emphasize that if, mathematically, the "Jacobi method" is "better" than the "Gauss-Seidel method" in the sense that it is more elegant, nevertheless numerically, the opposite is true. In effect, numerically, we call "iteration", an update of all the pixels. An iteration of the "numerical Jacobi method" allows to compute the approximations $\{u_{n+1}(x_k)\}_k$ from the approximations $\{u_n(x_k)\}_k$. For the "numerical Gauss-Seidel method", an iteration allows to compute the approximations $\{u_{n+|\mathcal{Z}_\rho|}(x_k)\}_k$ from the approximations $\{u_n(x_k)\}_k$ (where $|\mathcal{Z}_\rho|$ is the cardinal number of the set $\mathcal{Z}_\rho$). Also, unlike the "numerical Gauss-Seidel method", during one iteration of the "numerical Jacobi method", the update of the approximation of u at the pixel x_k does not use the update of the approximation of u at the previous pixels (of the same iteration). Therefore, one iteration of the "numerical Gauss-Seidel method" is more effective than one iteration of the "numerical Jacobi method".

R16.3 - In theorem 8, we can replace hypotheses (H17),(H20) and (H21) by hypotheses (H17'), (H20') and (H21')

(H17') $\forall \rho > 0, x \in \overline{\Omega}, u \in B(\overline{\Omega})$, the function $S_{\rho,x,u} : t \mapsto S(\rho, x, t, u)$ is continuous, nondecreasing and $lim_{t \to -\infty} S_{\rho,x,u}(t) \leq 0$.

(H20') $\forall \rho > 0$, there exists a supersolution of the scheme (4.8) (v^ρ is a supersolution of the scheme $S(\rho, x, u^\rho(x), u^\rho) = 0$ if $\forall x \in \overline{\Omega}, \quad S(\rho, x, v^\rho(x), v^\rho) \geq 0$).

(H21') $\forall \rho > 0$, there exists $M^\rho \in \mathbb{R}$ such that for all supersolutions v^ρ of (4.8), $\forall x \in \overline{\Omega}$, $v^\rho(x) \geq M^\rho$.

In this case, the sequence u_n we design is a nonincreasing sequence of supersolutions of the scheme (4.8).
The interest of this remark appears in practice. In effect it allows to prove the convergence of the algorithms with initial surfaces U_0 which are supersolutions. Also, the number of iterations required to obtain the convergence is much smaller when U_0 is a supersolution than when U_0 is a subsolution; see chapters 7 and 6.

R16.4 - Let us emphasize that theorem 8 does not impose regularity hypotheses with respect to the space variable x.

4.3.2 Stability of the implicit decentered schemes (4.3)

In this section, we prove the stability of the "scheme with Dirichlet conditions"

$$S(\rho, x, u^\rho(x), u^\rho) = 0$$

with S defined by

$$S(\rho, x, t, u) = \begin{cases} \tilde{S}(\rho, x, t, u) & \text{if } x \in \Omega^\rho, \\ t - \varphi(x) & \text{if } x \in \flat\Omega^\rho. \end{cases} \tag{4.10}$$

and $\tilde{S}$ defined by (see section 4.2)

$$\tilde{S}(\rho, x, t, u) = \lambda t + \sup_{a \in A} \left\{ \sum_{i=1}^{N} (f_i(x,a))_- \frac{t - u(x - h_i \overrightarrow{e_i})}{h_i} + \sum_{i=1}^{N} (f_i(x,a))_+ \frac{t - u(x + h_i \overrightarrow{e_i})}{h_i} - l(x,a) \right\}, \tag{4.11}$$

which can be rewritten as $\tilde{S}(\rho, x, t, u) = \lambda t +$

$$\sup_{a \in A} \left\{ t \sum_{i=1}^{N} \frac{|f_i(x,a)|}{h_i} - \sum_{i=1}^{N} \left(\frac{(f_i(x,a))_-}{h_i} u(x - h_i \overrightarrow{e_i}) + \frac{(f_i(x,a))_+}{h_i} u(x + h_i \overrightarrow{e_i}) \right) - l(x,a) \right\}. \tag{4.12}$$

A stability result based on subsolutions

Proposition 4 *Consider the scheme S described in (4.10) with $\tilde{S}$ defined by (4.11). Suppose that for all x in $\overline{\Omega}$, the functions $f(x,.) : a \mapsto f(x,a)$ and $l(x,.) : a \mapsto l(x,a)$ verify the hypotheses* (H6'), (H7') *and* (H23) *(descrided below). Suppose also that $\forall \rho > 0$, there exists a subsolution of the scheme S and that there exists $M^\rho \in \mathbb{R}$ such that for all subsolutions v^ρ of S, $\forall x \in \overline{\Omega}$, $v^\rho(x) \leq M^\rho$. Then the scheme S is stable.*
Also, if $M^\rho \equiv M \in \mathbb{R}$ does not depend on ρ then the stability is uniform.

(H6') *A is a compact topological space;*

(H7') *$f : A \to \mathbb{R}^N$ is continuous;*
$l : A \to \mathbb{R}$ is continuous and bounded.

(H23) *For all $x \in \Omega$, we have:*
there exists $a_x \in A$ such that $f(x, a_x) \neq 0$.

REMARKS 17.

R17.1 - Let us remind the reader that the (uniform) stability of an implicit decentered scheme given by (4.10) implies the (uniform) stability of the associated semi implicit scheme (4.6).

R17.2 - Proposition 4 holds for $\lambda \neq 0$ and $\lambda = 0$.

R17.3 - The difficulty for proving the stability of an implicit decentered scheme given by (4.10) lies in the proof of the existence of subsolutions and in the proof that the subsolutions are bounded. In the next subsection, we present some results for dealing with the HJB equation with null interest rate ($\lambda = 0$).

R17.4 - The hypotheses (H6') and (H7') do not impose regularity of f and l with respect to the space variable x.
Therefore, proposition 4 does not require the regularity with respect to x, to be applied.

NOTATION. Let B be a set. For a function

$$g : \begin{array}{ccc} B & \to & \mathbb{R}^N \\ x & \mapsto & (g_1(x), ..., g_i(x), ..., g_N(x)) \end{array} ,$$

we define

$$g_+ : \begin{array}{ccc} B & \to & \mathbb{R}^N \\ x & \mapsto & (g_{1+}(x), ..., g_{N+}(x)) \end{array} \quad \text{and} \quad g_- : \begin{array}{ccc} B & \to & \mathbb{R}^N \\ x & \mapsto & (g_{1-}(x), .., g_{N-}(x)) \end{array} .$$

Lemma 2 *Let $f : A \to \mathbb{R}^N$ and $l : A \to \mathbb{R}$ be such that the hypotheses* (H6') *and* (H7') *are verified. Then the function*

$$H(p) = \sup_{a \in A} \{-f(a) \cdot p - l(a)\}$$

is continuous.

PROOF. See lemma III.2.11 of Bardi and Capuzzo-Dolcetta 's book [1]. □

Lemma 3 *Let $f : A \to \mathbb{R}^N$ and $l : A \to \mathbb{R}$ be such that the hypotheses* (H6') *and* (H7') *are verified. Let*

$$\overline{f} : \begin{array}{ccc} A & \to & \mathbb{R}^{2N} \\ a & \mapsto & \begin{pmatrix} f(a)_+ \\ f(a)_- \end{pmatrix} \end{array}$$

and

$$\overline{H} : \begin{array}{ccc} \mathbb{R}^N \times \mathbb{R}^N & \to & \mathbb{R} \\ (p,q) & \mapsto & \sup_{a \in A} \left\{ -\overline{f}(a) \cdot \begin{pmatrix} p \\ q \end{pmatrix} - l(a) \right\} \end{array}$$

Then $\overline{H}$ is continuous.

PROOF. Since the hypotheses (H6') and (H7') hold for f, they also hold for $\overline{f}$, and lemma 2 applies to $\overline{H}$. □

Lemma 4 *Let S be defined by (4.10) with $\tilde{S}$ defined by (4.11). For all $\rho > 0$, $x \in \overline{\Omega}$ and $u : \overline{\Omega} \to \mathbb{R}$, the function $S_{\rho,x,u} : \mathbb{R} \to \mathbb{R} : t \mapsto S(\rho, x, t, u)$ is nondecreasing. If the hypothesis* (H23) *holds, then $\lim_{t \to +\infty} S_{\rho,x,u}(t) \geq 0$. Moreover if for all x in $\overline{\Omega}$, the functions $f(x,.) : a \mapsto f(x,a)$ and $l(x,.) : a \mapsto l(x,a)$ verify the hypotheses* (H6') *and* (H7'), *then the functions $S_{\rho,x,u}$ and $\breve{S}_{\rho,x}$ are continuous.*

PROOF. For $x \in \flat\Omega^\rho$, the result is obvious.
Let us fix x in Ω^ρ. We have $S_{\rho,x,u} = \tilde{S}_{\rho,x,u}$.
Since λ and $\sum_{i=1}^N \frac{|f_i(x,a)|}{h_i}$ are positive, the formulation (4.12) implies that $\tilde{S}_{\rho,x,u}$ is nondecreasing. Because of hypothesis (H23) there exists $a_x \in A$ such that $f(x,a_x) \neq 0$, therefore $\sum_{i=1}^N \frac{|f_i(x,a_x)|}{h_i} > 0$. By using the formulation (4.12), we have

$$\tilde{S}_{\rho,x,u}(t) \geq \left(\lambda + \sum_{i=1}^N \frac{|f_i(x,a_x)|}{h_i}\right) \; t \; + F(x,a_x)$$

where

$$F(x,a_x) = -\sum_{i=1}^N \left(\frac{(f_i(x,a_x))_-}{h_i} u(x - h_i\overrightarrow{e_i}) + \frac{(f_i(x,a_x))_+}{h_i} u(x + h_i\overrightarrow{e_i}) \right) - l(x,a_x).$$

Therefore $\lim_{t\to+\infty} \tilde{S}_{\rho,x,u}(t) = +\infty$.
By lemma 3, $\overline{H}$ is continuous. Let us fix $\rho > 0$ and $u : \overline{\Omega} \to \mathbb{R}$. The functions p and q

$$\begin{array}{rccc} p: & \mathbb{R} & \to & \mathbb{R}^N \\ & t & \mapsto & \begin{pmatrix} \frac{t-u(x+h_1\overrightarrow{e_1})}{h_1} \\ \vdots \\ \frac{t-u(x+h_N\overrightarrow{e_N})}{h_N} \end{pmatrix} \end{array} \qquad \begin{array}{rccc} q: & \mathbb{R} & \to & \mathbb{R}^N \\ & t & \mapsto & \begin{pmatrix} \frac{t-u(x-h_1\overrightarrow{e_1})}{h_1} \\ \vdots \\ \frac{t-u(x-h_N\overrightarrow{e_N})}{h_N} \end{pmatrix} \end{array}$$

are continuous. Since $\tilde{S}_{\rho,x,u}(t) = \lambda t + \overline{H}(x,p(t),q(t))$, the function $\tilde{S}_{\rho,x,u}$ is a composition of continuous functions, hence continuous. Therefore $S_{\rho,x,u}$ is continuous.
In the same way, we prove the continuity of $\check{S}_{\rho,x}$. □

PROOF OF PROPOSITION 4. We apply theorem 8.
Clearly the hypothesis (H16) is true ($\mathcal{V}_x^\rho = \{x \pm h_i\overrightarrow{e_i},\ i = 1..N\}$). The hypotheses (H17) and (H19) are true by lemma 4. Clearly (H18) is true.
Remark R16.1 allows us to deal with the uniform stability case. □

The difficulty in applying proposition 4 lies in the proof of the existence of subsolutions. In the case $\lambda = 0$ which is true for the SFS problems, things turn out to be simpler, as shown next.

Particular case of the HJB equations with null interest rate ($\lambda = 0$)

In this section we consider an HJB equation with null interest rate.
Concerning the existence of the subsolutions of the decentered schemes with Hamiltonians H verifying $H(x,0) \leq 0$, we have the following result:

Proposition 5 *Let H be an HJB Hamiltonian with null interest rate ($\lambda = 0$), defined on $\overline{\Omega} \times \mathbb{R}^N$. Let φ be a bounded function defined on a neighbourhood of $\partial\Omega$. If for all x in $\overline{\Omega}$, $H(x,0) \leq 0$ then all constant functions u on $\overline{\Omega}$ such that $u \leq min_x \varphi(x)$, are subsolutions of the associated decentered scheme S defined by (4.10).*

PROOF. If u is a constant function, we have

- $\forall x \in \Omega^\rho$,
$$\begin{aligned} S(\rho, x, u(x), u) &= \tilde{S}(\rho, x, u, u) \\ &= \sup_{a \in A}\{-l(x,a)\} \\ &= H(x,0) \\ &\leq 0 \ . \end{aligned}$$
- $\forall x \in \flat\Omega^\rho$,
$$S(\rho, x, u(x), u) = u - \varphi(x) \leq 0.$$

□

In order to apply proposition 4, we also need to prove that all the subsolutions of the scheme S are upper bounded.

NOTATION. For $K > 0$, we denote by $\mathcal{M}_K$ the set of ρs in $\mathcal{M}$ such that

$$\max_{i=1..N} h_i \ \leq \ K \ \min_{i=1..N} h_i.$$

In particular, if we choose ρ such that $h_1 = ... = h_N$, then $\rho \in \mathcal{M}_1$.

Proposition 6 *Consider an implicit decentered scheme S defined by (4.10) with $\lambda = 0$. Assume that Ω is a bounded open subset of $\mathbb{R}^N$.*
We suppose that for all x in $\overline{\Omega}$, there exists a control $a_x \in A$ such that for all $i = 1..N$, the sign of $f_i(x, a_x)$ does not depend on x. For $i = 1..N$, we denote by s_i the sign of $f_i(x, a_x)$. Also, let us suppose that there exists $\varepsilon > 0$ and j in $[1..N]$ such that $\forall x \in \overline{\Omega}$, $s_j f_j(x, a_x) \geq \varepsilon$. If l and φ are upper bounded (on $\overline{\Omega} \times A$ and on a neighbourhood of $\partial\Omega$) then all the subsolutions of S are upper bounded.
Also, for all $K > 0$, there exists $\mathtt{B}_K > 0$ such that $\forall \rho \in \mathcal{M}_K, \forall v_\rho$ subsolution of S, we have $v_\rho \leq \mathtt{B}_K$.

PROOF. Let v be a subsolution of the scheme S. By definition, for all $x \in \overline{\Omega}$,

$$S(\rho, x, v(x), v) \leq 0. \tag{4.13}$$

For all x in $\flat\Omega^\rho$, (4.13) implies $v(x) \leq \varphi(x)$. Thus for all x in $\flat\Omega^\rho$, $v(x) \leq \max \varphi$.
For all x in Ω^ρ, (4.13) implies

$$\sup_{a \in A} \left\{ \sum_{i=1}^{N} sign(f_i(x,a)) f_i(x,a) \frac{v(x) - v(x + sign(f_i(x,a)) h_i \overrightarrow{e_i})}{h_i} - l(x,a) \right\} \leq 0.$$

In particular,

$$\sum_{i=1}^{N} s_i f_i(x, a_x) \frac{v(x) - v(x + s_i h_i \overrightarrow{e_i})}{h_i} - l(x, a_x) \leq 0.$$

Let us note $w_i(x)$ the quantity $\frac{s_i f_i(x,a_x)}{h_i}$. We have

$$v(x) \sum_{i=1}^{N} w_i(x) \ \leq \ l(x, a_x) + \sum_{i=1}^{N} \ w_i(x) \ v(x + s_i h_i \overrightarrow{e_i}).$$

Therefore, by considering L, an upper bound of l, we have:

$$v(x) \leq \frac{L}{\sum_{k=1}^{N} w_k(x)} + \sum_{i=1}^{N} \frac{w_i(x)}{\sum_{k=1}^{N} w_k(x)} v(x + s_i h_i \overrightarrow{e_i});$$

Since $\sum_{k=1}^{N} w_k(x) \geq w_j(x) \geq \frac{\varepsilon}{h_j}$, then

$$v(x) \leq \frac{L h_j}{\varepsilon} + \sum_{i=1}^{N} \frac{w_i(x)}{\sum_{k=1}^{N} w_k(x)} v(x + s_i h_i \overrightarrow{e_i}).$$

We notice that $\sum_{i=1}^{N} \frac{w_i(x)}{\sum_{k=1}^{N} w_k(x)} \ v(x + s_i h_i \overrightarrow{e_i})$ is a barycentric combination of the $\{v(x + s_i h_i \overrightarrow{e_i})\}_{i=1..N}$, therefore

$$v(x) \leq \frac{L}{\varepsilon} h_j + \max_{i=1..N} v(x + s_i h_i \overrightarrow{e_i}).$$

Since $\overline{\Omega}$ is bounded and since $\forall i = 1..N$, s_i *does not depend on* x, then by recursivity

$$v(x) \leq (\frac{L}{\varepsilon} h_j)(\sum_{i=1}^{N} \frac{X}{h_i}) + \max_{y \in \flat\Omega^\rho} \varphi(y)$$

where $\overline{\Omega}$ is a subset of the box $[-\frac{X}{2}, \frac{X}{2}]^N$, and therefore v is bounded above. We continue with

$$v(x) \leq (\frac{L}{\varepsilon} h_j) NX \frac{1}{\min h_i} + \max \varphi,$$

$$v(x) \leq \frac{L}{\varepsilon} NX \frac{\max_i h_i}{\min_i h_i} + \max \varphi,$$

If $\rho \in \mathcal{M}_K$ (we can suppose that $K = \frac{\max_i h_i}{\min_i h_i}$), we have

$$v(x) \leq \frac{LKNX}{\varepsilon} + \max \varphi.$$

Let us denote $\mathtt{B}_K := \frac{LKNX}{\varepsilon} + \max \varphi$.
We have $v \leq \mathtt{B}_K$. □

REMARK 18. Let us emphasize that all the results described in this section (section 4.3) do not require regularity of the Hamiltonian with respect to the space variable x.

4.4 Convergence of the solutions of the approximation schemes toward the viscosity solutions

There exists basically only one method for proving the convergence of the solutions of an approximation scheme toward the viscosity solution of an Hamilton-Jacobi equation. This method, due to Barles and Souganidis [3], is based on the notion of weak limits[1].

4.4.1 Consistency of a scheme with an HJB equation and convergence of its solutions towards discontinuous viscosity solutions

We now give the definition of the *consistency* of an approximation scheme according to Barles and Souganidis [3].

[1] Other tools have been developed by F. Camilli et al.. Their work allows to approximate the "maximal" viscosity solutions of degenerate Hamilton-Jacobi equations. More precisely, in [8], F. Camilli and A. Siconolfi study and characterize the maximal solutions of a class of degenerate Hamilton-Jacobi equations with Dirichlet boundary conditions. Later on, F. Camilli and L. Grune [7] proposed a numerical approximation of the maximal solutions. In this report, we do not detail this approach. These tools have been applied to SFS problem by F. Camilli and M. Falcone [6, 16].

Remember that in the framework of discontinuous viscosity solutions, the PDE with Dirichlet boundary conditions must be rewritten as:

$$F(x, u(x), \nabla u(x)) = 0, \quad \forall x \in \overline{\Omega}; \tag{4.14}$$

where F is defined on $\overline{\Omega} \times \mathbb{R} \times \mathbb{R}^N$ by

$$F(x,u,p) = \begin{cases} H(x,u,p) & \text{for } x \text{ in } \Omega, \\ u(x) - \varphi(x) & \text{for } x \text{ on } \partial\Omega. \end{cases} \tag{4.15}$$

Definition 12 (consistency) *The scheme $S(\rho, x, u^\rho(x), u^\rho) = 0$ defined on $\overline{\Omega}$, is consistent with equation (4.14) if :*
$\forall x \in \overline{\Omega}$ *et* $\forall \phi \in C_b^\infty(\overline{\Omega})$

$$\limsup_{\rho \to 0,\ y \to x,\ \xi \to 0} \frac{S(\rho, y, \phi(y) + \xi, \phi + \xi)}{\rho} \leq F^*(x, \phi(x), \nabla\phi(x)),$$

and

$$\liminf_{\rho \to 0,\ y \to x,\ \xi \to 0} \frac{S(\rho, y, \phi(y) + \xi, \phi + \xi)}{\rho} \geq F_*(x, \phi(x), \nabla\phi(x)).$$

F^* and F_* are defined on page 19. In the sequel, we suppose that $\rho \in \mathbb{R}$. In other words we suppose that $\rho = h_1 = ... = h_N$.
Let us recall the definitions of the functions $\overline{u}$ and $\underline{u}$:

Definition 13 $\forall x \in \overline{\Omega}$,

$$\overline{u}(x) = \limsup_{\substack{\rho \to 0, \\ y \to x,\ y \text{ in } \overline{\Omega}}} u^\rho(y)$$

$$\underline{u}(x) = \liminf_{\substack{\rho \to 0, \\ y \to x,\ y \text{ in } \overline{\Omega}}} u^\rho(y)$$

With these definitions in hand we can now formulate the following theorem:

Theorem 9 *If an approximation scheme S is monotonous, uniformly stable and consistent with equation (4.14) then $\overline{u}$ and $\underline{u}$ are respectively viscosity subsolution and supersolution of this equation.*

PROOF. See theorem 2.1 of [3]. □

Thus, as soon as we have a strong uniqueness property (definition 6 on page 34, a proof of the convergence follows:

Theorem 10 (convergence toward the viscosity solution) *Let S be a monotonous, uniformly stable and consistent (with equation (4.14)) approximation scheme. Let us suppose that the strong uniqueness property is verified on a subset D of $\overline{\Omega}$. Then the solutions u^ρ of the scheme S converge on D toward the viscosity solution of (4.14) when $\rho \to 0$.*

PROOF. By theorem 9, the functions $\overline{u}$ and $\underline{u}$ are respectively viscosity subsolution and supersolution of the PDE (4.14). The strong uniqueness property involves $\overline{u} \leq \underline{u}$ on D. By definition, we have $\underline{u} \leq \overline{u}$, and hence:

$$\overline{u} = \underline{u} \quad (\text{ on } D).$$

For all $x \in D$, we now know that the limit $\lim_{\rho \to 0} u^\rho(x)$ exists and is equal to $u(x) := \overline{u}(x)$ (which is also equal to $\underline{u}(x)$). Finally, let v be a viscosity solution of (4.14). By definition 3, v^* and v_* is a subsolution and a supersolution, respectively; so the strong uniqueness property involves:

$$\forall x \in D, \quad \overline{u}(x) \leq v_*(x) \leq v^*(x) \leq \underline{u}(x)$$

Therefore $u = v_* = v^* = v$ on D and $\lim_{\rho \to 0} u^\rho(x) = v(x)$. □

REMARK 19. Note that despite the fact that we do not have uniqueness of the viscosity solution on $\overline{\Omega}$, we have it within D. Hence all viscosity solutions coincide on D.

4.4.2 Application to the decentered schemes

Theorem 10 applies to the implicit decentered schemes S (presented in section 4.2)

$$S(\rho, x, t, u) = \begin{cases} \tilde{S}(\rho, x, t, u) & \text{if } x \in \Omega^\rho, \\ t - \varphi(x) & \text{if } x \in \flat\Omega^\rho, \end{cases} \tag{4.16}$$

where $\tilde{S}$ is defined by

$$\tilde{S}(\rho, x, t, u) = \lambda t \; + \; \sup_{a \in A} \left\{ \sum_{i=1}^{N} (f_i(x,a))_- \frac{t - u(x - \rho \overrightarrow{e_i})}{\rho} + \sum_{i=1}^{N} (f_i(x,a))_+ \frac{t - u(x + \rho \overrightarrow{e_i})}{\rho} - l(x,a) \right\}.$$

It also applies to HJB equations, $\forall x \in \overline{\Omega}$, $F(x, u(x), \nabla u(x)) = 0$, where F is defined by

$$F(x, u, p) = \begin{cases} \lambda u + \sup_{a \in A} \{-f(x,a) \cdot p - l(x,a)\} & \text{if } x \in \Omega, \\ u - \varphi(x) & \text{if } x \in \partial\Omega. \end{cases} \tag{4.17}$$

In effect, we have following proposition:

Proposition 7 (consistency of the decentered schemes with HJB equations) *Let $f : \overline{\Omega} \times A \to \mathbb{R}^N$ and $l : \overline{\Omega} \times A \to \mathbb{R}$ be two functions such that the hypotheses* (H6)-(H8) *are verified. Then the scheme $S(\rho, x, u^\rho(x), u^\rho) = 0$ with*

$$S(\rho, x, t, u) = \begin{cases} \tilde{S}(\rho, x, t, u) & \text{if } x \in \Omega^\rho, \\ t - \varphi(x) & \text{if } x \in \flat\Omega^\rho. \end{cases}$$

$\tilde{S}$, defined by (4.3):

$$\tilde{S}(\rho, x, t, u) = \lambda t \; + \sup_{a \in A} \left\{ \sum_{i=1}^{N} (f_i(x,a))_- \frac{t - u(x - h_i \overrightarrow{e_i})}{h_i} + \sum_{i=1}^{N} (f_i(x,a))_+ \frac{t - u(x + h_i \overrightarrow{e_i})}{h_i} - l(x,a) \right\},$$

is consistent with the HJB equation

$$\forall x \in \overline{\Omega}, \qquad F(x, u(x), \nabla u(x)) = 0, \tag{4.18}$$

where F is defined by

$$F(x,u,p) = \begin{cases} \lambda u + \sup_{a \in A} \{-f(x,a) \cdot p - l(x,a)\} & \text{if } x \in \Omega, \\ u - \varphi(x) & \text{if } x \in \partial\Omega. \end{cases}$$

The proof of proposition 7 needs the following lemmas:

Lemma 5 *Let $f : \overline{\Omega} \times A \to \mathbb{R}^N$ and $l : \overline{\Omega} \times A \to \mathbb{R}$ be such that the hypotheses* (H6)-(H8) *are verified. Then the function*

$$H(x,p) = \sup_{a \in A} \{-f(x,a) \cdot p - l(x,a)\}$$

is continuous.

PROOF. See lemma III.2.11 of Bardi and Capuzzo-Dolcetta 's book [1]. □

Lemma 6 *Let $f : \overline{\Omega} \times A \to \mathbb{R}^N$ and $l : \overline{\Omega} \times A \to \mathbb{R}$ be such that the hypotheses* (H6)-(H8) *are verified. Let*

$$\begin{array}{rccc} \overline{f} : & \overline{\Omega} \times A & \to & \mathbb{R}^{2N} \\ & (x,a) & \mapsto & \begin{pmatrix} f(x,a)_+ \\ f(x,a)_- \end{pmatrix} \end{array}$$

and

$$\begin{array}{rccc} \overline{H} : & \overline{\Omega} \times \mathbb{R}^N \times \mathbb{R}^N & \to & \mathbb{R} \\ & (x,p,q) & \mapsto & \sup_{a \in A} \left\{ -\overline{f}(x,a) \cdot \begin{pmatrix} p \\ q \end{pmatrix} - l(x,a) \right\} \end{array}$$

Then $\overline{H}$ is continuous.

PROOF. See proof of lemma 3. □

PROOF OF 7. Instead of considering the scheme

$$S(\rho, x, u^\rho(x), u^\rho) = 0 \qquad \text{in } \overline{\Omega},$$

we consider the scheme

$$S'(\rho, x, u^\rho(x), u^\rho) = 0 \qquad \text{in } \overline{\Omega},$$

such that

$$S'(\rho, x, t, u) = \rho S(\rho, x, t, u).$$

Monotonicity, stability and solutions are exactly the same for both schemes.
We prove that S' is consistent with equation (4.18), i.e.:
$\forall x \in \overline{\Omega}$ et $\forall \phi \in C_b^\infty(\overline{\Omega})$

i) $\limsup_{\rho\to 0,\ y\to x,\ \xi\to 0} \frac{S'(\rho,y,\phi(y)+\xi,\phi+\xi)}{\rho} \leq F^*(x,\phi(x),\nabla\phi(x))$,

ii) $\liminf_{\rho\to 0,\ y\to x,\ \xi\to 0} \frac{S'(\rho,y,\phi(y)+\xi,\phi+\xi)}{\rho} \geq F_*(x,\phi(x),\nabla\phi(x))$.

We only prove i), the proof of ii) being identical. We consider two cases.

1. $x \in \Omega$:
   For ρ sufficiently small and y sufficiently close to x, we have $y \in \Omega^\rho$, and

$$\frac{S'(\rho, y, \phi(y)+\xi, \phi+\xi)}{\rho} = \tilde{S}(\rho, y, \phi(y)+\xi, \phi+\xi)$$
$$= \lambda(\phi(y)+\xi) \ +$$
$$\sup_{a\in A}\left\{\sum_{i=1}^N (f_i(y,a))_- \frac{\phi(y)-\phi(y-\rho\overrightarrow{e_i})}{\rho} + \sum_{i=1}^N (f_i(y,a))_+ \frac{\phi(y)-\phi(y+\rho\overrightarrow{e_i})}{\rho} - l(y,a)\right\}.$$

   Since $\phi \in C^2$, we have

$$\lim_{\rho\to 0,\ y\to x} \frac{\phi(y)-\phi(y-\rho\overrightarrow{e_i})}{\rho} = \partial_{\overrightarrow{e_i}}\phi(x),$$

$$\lim_{\rho\to 0,\ y\to x} \frac{\phi(y)-\phi(y+\rho\overrightarrow{e_i})}{\rho} = -\partial_{\overrightarrow{e_i}}\phi(x),$$

   and the function K

$$K : (\rho, y) \mapsto \left(y, \left(\frac{\phi(y)-\phi(y-\rho\overrightarrow{e_i})}{\rho}\right)_{i=1..N}, \left(\frac{\phi(y)-\phi(y+\rho\overrightarrow{e_i})}{\rho}\right)_{i=1..N}\right)$$

is continuous on $\mathcal{M} \times \Omega$ and

$$\lim_{\rho \to 0,\ y \to x} K(\rho, y) = \left(x, \left(\partial_{\vec{e_i}} \phi(x)\right)_{i=1..N}, \left(-\partial_{\vec{e_i}} \phi(x)\right)_{i=1..N}\right).$$

Since f and l verify the hypotheses (H6)-(H8), lemma 6 involves:

$$\begin{aligned}
&\limsup_{\rho \to 0,\ y \to x,\ \xi \to 0} \tilde{S}(\rho, y, \phi(y) + \xi, \phi + \xi) \\
&= \lambda \phi(x) \ + \ \sup_{a \in A} \left\{ \sum_{i=1}^{N} (f_i(x,a))_- \, \partial_{\vec{e_i}} \phi(x) + \sum_{i=1}^{N} (f_i(x,a))_+ \, (-\partial_{\vec{e_i}} \phi(x)) - l(x,a) \right\} \\
&= \lambda \phi(x) \ + \ \sup_{a \in A} \left\{ \sum_{i=1}^{N} -f_i(x,a) \ \partial_{\vec{e_i}} \varphi(x) - l(x,a) \right\} \\
&= \lambda \phi(x) \ + \ \sup_{a \in A} \{ -f(x,a) \cdot \nabla \phi(x) - l(x,a) \} \\
&= H(x, \phi(x), \nabla \phi(x))
\end{aligned}$$

where $H(x,u,p) = \lambda u + \sup_{a \in A} \{-f(x,a) \cdot p - l(x,a)\}$.
Since x is in Ω, for all y sufficiently close to x, $F(y,u,p) = H(y,u,p)$. By continuity of H (by lemma 5), we have $F^*(x,u,p) = F(x,u,p) = H(x,u,p)$. Thus

$$\limsup_{\rho \to 0,\ y \to x,\ \xi \to 0} \frac{S'(\rho, y, \phi(y) + \xi, \phi + \xi)}{\rho} = F^*(x,u,p).$$

2. $x \in \partial\Omega$:
In the same way, by continuity of the involved functions, we have:

$$\begin{aligned}
&\limsup_{\rho \to 0,\ y \to x,\ \xi \to 0} S(\rho, y, \phi(y) + \xi, \phi(y) + \xi) \\
&= \max\left(H(x, \phi(x), \nabla \phi(x)), \phi(x) - \varphi(x)\right) \\
&= F^*(x, \phi(x), \nabla \phi(x)).
\end{aligned}$$

We deal the same way with point ii), comparing the inferior limit and F_*. Thus, the scheme S' is consistent with the equation (4.18); This ends the proof of proposition 7. □
We can now state the main result of this chapter.

Proposition 8 (convergence for the decentered schemes and HJB equations)
Consider the decentered scheme S defined by (4.16) and the associated HJB equation (4.17). Suppose that f and l verify the hypotheses (H6)-(H8).
Suppose that there exist subsolutions of the scheme S and $M \in \mathbb{R}$ such that $\forall \rho > 0$, $\forall v^\rho$ subsolution of S, $\forall x \in \overline{\Omega}$, $v^\rho(x) \leq M$. Suppose also that the strong uniqueness property is verified on a subset D of $\overline{\Omega}$.
Then the solutions u^ρ of the scheme S converge on D toward the unique restriction to D of the viscosity solutions of the HJB equation when ρ vanishes to zero.

PROOF. The monotonicity of the scheme S is clear. The uniform stability is given by proposition 4. The consistency of S with the HJB equation is given by proposition 7. Theorem 10 allows to conclude. □

REMARK 20. Since the solutions of the semi-implicit scheme (4.6) are the same as the solutions of the implicit scheme (4.10), the conclusion of proposition 8 applies also to the semi-implicit scheme.

Chapter 5

Decentered schemes for SFS

In the previous chapter, we have described approximation schemes allowing to "solve" HJB equations. In sections 4.3 and 4.4, we proved theorems and propositions which ensure the stability and the convergence (toward the viscosity solution) of these schemes.
In this chapter, we show that these results apply to SFS problems.

5.1 Stability of the Decentered schemes for SFS

In chapters 2 and 3, we show that the SFS problems lead to solving PDEs and that the associated Hamiltonians are special cases of a "generic" Hamiltonian H_g. In section 3.3.2 we proved that the "generic" Hamiltonian H_g is a HJB Hamiltonian. Therefore the implicit (and semi implicit) schemes we described in section 4.2 allow to approximate SFS PDEs. Following the notations introduced in Definition 4 (page 21), we have $\lambda = 0$, $N = 2$, and Ω is bounded.

By using proposition 4 stated on page 54, we can prove the stability of the decentered schemes with SFS Hamiltonians.

First, it is easy to verify that the generic Hamiltonian H_g verifies the hypotheses (H6') and (H7'). Also, x being fixed, we have for the "generic Hamiltonian" H_g,

$$\forall a \in A,\ f_g(x,a) = 0 \Longleftrightarrow \overrightarrow{w_x} = 0 \text{ and } \kappa_x = 0$$

(since $f_g(x,0) = 0$ involves $\overrightarrow{w_x} = 0$ because of equation (3.24) on page 30; we conclude by using the definition of Dil_x, equation (3.18) on page 24, the fact that $\mu_x \neq 0$ and $\nu_x \neq 0$).
Therefore the hypothesis (H23) is true iff for all x in $\overline{\Omega}$, $\kappa_x \neq 0$ or $\overrightarrow{w_x} \neq 0$.
For $H^{orth}_{R/T}$ and $H^{orth}_{D/O}$, we have $\overrightarrow{w_x} = \mathrm{l}$, therefore, if $\mathrm{l} \neq 0$ then the hypothesis (H23) holds ($I(x)$ can be null). In the case where $\mathrm{l} = 0$, the hypothesis (H23) holds iff $I(x) \neq 0$.
For H^{orth}_{Eiko} and H^{pers}_{F}, the hypothesis (H23) holds iff $I(x) \neq 0$.
For H^{pers}_{1}, $\overrightarrow{w_x} = 0$ iff $x = -\frac{f}{\gamma}\mathrm{l}$. Therefore the hypothesis (H23) holds iff $I(-\frac{f}{\gamma}\mathrm{l}) \neq 0$.

REMARK 21. In practice, for H^{orth}_{Eiko} and H^{pers}_{F}, and for H^{pers}_{1}, H^{pers}_{2}, $H^{orth}_{R/T}$ and $H^{orth}_{D/O}$ with $\mathrm{l} = 0$, there are no shadows, therefore, $I(x)$ is never null.

Second, since the intensity image I verifies $I(x) \leq 1$, proposition 5 applies to the SFS Hamiltonians H^{orth}_{Eiko}, $H^{orth}_{(0,0,1)}$, H^{pers}_{F}, $H^{pers}_{(0,0,1)}$, $H^{orth}_{D/O}$ and H^{pers}_{2}. Thus for these SFS Hamiltonians, the associated decentered schemes (4.10) have subsolutions.
Concerning the Hamiltonian $H^{orth}_{R/T}$, we prove that $u_0(x) := -\frac{1}{\gamma}\,\mathrm{l}\cdot x + C$ (where C is chosen such that $\forall x \in \overline{\Omega}$, $u_0(x) \leq \min_x \varphi(x)$) is a subsolution of the associated decentered scheme (4.10).

PROOF.

- $\forall x \in \Omega^\rho$, we have $S(\rho, x, u_0(x), u_0) = \tilde{S}(\rho, x, u_0(x), u_0)$.
  Since
  $$\frac{u_0(x) - u_0(x - h_1\overrightarrow{e_1})}{h_1} = -\frac{\alpha}{\gamma}, \qquad \frac{u_0(x) - u_0(x + h_1\overrightarrow{e_1})}{h_1} = \frac{\alpha}{\gamma},$$
  $$\frac{u_0(x) - u_0(x - h_2\overrightarrow{e_2})}{h_2} = -\frac{\beta}{\gamma}, \qquad \frac{u_0(x) - u_0(x + h_2\overrightarrow{e_2})}{h_2} = \frac{\beta}{\gamma};$$
  then
  $$\begin{aligned} S(\rho, x, u_0(x), u_0) &= \sup_{a\in A} f(x,a)\cdot \tfrac{1}{\gamma}\mathrm{l} - l(x,a) \\ &= H(x, -\tfrac{1}{\gamma}\mathrm{l}) \\ &\leq 0. \end{aligned}$$
- $\forall x \in \flat\Omega^\rho$,
  $$S(\rho, x, u_0(x), u_0) = u_0(x) - \varphi(x) \leq 0.$$

□

We have not found subsolutions of the decentered scheme (4.10) associated with the Hamiltonian H^{pers}_{1}. The viscosity subsolution proposed in section 3.5.1 is not a subsolution the decentered scheme (4.10). This shows the interest of the Hamiltonian H^{pers}_{2}, and more generally the interest of the Hamiltonians which verify $H(x, 0) \leq 0$.

Third, if κ_x, K_x, $\overrightarrow{v_x}$ and c_x are bounded then the running cost l_g of H_g is bounded. Moreover, if, for all x in $\overline{\Omega}$, we consider [1] $a_x = Dil_x^{-1}\left[\begin{pmatrix} 1 \\ 1 \end{pmatrix} - \overrightarrow{w_x}\right]$, then we have $f_g(x, a_x) = -\begin{pmatrix} 1 \\ 1 \end{pmatrix}$. Therefore proposition 6 (page 58) applies with the generic Hamiltonian H_g. Hence the subsolutions are bounded by a same constant (uniformly for ρ in $\mathcal{M}_K$).

[1] We assume that $\forall x \in \overline{\Omega}\ \kappa_x \neq 0$

The reader will also easily verify that proposition 6 applies with all SFS Hamiltonians H_*^{orth} and H_*^{pers} [2].

Consequently, proposition 4 applies with all SFS Hamiltonians[3]. Therefore, for all SFS Hamiltonians, the implicit (and therefore semi-implicit) decentered schemes are stable (uniformly for ρ in $\mathcal{M}_K$).

REMARK 22. **SFS with discontinuous images and shadows:**
Let us emphasize that the continuity of the intensity image I is not required for obtaining the stability of our SFS schemes. Therefore our numerical SFS method is still relevant when the intensity image is discontinuous and when there are shadows.

5.2 Convergence toward the viscosity solutions of SFS

In the previous section we have described some sufficient conditions ensuring the stability of the implicit schemes (and therefore of the semi-implicit schemes) associated with the SFS Hamiltonians. In other words, the SFS schemes we propose have uniformly bounded solutions. Now, we claim that (with some weak hypotheses) these solutions converge towards the viscosity solutions of the SFS PDEs when the size of the mesh vanishes to zero. This assertion can be proved easily by using proposition 8:

1. If the intensity image I is Lipschitz continuous then hypotheses (H6)-(H8) are verified for all the SFS Hamiltonians[4]: see section 3.4.2 in which we detail the conditions for which the generic Hamiltonian H_g verifies the hypotheses (H6)-(H8).

2. Questions about subsolutions have also been studied in the previous section.

3. Some conditions involving the strong uniqueness property for the SFS equations are described at the end of section 3.5.2.

The reader will conclude without difficulty.

[2] $\forall x \in \overline{\Omega}, I(x) \neq 0$
[3] except for H_1^{pers}, because we have not found subsolutions of the associated scheme.
[4] For the Hamiltonian H_{Eiko}^{orth}, we also need to impose $I > 0$ on $\overline{\Omega}$. In practice, this is not a problem; see the remark below.

Chapter 6

Numerical algorithm associated with a monotonous scheme of the form $S(\rho, x, u^\rho(x), u^\rho) = 0$; Some new SFS algorithms

6.1 Numerical algorithm for monotonous schemes of the form $S(\rho, x, u^\rho(x), u^\rho) = 0$;

In section 4, we considered monotonous schemes of the form $S(\rho, x, u^\rho(x), u^\rho) = 0$. Theorem 8 describes sufficient conditions ensuring the stability of such schemes. Later, theorem 10 establishes that the strong uniqueness property involves the convergence of the solutions u^ρ toward the unique viscosity solution of the associated equation. We are now going to describe an algorithm that computes an approximation of u^ρ, for each value of $\rho > 0$. We also prove the convergence of our algorithm. It is important to keep in mind that this algorithm converges toward u^ρ but not toward the viscosity solution.

For a fixed $\rho > 0$, let us denote

- $x_k = \begin{pmatrix} k_1 h_1 \\ \vdots \\ k_N h_N \end{pmatrix}$ for k in $\mathbb{Z}^N$,
- $Q := \{k \in \mathbb{Z}^N \text{ such that } x_k \in \overline{\Omega}\}$.

We call "pixel" a point x_k in $\overline{\Omega}$. We suppose that $\overline{\Omega}$ is bounded; therefore the number of pixels is finite. The following algorithm computes for all $k \in Q$ a sequence of approximations U_k^n of $u^\rho(x_k)$:

Algorithm 1 *1. Initialisation ($n = 0$):*

$$\forall k \in Q, \qquad U_k^0 = u_0(x_k),$$

where u_0 is a subsolution of the considered scheme.

2. Choice of a pixel x_k and modification (step $n+1$) of U_k^n: We choose

$$U^{n+1} = \sup \{V = (V_l)_{l \in Q} \text{ such that } \forall l \neq k, \quad V_l = U_l^n \quad \text{and} \quad S(\rho, x_k, V_k, V) = 0\}.$$

In other words, we choose U^{n+1} such that

$$\left\{ \begin{array}{l} U_l^{n+1} = U_l^n \quad \text{if} \quad l \neq k, \\ U_k^{n+1} = \max \{\ t \mid S(\rho, x_k, t, U^n) = 0\ \}. \end{array} \right.$$

3. Choose the next pixel x_k in such a way that all pixels are regularly visited and go back to 2.

Definition 14 *The algorithm 1 is* well-defined *if for all steps, the set of V's defined at step (2) of the algorithm, is not empty and bounded; in other words, if for all steps we can compute the next approximation.*

We have the following theorem:

Theorem 11 *If the hypotheses of theorem 8 are satisfied, algorithm 1 is well-defined and the constructed sequence U^n is increasing and converges when $n \longrightarrow +\infty$ towards the solution u^ρ of the considered scheme.*

PROOF. The elements of the sequence U^n are the restrictions to $\{x_k\}_{k \in Q}$ of the functions u_n introduced in the proof of the remark R16.2 (page 52). □

REMARKS 23.

R23.1 - The algorithm we propose here is a Gauss-Seidel algorithm. The associated Jacobi algorithm also converges (see the proof of theorem 8), nevertheless it is less effective.

R23.2 - Let us emphasize the fact that the limit does not depend on the particular path used to traverse the pixels. Nevertheless, the convergence velocity strongly depends on this choice. For example, the strategy which consists in following back and forth the path indicated in figure 6.1 is the most effective one we have tested so far[1].

R23.3 - If hypotheses (H17'), (H20') and (H21') described in the remark R16.3 (page 52) are verified then the conclusion of theorem 11 holds even if the initial function u_0 (used at step 1 of algorithm 1) is a supersolution.

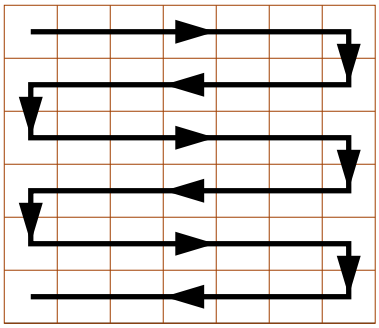

Figure 6.1: Most effective path we have tested.

6.2 New "generic" algorithms for SFS

6.2.1 Two "generic" SFS algorithms

In section 4.2 we have described two approximation schemes of the form $S(\rho, x, u^\rho(x), u^\rho) = 0$ (an implicit scheme and a semi-implicit one) allowing to approximate the solutions of HJB PDEs. Since the various models of the SFS problem we present all led to HJB equations, we have at our disposal two new approximation schemes, hence *two new algorithms* for computing numerical solutions of each formulation of the SFS problem.

We have *implemented* the algorithms associated with the implicit scheme and with the semi-implicit scheme, for the *"generic SFS" Hamiltonian.* Thus the code applies to all SFS Hamiltonians. Let us emphasize the interest of the "generic" formulation of the SFS problems. In effect, instead of implementing an algorithm for each formulation of the SFS problem, we implement only one code. In particular, a single code allows to compute numerical solutions of the "perspective SFS" problem and of the "orthographic SFS" problem.

[1] Path described by Dupuis and Oliensis in [12].

In return, our code is clearly not optimal for a particular formulation of the SFS problem. Nevertheless, it is very easy to optimize the code for a specific algorithm.

In other respects, let us remark that the implemention of the implicit algorithm is more difficult than that of the semi-implicit algorithm. Also, the cost of one iteration of the implicit scheme is greater than the cost of one iteration of the semi-implicit scheme. Nevertheless, the number of iterations required for reaching the convergence is much smaller for the implicit scheme than for the semi-implicit scheme. For a quantitative comparison see chapter 7.

REMARK 24. The algorithm proposed by Rouy and Tourin in [39] is a particular case of the implicit algorithm with the Eikonal Hamiltonian.
The first algorithm proposed by Dupuis and Oliensis in [12] is a particular case of the semi-implicit algorithm with the Hamiltonian $H_{D/O}^{orth}$ [2].
Therefore, from an algorithmic point of view, our work can be interpreted as a generalization and a unification of the work of Rouy and Tourin [39] and the work of Dupuis and Oliensis [12]. Let us remind the reader that the implicit scheme and the semi-implicit scheme have the same solutions; see remark R12.2 in section 4.2.

6.2.2 Comments about initialisation

The algorithms we propose are iterative. Also, the behaviour of the sequence of approximations U^n strongly depends on the choice of the initial surface u_0. Nevertheless, in this section, we prove that in all cases (when u_0 is a subsolution and when u_0 is a supersolution) the sequence of approximations (computed with the implicit or the semi-implicit algorithm) converges toward the solution of the scheme. Finally, we remark that the convergence velocity stongly depends on the choice of u_0.

If u_0 is a subsolution

By using theorem 11, proposition 4 and the previous chapter, the reader will verify easily that, *if u_0 is a subsolution* [3], then the numerical approximations computed with the associated *implicit* SFS algorithms converge toward the solutions of the scheme associated with the SFS Hamiltonians.
Concerning the algorithms provided by the *optimal semi-implicit scheme* (described in the

[2] In [12], Dupuis and Oliensis describe two schemes and algorithms for computing numerical solutions of the orthographic SFS problem. The first algorithm is the algorithm associated with the semi-implicit scheme applied to the Hamiltonian $H_{D/O}^{orth}$; the second algorithm is an other semi-implicit scheme based on the differential games instead of the control theory;

[3] The semi-implicit schemes and the implicit schemes have exactly the same supersolutions, the same subsolutions and the same solutions

remark R12.1 at page 47) the reader will verify without difficulty that the hypotheses of theorem 8 are satisfied with all SFS Hamiltonians:

- the hypotheses (H17) and (H18) are always true,
- the hypothesis (H19) is true if for all x in $\overline{\Omega}$, the functions $f(x,.) : a \mapsto f(x,a)$ and $l(x,.) : a \mapsto l(x,a)$ verify the hypotheses (H6') and (H7'),
- the subsolutions of the semi-implicit schemes are exactly the same as the subsolutions of the implicit schemes. Therefore, the study of the hypotheses (H20) and (H21) has been done previously.

Thereby, *if u_0 is a subsolution of the scheme*, then the numerical approximations computed with the SFS *semi-implicit* algorithms converge toward the solutions of the associated scheme.
Nevertheless, let us emphasize that in practice, the semi-implicit algorithms starting from a subsolution are really not effective.

If u_0 is a supersolution

We prove easily that the hypotheses (H20') and (H21') described in the remark R16.3 (page 49) are verified with the SFS implicit schemes and the SFS semi-implicit schemes. Therefore, if the hypothesis (H17') holds, we can conclude that:

if the initial function u_0 is a supersolution, then the numerical approximations computed with the SFS implicit / semi-implicit algorithms converge toward the solutions of the associated schemes.

Clearly, the hypothesis (H17') holds with the semi-implicit schemes. Nevertheless, (H17') is not always true with the implicit schemes. For proving that (H17') holds with a specific implicit scheme, we can use the following proposition:

Proposition 9 *Let us consider an implicit scheme S as presented in section 4.2.1. We assume that A is a compact subset of $\mathbb{R}^N$, that for all $x \in \overline{\Omega}$, the function $f(x,.) : a \mapsto f(x,a)$ is a homeomorphism (we denote $f^{-1}(x,.)$ its inverse), and that the function $l(x,.) : a \mapsto l(x,a)$ is continuous on A.*
Therefore: If $\lambda \neq 0$, then

$$\lim_{t \to -\infty} S_{p,x,u}(t) \leq 0,$$

else, if there does not exist $a \in A$ such that $f(x,a) = 0$ or if

$$l(x, f^{-1}(x,0)) \geq 0,$$

then we have the same conclusion.

REMARK 25.
Since for the "generic" Hamiltonian, we have $H_g^*(x,q) = l_g(x,[-f_g]^{-1}(x,q))$ and $f_g^{-1}(x,0) = [-f_g]^{-1}(x,0)$ (we note $[-f_g]$ the opposite of the function f_g), then the condition $l_g(x,f_g^{-1}(x,0)) \geq 0$ is equivalent to $H^*(x,0) \geq 0$.
By the previous proposition and the remark 25, for all SFS Hamiltonians such that $H(x,0) \leq 0$ (H_{Eiko}^{orth}, $H_{(0,0,1)}^{orth}$, H_F^{pers}, $H_{(0,0,1)}^{pers}$, H_2^{pers} and $H_{D/O}^{orth}$), the numerical approximations computed with an implicit algorithm converge toward the solution of the adequate scheme, when u_0 is a supersolution.
The reader will verify easily that this is also true for the Hamiltonian $H_{R/T}^{orth}$.

REMARK 26. By considering for example the Hamiltonian $H_{R/T}^{orth}$, the reader can verify that, when x converges toward a critical point x_0, then

$$\lim_{x \to x_0} l_g(x, f_g^{-1}(x,0)) = 0.$$

Thus, in a neighbourhood of such a point, the equation in t

$$S(\rho, x_{ij}, t, U) = 0 \tag{6.1}$$

is almost degenerate. In particular, if we do not implement carefully the resolving of the equation (6.1), it is possible that *numerically*, we do not obtain solutions of the equation (6.1) (even if theorically there exists a solution). In this case, instead of solving the equation (6.1), we can compute the value t which minimizes $S(\rho, x_{ij}, t, U)$. Another alternative consists in corrupting slightly the values of the intensity image, considering the image I_ε instead of I; where I_ε is the image: $I_\varepsilon(x) = I(x)$ if $I(x) > \varepsilon$, else $I_\varepsilon(x) = \varepsilon$.

REMARK 27. Let us note that, in practice, we do not compute the supersolution u_0 required for starting the algorithm. In effect a large constant function u_0 with the appropriated boundary data does the trick!

About the convergence velocity

Finally, let us remark that *in practice, the speed of convergence strongly depends on the initial surface* u_0 used at step one of the algorithm. *For an optimal velocity, we can start from a supersolution*; a quantitative comparison can be found in chapter 7.

PROOF OF PROPOSITION 9. We consider the case where $\lambda = 0$ (the case where $\lambda \neq 0$ is easier to prove). Let us assume that

$$\lim_{t\to-\infty} \sup_{a\in A} \left\{ \sum_{i=1}^{N} (-f_i(x,a)) \frac{t - u(x + s_i(x,a)h_i\overrightarrow{e_i})}{-s_i(x,a)h_i} - l(x,a) \right\} \quad > \quad 0, \tag{6.2}$$

where $s_i(x,a)$ is the sign of $f_i(x,a)$.
For all $(s_1,..,s_N) \in \{\pm 1\}^N$, we denote $A_{s_1,..,s_N} := \{a \in A \mid \forall i = 1..N,\ s_i f_i(x,a) \geq 0\}$.
By (6.2) there exists $(s_1,..,s_N) \in \{\pm 1\}^N$, such that

$$\lim_{t\to-\infty} \sup_{a\in A_{s_1,..,s_N}} \left\{ \sum_{i=1}^{N} (-f_i(x,a)) \frac{t - u(x + s_i h_i\overrightarrow{e_i})}{-s_i h_i} - l(x,a) \right\} > 0. \tag{6.3}$$

Since $f(x,.)$ and $l(x,.)$ are continuous, there exists a control a_t maximizing the supremum of (6.3). Therefore, we have

$$\lim_{t\to-\infty} \sum_{i=1}^{N} \frac{f_i(x,a_t)}{s_i h_i} (t - u(x + s_i h_i\overrightarrow{e_i})) - l(x,a_t) \quad > \quad 0.$$

We now proceed in two steps.

- Now, let us assume that there does not exist a in A such that $f(x,a) = 0$. Therefore, by compactness of $A_{s_1,..,s_N}$, there exists $\varepsilon > 0$ such that

  $$\forall a \in A_{s_1,..,s_N}, \quad \sum_{i=1}^{N} \frac{f_i(x,a)}{s_i h_i} \geq \varepsilon.$$

  Therefore, for all t sufficiently small ($t \leq \min_i u(x + s_i h_i\overrightarrow{e_i})$),

  $$\sum_{i=1}^{N} \frac{f_i(x,a_t)}{s_i h_i} (t - u(x + s_i h_i\overrightarrow{e_i})) \ \leq \ \varepsilon \left(t - \min_i u(x + s_i h_i\overrightarrow{e_i}) \right).$$

  Since $l(x,.)$ is bounded[4],

  $$\lim_{t\to-\infty} \sum_{i=1}^{N} \frac{f_i(x,a_t)}{s_i h_i} (t - u(x + s_i h_i\overrightarrow{e_i})) - l(x,a_t) \ = \ -\infty.$$

  We obtain a contradiction. Therefore if there does not exist a in A such that $f(x,a) = 0$, then

  $$\lim_{t\to-\infty} S_{p,x,u}(t) \leq 0.$$

[4] Because $l(x,.)$ is continuous on the compact set A.

◦ Henceforth, we assume that there exists a in A such that $f(x,a) = 0$. Since $l(x,.)$ is bounded and since for all $i = 1..N$, $\frac{f_i(x,a_t)}{s_i h_i}$ is positive[5], we prove easily as above that:

$$\lim_{t \to -\infty} f(x, a_t) = 0.$$

$f(x,.)$ being a homeomorphism, we obtain

$$\lim_{t \to -\infty} a_t = f^{-1}(x, 0).$$

In other respects, since

$$\lim_{t \to -\infty} \sum_{i=1}^{N} \frac{f_i(x,a_t)}{s_i h_i}(t - u(x + s_i h_i \overrightarrow{e_i})) - l(x, a_t) \; > \; 0,$$

and since for all t sufficiently small ($t \leq \min_i u(x + s_i h_i \overrightarrow{e_i})$), we have

$$\sum_{i=1}^{N} \frac{f_i(x,a_t)}{s_i h_i}(t - u(x + s_i h_i \overrightarrow{e_i})) \leq 0,$$

then

$$\lim_{t \to -\infty} -l(x, a_t) > 0.$$

By continuity of $l(x,.)$, we conclude that

$$l(x, f^{-1}(x, 0)) < 0.$$

□

[5] because a_t is in $A_{s_1,..,s_N}$;

6.2.3 SFS algorithms with discontinuous images and black shadows

All the results presented in this chapter are correct for *discontinuous images*. Also, for all intensity images, the numerical solutions computed by our algorithms always converge toward a solution of the adequate scheme. In particular, this is true in the case of black shadows, i.e. zones of 0 intensity in the image.

Let us remark that, in general, in the case where there exist shadows[6] in the image, our algorithms return approximations of the exact solutions in shading areas and return the raising light in black shadows areas; see figure 6.2.

REMARK 28. For images containing black shadows, the algorithm proposed by Falcone [17] for the "orthographic SFS" returns the same numerical solution as ours.

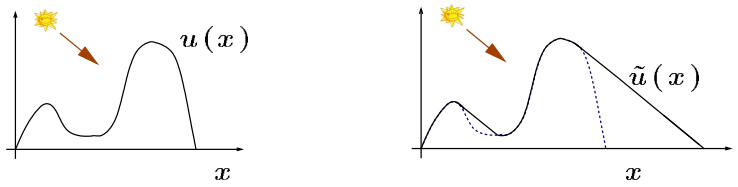

Figure 6.2: a) Original surface u; b) Solution computed by our and Falcone's algorithms [17].

[6] We assume that the critical points (of the image obtained using the irradiance equation without black shadows) and the boundary of the image are not covered by the black shadows . **Note : comment les points critiques, $I = 1$, peuvent-ils etre dans l'ombre, $I = 0$?**

Chapter 7

Experimental results

We have implemented for the **"generic Hamiltonian"** H_g the algorithms described in the previous chapter for approximating the solutions of the "schemes with Dirichlet conditions"

$$S(\rho,x,t,u) = \left\{ \begin{array}{ll} \tilde{S}(\rho,x,t,u) & \text{if } x \in \Omega^\rho, \\ t - \varphi(x) & \text{if } x \in \flat\Omega^\rho, \end{array} \right.$$

for the **implicit** decentered scheme defined by

$$\tilde{S}(\rho,x,t,u) = \sup_{a\in A} \left\{ \sum_{i=1}^{N} (f_i(x,a))_- \frac{t - u(x - h_i\overrightarrow{e_i})}{h_i} + \sum_{i=1}^{N} (f_i(x,a))_+ \frac{t - u(x + h_i\overrightarrow{e_i})}{h_i} - l(x,a) \right\},$$

and for the (optimal) **semi-implicit** decentered scheme defined by

$$\tilde{S}(\rho,x,t,u) = (1 + \frac{\lambda}{\sum_{j=1}^{N} |f_j(x,a_0)|/h_j})\ t - \sum_{i=1}^{N} \frac{|f_i(x,a_0)|/h_i}{\sum_{j=1}^{N} |f_j(x,a_0)|/h_j}\ u(x + s_i h_i \overrightarrow{e_i}) - \frac{1}{\sum_{j=1}^{N} |f_j(x,a_0)|/h_j}\ l(x,a_0),$$

where a_0 is the optimal control of (4.6); see remark 12 at page 47.

REMARK 29.

- In [37] and [38], we have implemented and tested the algorithm associated with the implicit decentered scheme for the "orthographic SFS" problem (with the Hamiltonian $H^{orth}_{R/T}$) in the case where $\mathbf{l} = (\alpha, 0)$.

- In [36], we have implemented and tested the algorithm associated with the implicit decentered scheme for the "perspective SFS" problem.

In the following subsections, we compare the results obtained with all our algorithms. This comparison is based on the speed of convergence and the reconstruction error, when the groundtruth data is available.

We start with the algorithms associated with the orthographic SFS problem. In this context, we emphasize the comparison of the implicit and semi-implicit algorithms, and the influence of the initial surface u_0 on the speed of convergence. We have tested our algorithms with synthetic images generated by shapes with several degrees of regularity e.g. C^∞ (a paraboloid, a sinusoid and a smoothed vase, see figures 7.1, 7.2, 7.14), or C^0 (a pyramid, see figures 7.3, 7.15), to demonstrate the ability of our method to work with smooth and nonsmooth objects.

Next, we deal with the perspective SFS algorithms. In particular we compare the results obtained by the orthographic SFS algorithms and the perspective SFS algorithms for synthetic perspective images.

Let us emphasize that the theory shows that we need to impose Dirichlet boundary conditions on $\partial\Omega' = \partial\Omega \cup \{x \mid I(x) = 1\}$ for characterizing a solution (see section 3.5). Therefore, in order to compute the correct solution (i.e. the original surface used for creating the image; remember that there exist several viscosity solution), we must provide the "height" of the solution at the boundary of the image and at all critical points (the pixels x_{ij} such that $I(x_{ij}) = 1$).

In all the examples, the parameters are n, the number of iterations, ε_1, ε_2 and ε_∞ the mean absolute errors between the reference and reconstructed surfaces measured according to the L_1, L_2 and L_∞ norms, respectively, θ the angle of the direction of illumination with the z-axis. We denote $\mathbf{L} = (1, \gamma)$ the light vector and f the focal length.

7.1 Experimental results for the general "orthographic SFS"

7.1.1 Comparison of the implicit algorithm and the semi-implicit algorithm

We tested the orthographic SFS algorithms (i.e. the algorithms associated with the Hamiltonians H_*^{orth}) with synthetic images generated by an orthographic projection.
In all cases, we show the original object, the input image and the reconstructed surface.

First we show that the accuracy of the implicit algorithm is approximately the same as that of the semi-implicit algorithm. This confirms the prediction of the theory which states that an implicit scheme and its associated semi-implicit scheme have the same solutions, and that the computed numerical approximations converge towards the solution of these schemes. Figures 7.1 and 7.2 show the reconstructions of smooth surfaces obtained by the implicit algorithm (associated with the Hamiltonian $H_{R/T}^{orth}$) and by the semi-implicit algorithm, starting from a subsolution and from a supersolution. Since, in practice, the combination of the semi-implicit algorithms with the subsolutions is really not effective, we only return the results obtained with the three other combinations. Also, in these three other cases, we recover almost exactly the same surface.
Contrariwise, the numbers of iterations required for converging are very different. Globally, the number of iterations required for converging with a semi-implicit algorithm is very larger than with an implicit algorithm. For example, when u_0 is a supersolution, approximately 100 iterations are required for obtaining the sinusoidal surface with the semi-implicit algorithm (figure 7.2-d), when only 20 iterations are sufficient with the implicit algorithm (figure 7.2-e). Furthermore, the number of iterations required when the approximation sequence starts from a subsolution is very larger than when it starts from a supersolution. For the example of the sinusoidal surface displayed in figure 7.2, the implicit algorithm requires approximately 600 iterations for converging when u_0 is a subsolution; when only $simeq20$ iterations are required when u_0 is a supersolution.
Clearly, the optimal algorithm is the implicit algorithm starting from a supersolution.

To demonstrate the ability of our method to deal with nonsmooth objects, we have tested our algorithms with a pyramidal surface; see figure 7.3. The previous remarks about accuracy and speed of convergence are still true for nonsmooth surfaces.

REMARKS 30.

R30.1 - In [12], Dupuis and Oliensis propose two numerical algorithms for the orthographic SFS. Their first algorithm is our semi-implicit algorithm. Their second algorithm, based on the differential games, is faster than their first one because the control dependency is

quadratic[1]The scheme associated with this original algorithm is still semi-implicit; therefore, it is "theoretically" less effective than our implicit algorithm.

R30.2 - In figures 7.1, 7.2 and 7.3, we show results obtained by applying the Gauss-Seidel method. Convergence using the Jacobi updating is much slower. As explained by Dupuis and Oliensis [12] the expected convergence time for the Jacobi method is on the order of the maximum length of the optimal path. In effect, when we perform an iteration (i.e. we once scan of all pixels) of the Jacobi method, the information is only able to propagate by "one pixel" along the optimal path. For a Gauss-Seidel method, the information is able to propagate all along the optimal path in only one iteration. Note that for obtaining convergences as fast as those we obtain, we need to use the path indicated in the remark 6.1. In effect, this path provides a homogeneous propagation [2] of the information.

Figures 7.4-7.6 show the speed of convergence of the two algorithms for two different initial conditions, i.e. a subsolution (except for the semi-implicit scheme, as mentioned above) and a supersolution. Clearly, as shown in tables 7.1-7.3, the combination (implicit, supersolution) is the best.

[1] see [12], for more details...
[2] i.e in all directions and in all senses

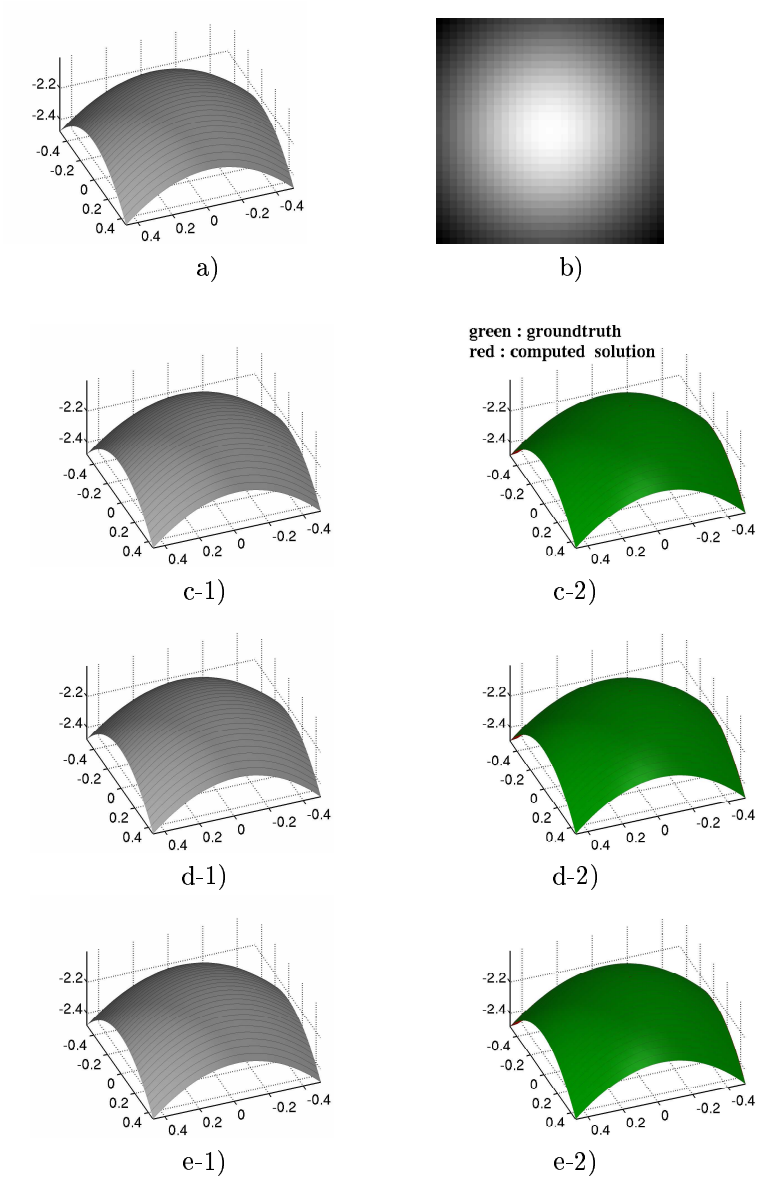

Figure 7.1: Results for a synthetic image generated by a paraboloidal surface sampled on a grid of size 32×32 with $\mathbf{l} = (0, 0)$ ($\theta \simeq 0°$):
a) original surface (groundtruth), b) original image,
c) surface reconstructed from b) with the implicit algorithm starting from a subsolution: $n = 18$, $\varepsilon_1 = 0.0015$, $\varepsilon_2 = 2.10e-05$, $\varepsilon_\infty = 0.0021$;
d) surface reconstructed from b) with the semi-implicit algorithm starting from a supersolution: $n = 15$, $\varepsilon_1 = 0.0014$, $\varepsilon_2 = 2.09e-05$, $\varepsilon_\infty = 0.0020$;
e) surface reconstructed from b) with the implicit algorithm starting from a supersolution: $n = 5$, $\varepsilon_1 = 0.0015$, $\varepsilon_2 = 2.10e-05$, $\varepsilon_\infty = 0.0020$;

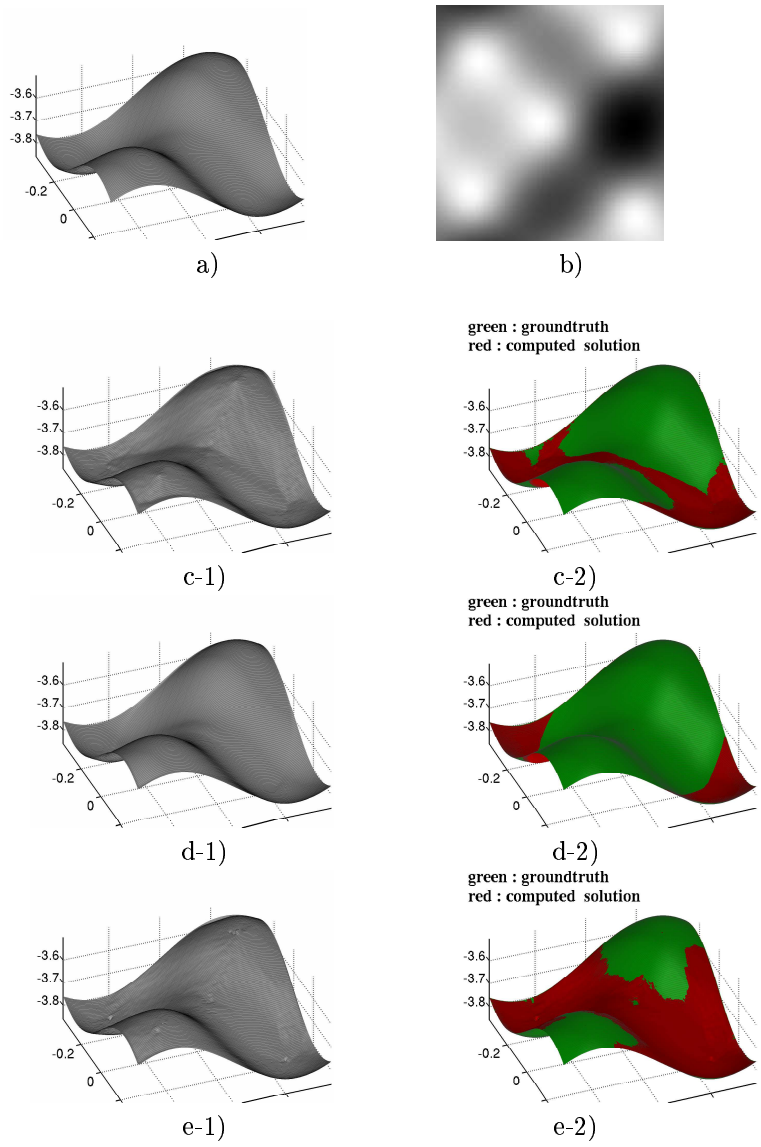

Figure 7.2: Results for a synthetic image generated by a sinusoidal surface sampled on a grid of size 200×200 with $\mathbf{l} = (0.1, 0.3)$ ($\theta \simeq 18.5°$):
a) original surface, b) original image,
c) surface reconstructed from b) with the implicit algorithm starting from a subsolution: $n \simeq 700$, $\varepsilon_1 = 0.003902$, $\varepsilon_2 = 2.881e-05$, $\varepsilon_\infty = 0.00740$;
d) surface reconstructed from b) with the semi-implicit algorithm starting from a supersolution: $n \simeq 120$, $\varepsilon_1 = 0.003900$, $\varepsilon_2 = 2.881e-05$, $\varepsilon_\infty = 0.00747$;
e) surface reconstructed from b) with the implicit algorithm starting from a supersolution: $n \simeq 25$, $\varepsilon_1 = 0.003905$, $\varepsilon_2 = 2.884e-05$, $\varepsilon_\infty = 0.00747$;

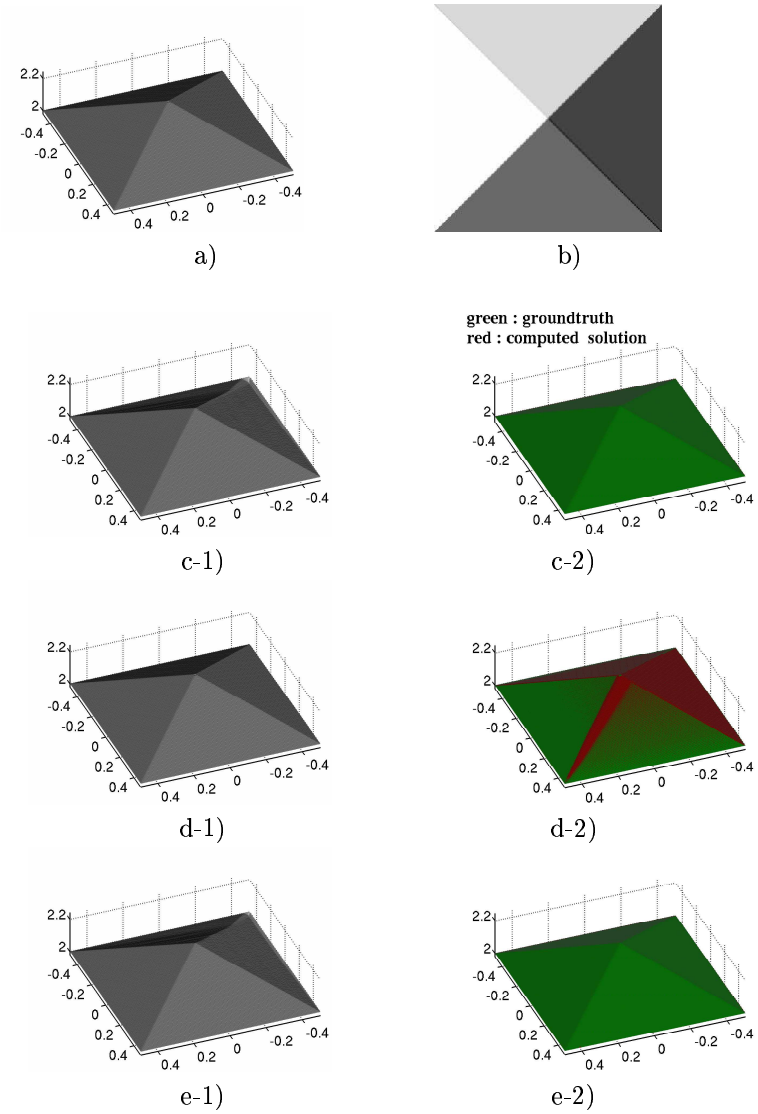

Figure 7.3: Results for a synthetic image generated by a pyramidal surface sampled on a grid of size 200×200 with $\mathbf{l} = (0.5, 0.3)$ ($\theta \simeq 35.6°$):
a) original surface, b) original image,
c) surface reconstructed from b) with the implicit algorithm starting from a subsolution: $n \simeq 1000$, $\varepsilon_1 = 8.461e-05$, $\varepsilon_2 = 8.058e-07$, $\varepsilon_\infty = 0.000940$;
d) surface reconstructed from b) with the semi-implicit algorithm starting from a supersolution: $n \simeq 110$, $\varepsilon_1 = 8.461e-05$, $\varepsilon_2 = 8.058e-07$, $\varepsilon_\infty = 0.000940$;
e) surface reconstructed from b) with the implicit algorithm starting from a supersolution: $n \simeq 50$, $\varepsilon_1 = 8.461e-05$, $\varepsilon_2 = 8.058e-07$, $\varepsilon_\infty = 0.000940$;

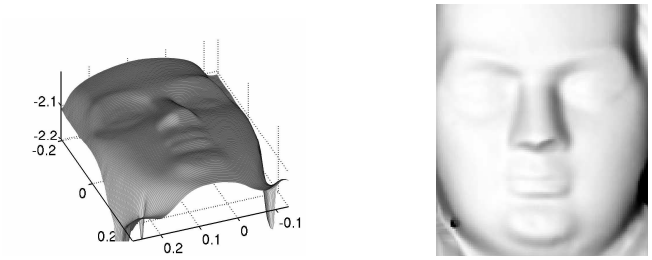

a) b)

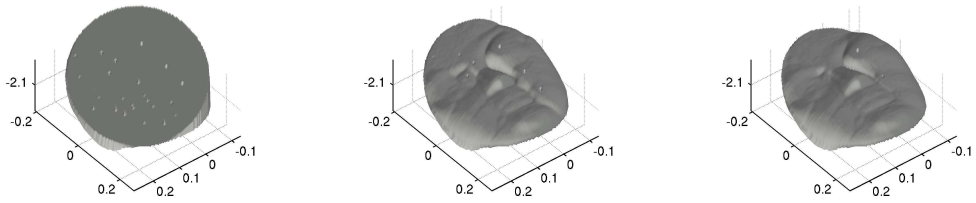

c) $n = 0$ d) $n = 30$ e) $n = 60$

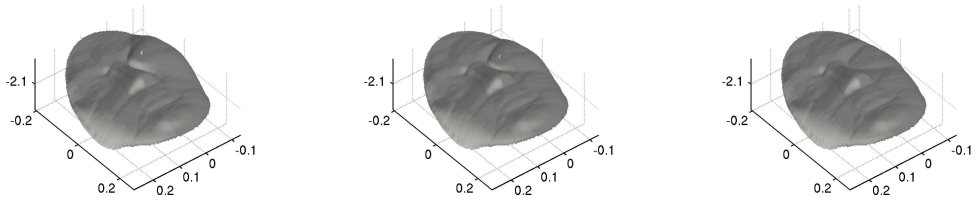

f) $n = 90$ g) $n = 120$ h) $n = 150$

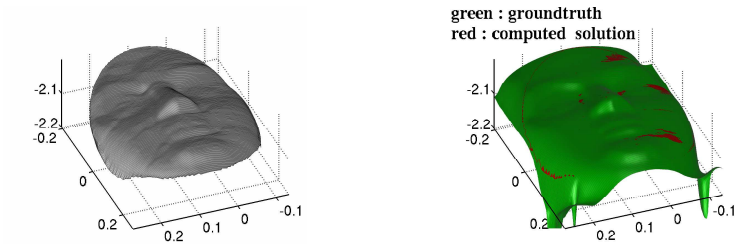

i) j)

a) Original surface of size $\simeq 150 \times 150$,
b) synthetic image generated from the original surface a) with $\mathbf{l} = (0.2, 0.1)$ ($\theta \simeq 13°$),
c) to h) surface U^n at the n^{th} iteration for $n = 0$, $n = 30$, $n = 60$, $n = 90$, $n = 120$ and $n = 150$, respectively.
i) Final result : $n = 200$
j) visual comparison of the final result i) with the original surface a).
Error : $\varepsilon_1 \simeq 0.002$, $\varepsilon_2 \simeq 2.16e-05$, $\varepsilon_\infty \simeq 0.034$;
The errors of each iteration are given in the table 7.1.

Figure 7.4: Experimental results obtained with the *implicit algorithm* starting from a *subsolution*, for a synthetic image representing Mozart's face.

iteration	ε_1 error	ε_2 error	ε_∞ error
30	0.0182615	0.000252425	0.112334
60	0.0100561	0.00016248	0.0664543
90	0.00679089	0.000118694	0.050051
120	0.0049317	8.55249e-05	0.0391274
150	0.0035902	5.70633e-05	0.0336975
200	0.00202838	2.16304e-05	0.0336975

Table 7.1: Errors associated to figure 7.4 (implicit algorithm starting from a subsolution).

iteration	ε_1 error	ε_2 error	ε_∞ error
8	0.0215886	0.000238949	0.0881951
16	0.00840164	0.000104874	0.056211
24	0.00420738	5.73969e-05	0.0389878
32	0.00288298	3.85285e-05	0.0335179
40	0.00234463	2.76988e-05	0.0335179
48	0.00206178	2.21822e-05	0.0335179

Table 7.2: Errors associated to figure 7.5 (semi-implicit algorithm starting from a supersolution).

iteration	ε_1 error	ε_2 error	ε_∞ error
4	0.00281226	3.05393e-05	0.0432186
8	0.00217095	2.28104e-05	0.0333782
12	0.00203401	2.14676e-05	0.0335754
16	0.00199646	2.11285e-05	0.033603
20	0.00199058	2.10833e-05	0.03361
24	0.00198982	2.10783e-05	0.03361
28	0.00198976	2.10779e-05	0.03361

Table 7.3: Errors associated to figure 7.6 (implicit algorithm starting from a supersolution).

7.1.2 Robustness to noise

We also show the stability of our method with respect to two types of errors.
The first type is image intensity errors due to noise. Uniformly distributed white noise has been added to all pixels of the input images and the corresponding reconstructed surfaces are shown, see figure 7.9 for the sinusoidal surface and 7.10 for the pyramidal surface. The Signal to Noise Ratio (SNR) is equal to 3.2 in figure 7.10 and to 2.7 in figure 7.9. As seen from these figures, our algorithms are very robust to intensity noise, as also observed in [39, 12].

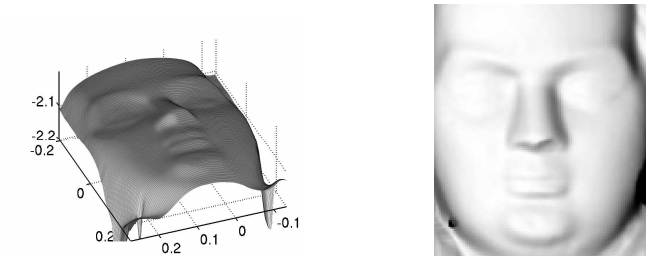

a) b)

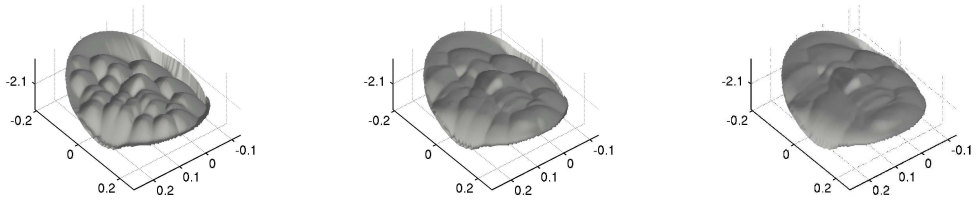

c) $n = 8$ d) $n = 16$ e) $n = 24$

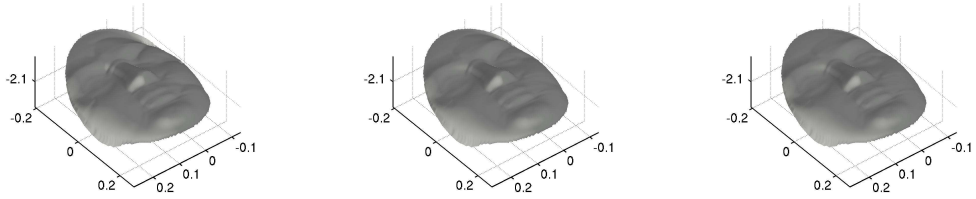

f) $n = 32$ g) $n = 40$ h) $n = 48$

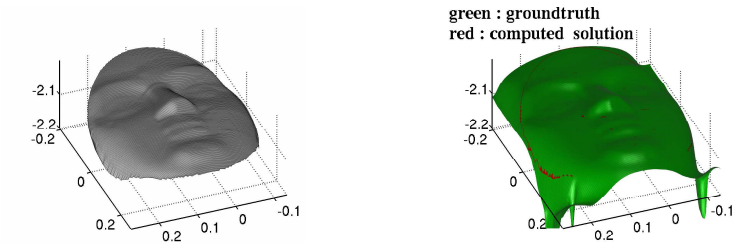

i) j)

a) Original surface of size $\simeq 150 \times 150$,
b) synthetic image generated from the original surface a) with $\mathbf{l} = (0.2, 0.1)$ ($\theta \simeq 13°$),
c) to h) surface U^n at the n^{th} iteration for $n = 8$, $n = 16$, $n = 24$, $n = 32$, $n = 40$ and $n = 48$, respectively.
i) Final result : $n \leq 50$;
j) visual comparison of the final result i) with the original surface a).
Error : $\varepsilon_1 \simeq 0.002$, $\varepsilon_2 \simeq 2.22e-05$, $\varepsilon_\infty \simeq 0.034$;
The errors of each iteration are given in the table 7.2.

Figure 7.5: Experimental results obtained with the *semi-implicit algorithm* starting from a *supersolution*, for a synthetic image representing Mozart's face.

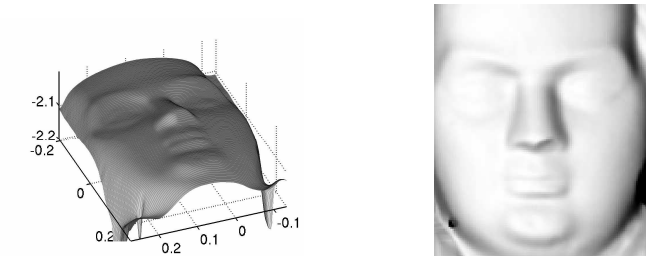

a) b)

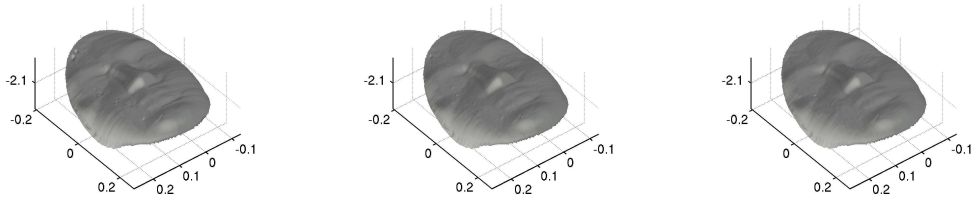

c) $n = 4$ d) $n = 8$ e) $n = 12$

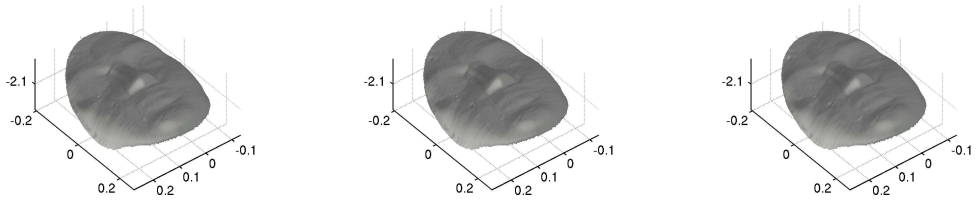

f) $n = 16$ g) $n = 20$ h) $n = 24$

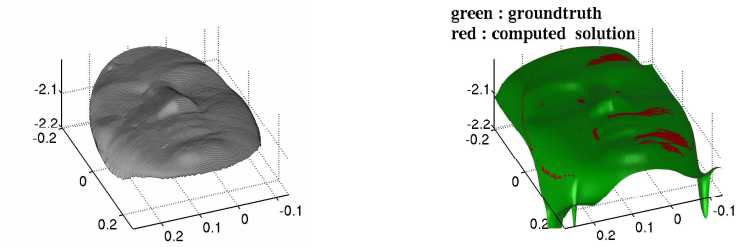

i) j)

a) Original surface of size $\simeq 150 \times 150$,
b) synthetic image generated from the original surface a) with $\mathbf{l} = (0.2, 0.1)$ ($\theta \simeq 13°$),
c) to h) surface U^n at the n^{th} iteration for $n = 4$, $n = 8$, $n = 12$, $n = 16$, $n = 20$ and $n = 24$, respectively.
i) Final result : $n = 30$;
j) visual comparison of the final result i) with the original surface a).
Error : $\varepsilon_1 \simeq 0.002$, $\varepsilon_2 \simeq 2.11e-05$, $\varepsilon_\infty \simeq 0.034$;
The errors of each iteration are given in the table 7.3.

Figure 7.6: Experimental results obtained with the *implicit algorithm* starting from a *supersolution*, for a synthetic image representing Mozart's face.

The second type of error is due to an incorrect estimation of the direction of the illumination **L**. Starting with the sinusoidal object of figure 7.2, we show in figure 7.11. that an error of roughly 9° on the parameter **L** does not affect much the reconstructed surface whereas for a larger error of 15°, the result is more distorted.

We continue with the pyramidal shape of figure 7.3; figure 7.12 shows a similar trend: a small error of approximately 5° already affects the results and later we introduce a large error of (9°).

Our algorithms seem to be fairly robust to small inaccuracies in the estimation of the direction of the light source **L** (Fig.7.11-a) and Fig.7.12-a)). Nevertheless, when the error grows larger, the results are not as good because some undesirable edges are created.

The third type of error is the gamma factor. Most of the usual image acquisition devices do not have a linear response in intensity. The actual response is usually well approximated by a power law, whose exponent is the gamma factor. If $\gamma = 1$ the response is linear. Typical values of γ range between 0.5 and 2.5. Figure 7.13-d) shows the reconstruction results when the algorithm is run on the original image raised to the power 2; they are somewhat disappointing. Figure 7.13-e) corresponds to a γ of .5 resulting in a flatter than real reconstructed surface.

7.1.3 Some remarks

1. The pyramid example shows the remarkable ability of the numerical algorithms to deal with *surfaces which are only continuous* as well as with *discontinuous images*.

2. Figures 7.7 and 7.8 show the ability of the numerical algorithms to deal with *shadows*, as predicted by the theory and pointed out in section 6.2.3.

3. An example with a real image is shown in [37] or [38].

4. In these references and in [36] the results have been with obtained with the implicit algorithms starting from subsolutions.

5. The synthetic surfaces of the vase and of Mozart's face, as well as other surfaces are available by anonymous ftp under the pub/tech_paper/survey directory at eustis.cs.ucf.edu (132.170.108.42). They are associated to the paper by Zhang et al. [43].

7.2 Experimental results for "perspective SFS"

We have tested the "perspective" algorithms (i.e. the algorithms associated with the Hamiltonians H_*^{pers}) with synthetic images generated by using a "perspective" projection. The previous remarks about the speed of convergence of the orthographic SFS algorithms still hold for the perspective SFS algorithms. In the following results, the solutions are computed with the implicit algorithm associated with the Hamiltonian H_1^{pers} starting from supersolutions (figures 7.14, 7.15 and 7.16) or from a subsolutions (figures 7.17 7.18 and 7.19).
In all cases we show the original object, the input image, the surface reconstructed by the new "perspective algorithm" and the surface reconstructed by the "general orthographic algorithm". We denote r the ratio of the focal and object distances (the object distance is the mean distance of the points of the surface to the optical center). We notice that, as soon as the ratio r is larger than 2, the "orthographic algorithm" produces important errors whereas the quality of the results obtained by the "perspective algorithm" remain very good (see figures 7.14, 7.15 and 7.16).

As for the orthographic algorithms, we demonstrate the stability of the perspective SFS algorithms with respect to various types of errors. The first type is image intensity errors due to noise (see figure 7.17, SNR$\simeq$ 3.7). The second type of error is due to an incorrect estimation of the direction of illumination $\mathbf{L}$ (see figure 7.18). The third type of error is due to an incorrect estimation of the focal length (see figure 7.19). As seen from these figures, the algorithms are quite robust to intensity noise; they are also robust to small inaccuracies in the light and focal parameters. But large errors on these parameters create some spurious edges.

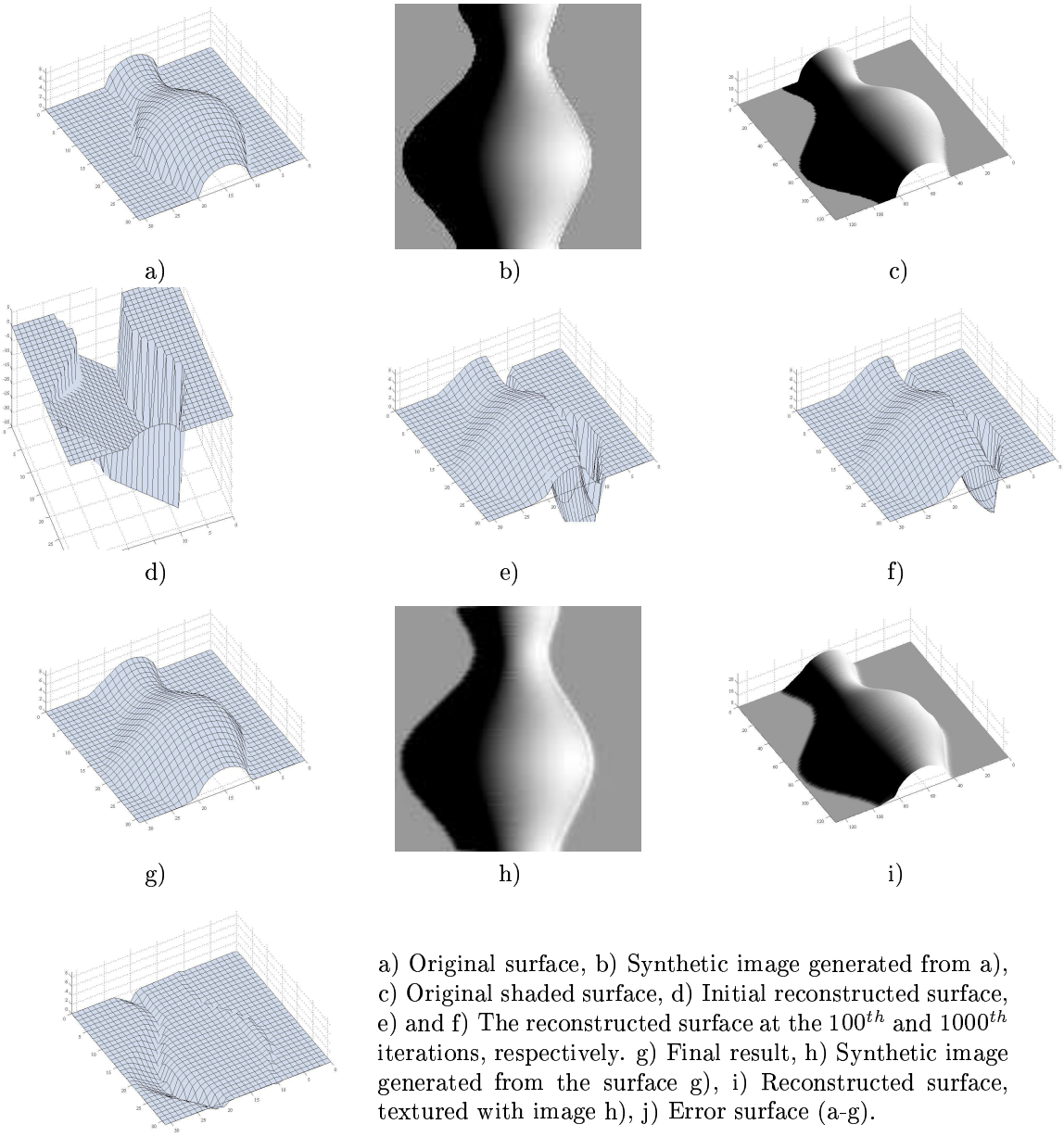

a) Original surface, b) Synthetic image generated from a), c) Original shaded surface, d) Initial reconstructed surface, e) and f) The reconstructed surface at the 100^{th} and 1000^{th} iterations, respectively. g) Final result, h) Synthetic image generated from the surface g), i) Reconstructed surface, textured with image h), j) Error surface (a-g).

Size of the image $= 256 \times 256$.
Algorithm: implicit algorithm starting from a subsolution: $n < 2500$.
$\mathbf{L} = (\alpha, \beta, \gamma) = (0.8,\ 0.0,\ 0.6)$ i.e. $\theta = 53°$.

Figure 7.7: First example of a reconstruction from an image with black shadows: the case of the vase.

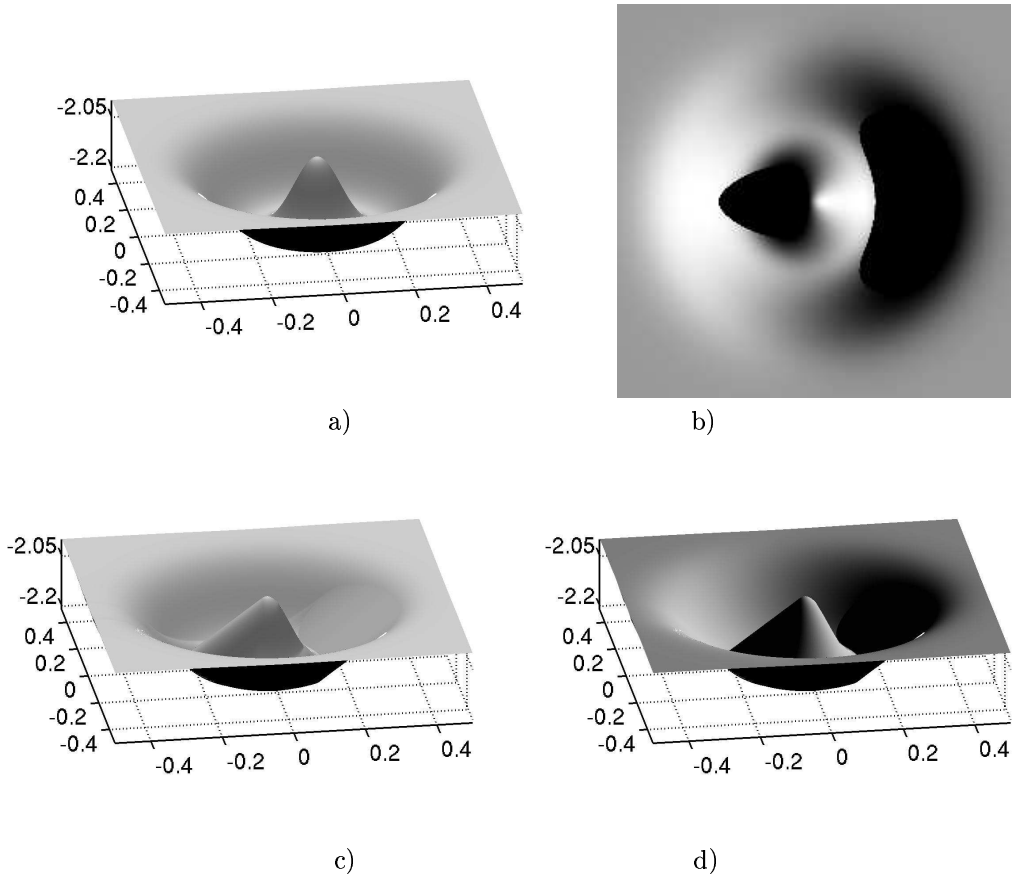

Size of the image $\simeq$ 1000×1000.
Algorithm: implicit algorithm starting from a supersolution: $n < 90$.

Figure 7.8: Second example of a reconstruction from an image with black shadows: the case of the Mexican hat. a) Original surface (the direction of the visualisation light is $(0, 0, 1)$), different from $\mathbf{L}$; b) Synthetic image computed from the surface a) with $\mathbf{L} = (0.8, 0.0, 0.6)$ (the angle between the light direction $\mathbf{L}$ and the camera axis is around $53°$); c) Solution recovered by our algorithm from the image b) (the direction of the visualisation light is $(0, 0, 1)$); d) Surface c) illuminated by a light of direction $(0.8, 0.0, 0.6)$.

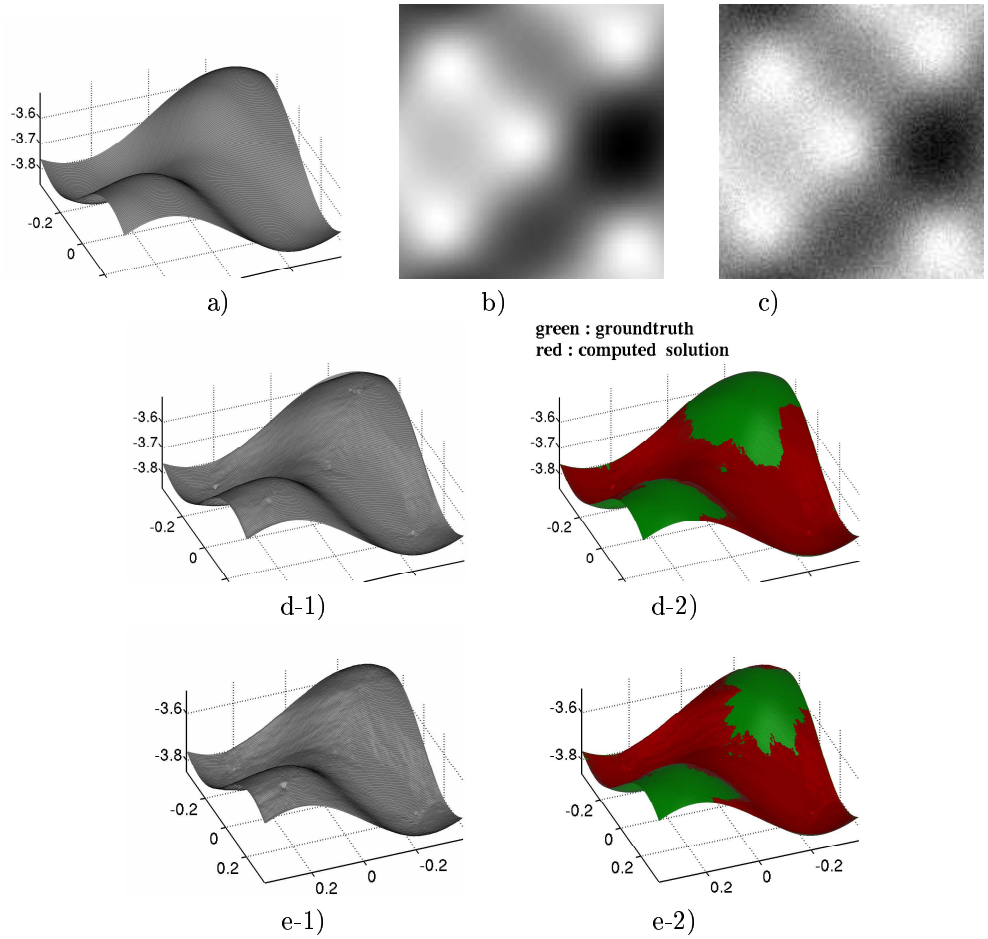

a) Original surface, b) Original image, c) Noisy image;
d) Reconstructed surface from b): $n \simeq 25$, $\varepsilon_1 = 0.003905$, $\varepsilon_2 = 2.884e-05$, $\varepsilon_\infty = 0.00747$;
e) Reconstructed surface from c): $n \simeq 30$, $\varepsilon_1 = 0.003905$, $\varepsilon_2 = 2.883e-05$, $\varepsilon_\infty = 0.00748$

Figure 7.9: Results for a *noisy* image generated by a sinusoidal surface sampled on a grid of size 200×200 with $\mathbf{l} = (0.1, 0.3)$ $(\theta = 18.5°)$.

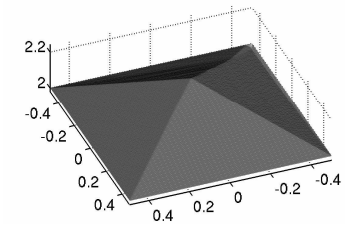

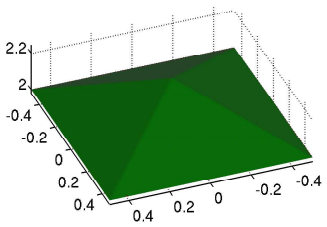

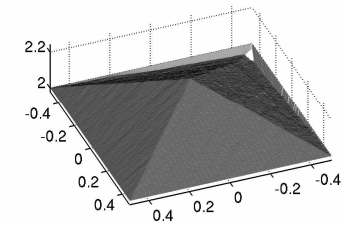

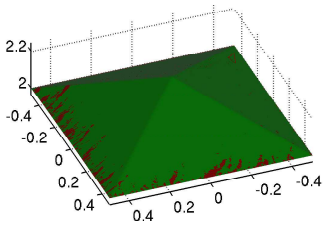

a) original surface, b) original image, c) noisy image;
d) surface reconstructed from b): $n \simeq 50, \varepsilon_1 = 8.461e{-}05, \varepsilon_2 = 8.058e{-}07, \varepsilon_\infty = 0.000940$;
e) surface reconstructed from c): $n \simeq 50, \varepsilon_1 = 0.00467, \varepsilon_2 = 4.58e-05, \varepsilon_\infty = 0.044$.

Figure 7.10: Results for a *noisy* image generated by a pyramidal surface sampled on a grid of size 200×200 with $\mathbf{l} = (0.5, 0.3) \quad (\theta = 35.6°)$.

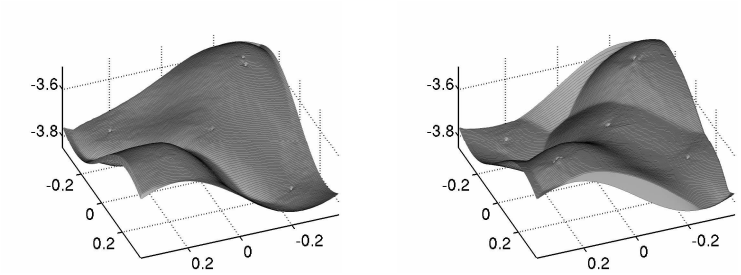

a) b)

Figure 7.11: Sinusoidal surface of figure 7.2 reconstructed from the image 7.2-b) with an error on the light parameter $\mathbf{L}$.
The light parameter used for obtaining the image 7.2-b) was $\mathbf{l} = (0.1, 0.3)$.
a) surface reconstructed with $\mathbf{l} = (0.0, 0.3)$ $(\varepsilon_\theta \simeq 9.3°)$:
$n \simeq 40$, $\varepsilon_1 = 0.0171$, $\varepsilon_2 = 0.000157$, $\varepsilon_\infty = 0.0729$;
b) surface reconstructed with $\mathbf{l} = (0.3, 0.2)$ $(\varepsilon_\theta \simeq 15.4°)$:
$n \simeq 35$, $\varepsilon_1 = 0.0394$, $\varepsilon_2 = 0.000342$, $\varepsilon_\infty = 0.142$.

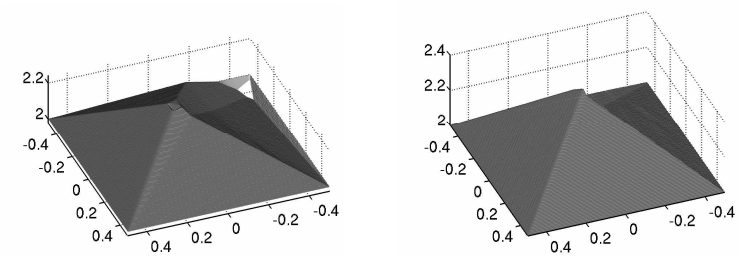

a) b)

Figure 7.12: Pyramidal surface of figure 7.3 reconstructed from the image Fig.7.3-b) with an error on the light parameter $\mathbf{L}$.
The light parameter used for obtaining the image Fig.7.3-b) was $\mathbf{l} = (0.5, 0.3)$.
a) surface reconstructed with $\mathbf{l} = (0.3, 0.2)$ $(\varepsilon_\theta \simeq 5.3°)$:
$n \simeq 40$, $\varepsilon_1 = 0.0407$, $\varepsilon_2 = 0.000278$, $\varepsilon_\infty = 0.177$;
b) surface reconstructed with $\mathbf{l} = (0.4, 0.4)$ $(\varepsilon_\theta \simeq 8.8°)$:
$n \simeq 40$, $\varepsilon_1 = 0.0251$, $\varepsilon_2 = 0.000167$, $\varepsilon_\infty = 0.103$.

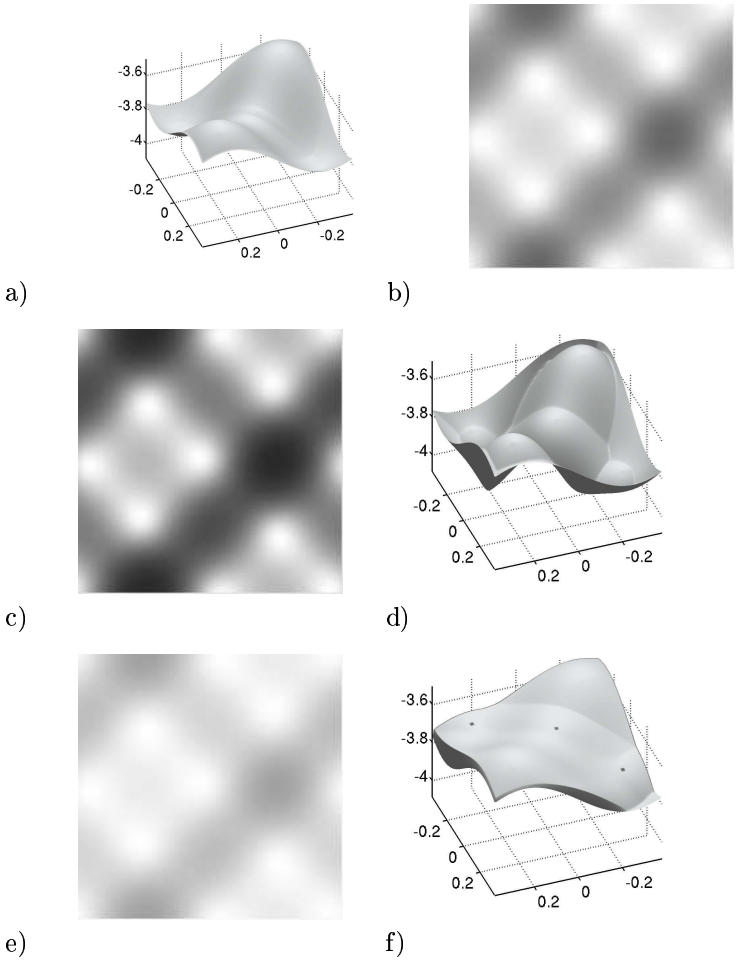

a) Original surface, b) Synthetic image generated from the original surface a) :
size $\simeq 200 \times 200$, $\mathbf{l} = (0.1, 0.3)$ $\Rightarrow \theta = 18.5°$.
c) Corrupted image: $\gamma = 2$, d) result computed from c)
$n \simeq 40$, $\varepsilon_1 = 0.0587$, $\varepsilon_2 = 0.00051$, $\varepsilon_\infty = 0.259$;
e) Corrupted image: $\gamma = 0.5$, f) result computed from e) $(n = 40)$;
$n \simeq 40$, $\varepsilon_1 = 0.0642$, $\varepsilon_2 = 0.00052$, $\varepsilon_\infty = 0.165$;

Figure 7.13: Results with a synthetic image corrupted by the gamma corrections $\gamma = 2$ and $\gamma = 0.5$, i.e. instead of using the real image I we used I^2 and $\sqrt{I}$, as if the gamma distortion had not been compensated for.

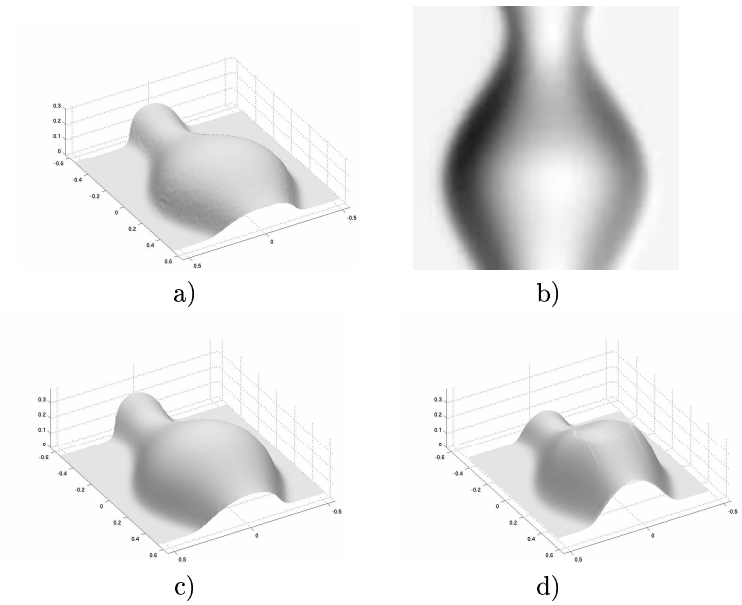

Figure 7.14: "Perspective SFS" results for an image generated by a smooth surface (computed by the implicit algorithm starting from a subsolution):
a) original surface, b) original image
($\mathbf{l} = (0.2, 0.2)$, $r = 2.5$, size=128×128),
c) surface reconstructed from b) by the "perspective algorithm":
$n \simeq 1000$, $\varepsilon_1 = 0.0041$, $\varepsilon_2 = 3.01e-05$, $\varepsilon_\infty = 0.00814$;
d) surface reconstructed from b) by the "orthographic algorithm":
$n \simeq 1000$, $\varepsilon_1 = 0.0201$, $\varepsilon_2 = 6.06e-05$, $\varepsilon_\infty = 0.035$;

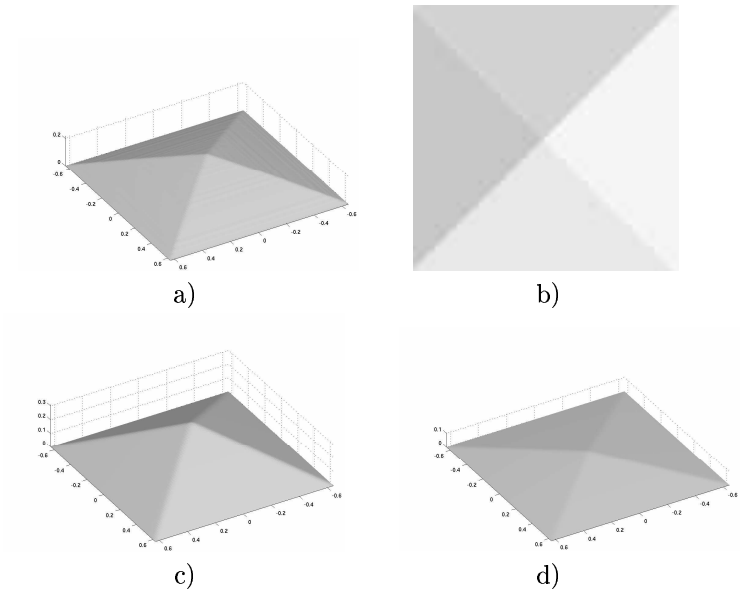

Figure 7.15: "Perspective SFS" results for an image generated by a pyramidal surface (computed by the implicit algorithm starting from a subsolution):
a) original surface, b) original image ($\mathbf{l} = (0.2, 0.2)$, $r = 2.1$, size$= 100 \times 100$),
c) surface reconstructed from b) by the "perspective algorithm":
$n \simeq 76$, $\varepsilon_1 \simeq 0.00015$, $\varepsilon_2 \simeq 1.50e-05$, $\varepsilon_\infty \simeq 0.00110$;
d) surface reconstructed from b) by the "orthographic algorithm":
$n = \simeq 83$, $\varepsilon_1 = 0.063$, $\varepsilon_2 = 0.0013$, $\varepsilon_\infty = 0.135$;

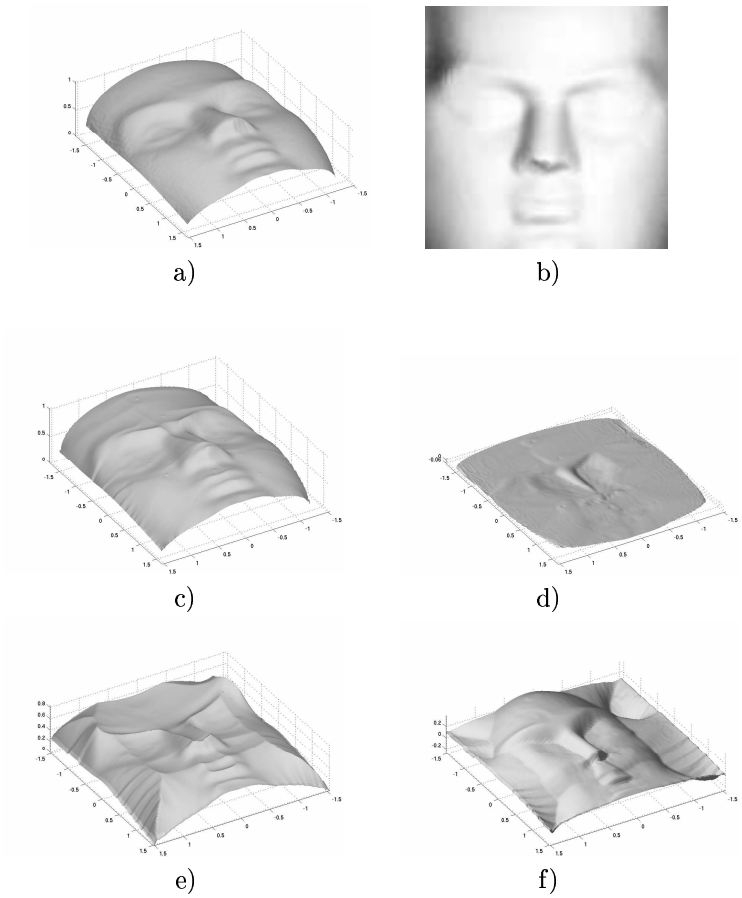

Figure 7.16: "Perspective SFS" results for an image generated by Mozart's face (computed by the implicit algorithm starting from a subsolution):
a) original surface, b) original image ($\mathrm{l} = (0.1, 0.1)$, $r \approx 1.6$, size$= 128 \times 128$),
c) surface reconstructed from b) by the "perspective algorithm",
d) the associate error surface:
$n \simeq 4000$, $\varepsilon_1 \simeq 0.00255$, $\varepsilon_2 \simeq 3.242e-05$, $\varepsilon_\infty \simeq 0.012$;
e) surface reconstructed from b) by the "orthographic algorithm" and f) the associate error surface:
$n \simeq 5000$, $\varepsilon_1 = 0.0495$, $\varepsilon_2 = 9.277e-04$, $\varepsilon_\infty = 0.20$;

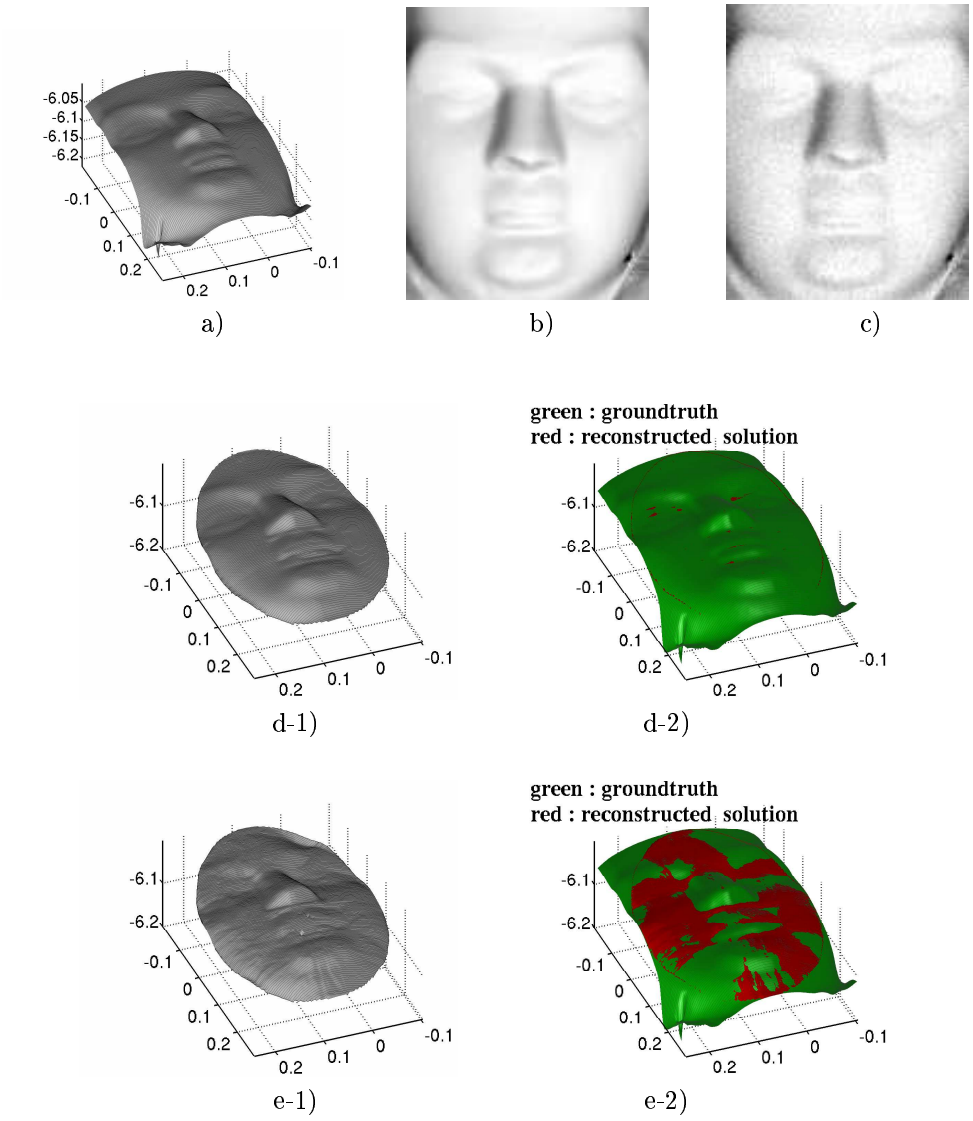

Figure 7.17: "Perspective SFS" results for an image of Mozart's face corrupted by a uniformly distributed noise.
Size of the grid $\simeq$ 200×200;
light parameter: $\mathbf{l} = (0.1, 0.3)$ $(\theta = 18.4°)$; focal length: $f = 4$.
a) original surface, b) original image, c) noisy image;
d) surface reconstructed from b): $n \simeq 5$, $\varepsilon_1 = 0.00197$, $\varepsilon_2 = 1.69e-05$, $\varepsilon_\infty = 0.00721$;
e) surface reconstructed from c): $n \simeq 7$, $\varepsilon_1 = 0.00247$, $\varepsilon_2 = 2.25e-05$, $\varepsilon_\infty = 0.0116$.

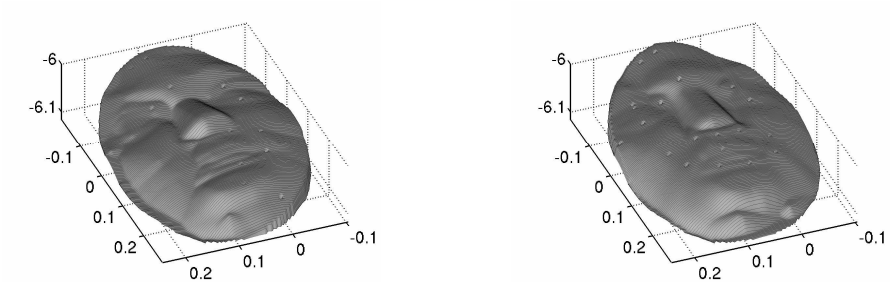

a) b)

The light parameter l used for design the image 7.17-b) is $\mathrm{l} = (0.1, 0.3)$.
a) Result obtained with the corrupted parameter $\mathrm{l} = (0.3, 0.3)$; $n \leq 10$;
$\varepsilon_1 = 0.0131$, $\varepsilon_2 = 0.000122$, $\varepsilon_\infty = 0.0466$.
b) Result obtained with the corrupted parameter $\mathrm{l} = (0.1, 0.5)$; $n \leq 10$;
$\varepsilon_1 = 0.0226$, $\varepsilon_2 = 0.000198$, $\varepsilon_\infty = 0.0547$.

Figure 7.18: "Perspective SFS" results for Mozart's face of the figure 7.17-a) reconstructed with an error on the light parameter **L**.

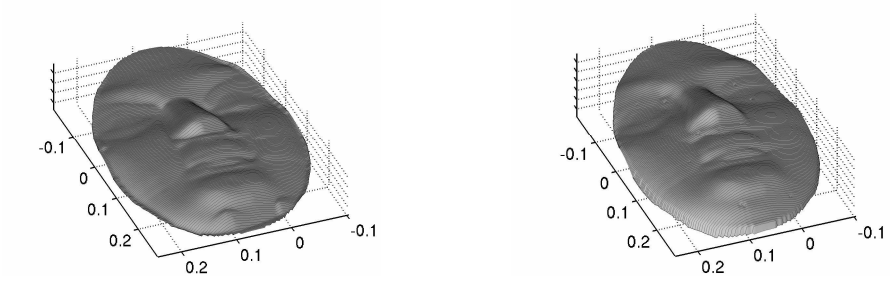

a) b)

Figure 7.19: "Perspective SFS" results for Mozart's face of the figure 7.17-a) reconstructed with an error on the focal length parameter f:
The focal length used for design the image 7.17-b) is equal to 5.
a) Result obtained with the corrupted focal $f = 4$; $n \simeq 6$.
b) Result obtained with the corrupted focal $f = 6$; $n \leq 6$.

Chapter 8

Conclusion

In this report we have extended the SFS methods to deal with perspective projection (pinhole) cameras, we have presented a complete mathematical and algorithmic study of the "orthographic" and "perspective SFS" problems, and we have proposed a general method for solving numerically the Hamilton-Jacobi-Bellman equations. More precisely:

- we have proposed some new formulations of the SFS problem by modeling the camera as a pinhole. The scene can be illuminated by a single point light source located at the infinity or located at the optical center. This allows to extend the SFS methods to more realistic image acquisition models. Moreover, our formulations lead to new PDEs which allow to develop a complete mathematical study of the problem.
- By using the theory of viscosity solutions, we have proved the existence and characterized the solutions of the "orthographic" and "perspective SFS" problems. In particular, this allows us to choose a particular solution of interest before starting to produce numerical results.
- We have described a general method dealing with monotonous schemes. In particular, we state and prove a general theorem ensuring the stability of monotonous schemes. Some convergence results for the associated algorithms follow automatically. Moreover, we design some monotonous approximation schemes adapted to (and consistent with) all Hamilton-Jacobi-Bellman equations and we apply our stability results to them.
- By introducing a "generic" Hamiltonian, we unify the "orthographic" and "perspective SFS" problems, and we simplify the formalism. After having proved that the "generic SFS Hamiltonian" is a Hamilton-Jacobi-Bellman Hamiltonian, we apply our numerical theory to it. This allows to design a unique SFS algorithm which can be used to solve numerically the various formulations of the SFS problem. Also, we prove the convergence of the numerical solutions computed by our algorithm toward the viscosity solution of the considered SFS problem.

- Our algorithm is robust to pixel noise and to the errors made on the parameters (light direction and focal length) and seems to be one of the more efficient iterative SFS algorithms of the SFS literature.
- Our algorithm can deal with discontinuous images and images containing black shadows. We prove the stability of our SFS scheme and the convergence of our SFS algorithm with such images.

We are extending our approach for recovering non Lambertian surfaces and for removing the requirement for boundary conditions.

Appendix A

How to transform a convex Hamiltonian into a HJB Hamiltonian; Legendre Tranform

In this section, we propose a method for transforming a convex Hamiltonian $H(x, \nabla u)$ into a HJB Hamiltonian.

In general, the Hamiltonian H is not given in the form

$$H(x,p) = \sup_{a \in A} \{-f(x,a) \cdot p - l(x,a)\}$$

but explicitly. In the case where $H(x,p)$ is a convex continuous function with respect to p (and Lipschitz continuous at least locally in x), it is possible to write $H(x,p)$ as a supremum of affine functions: We note H^* the dual convex function of H (also called the "Legendre transform" of H):

$$H^*(x,a) = \sup_{p \in \mathbb{R}^N} \{p.a - H(x,p)\} \ \leq +\infty.$$

We know that

$$H(x,p) = \sup_{a \in Dom(H^*(x,.))} \{p.a - H^*(x,a)\},$$

see for example [15]. We notice that in general $D_x := Dom(H^*(x,.))$ depends on x. To remove this dependency we change variables (see below).

In the case where the Hamiltonian is C^1 with respect to p, we can compute H^* explicitly through differential calculus. The method consists in computing the gradient $\overrightarrow{\nabla_p H}$, solving equation $\overrightarrow{\nabla_p H}(p_0) = 0$ (p_0 depends on x), and calculating $H(x, p_0)$.

EXAMPLE : for the Hamiltonian

$$H^{orth}_{R/T}(x,p) = I(x)\sqrt{1+|p|^2} + p\cdot 1 - \gamma,$$

we find

$$H^{orth^*}_{R/T}(x,a) = \begin{cases} -\sqrt{I(x)^2 - |a-1|^2} + \gamma & \text{if } x \in \overline{B}(1, I(x)) \\ +\infty & \text{otherwise.} \end{cases}$$

Therefore we have

$$H^{orth}_{R/T}(x,p) = \sup_{a\in\overline{B}(1,I(x))} \{p.a + \sqrt{I(x)^2 - |a-1|^2} - \gamma\}.$$

In this example, $D_x = \overline{B}(1, I(x))$ depends of x. The change of variables $b = (a-1)/I(x)$ removes this dependency. Thus

$$H^{orth}_{R/T}(x,p) = \sup_{b\in\overline{B}(0,1)} \{\underbrace{-(-I(x)b-1)}_{f^{orth}_{R/T}(x,b)}\cdot p - \underbrace{(\gamma - I(x)\sqrt{1-|b|^2})}_{l^{orth}_{R/T}(x,b)}\},$$

and $H^{orth}_{R/T}$ has the desired form.

REMARKS 31.

R31.1 - With this method based on the Legendre transform, the set A of the controls has the same dimension as p (the second variable of $H(x,p)$). There exist other methods for rewriting H as a supremum. For example, for

$$H^{orth}_{R/T}(x,p) = I(x)\sqrt{1+|p|^2} + p\cdot 1 - \gamma,$$

with $p \in \mathbb{R}^2$, Falcone [17] uses the identity

$$\forall X \in \mathbb{R}^3, |X| = \sup_{a\in B_3(0,1)} \{a\cdot X\},$$

where $B_3(0,1)$ is the unit ball of center 0 in $\mathbb{R}^3$. Thus, for $X = \begin{pmatrix} p \\ 1 \end{pmatrix}$:

$$\sqrt{1+|p|^2} = \sup_{(a_1,a_2,a_3)\in B_3(0,1)} \left\{ p\cdot \begin{pmatrix} a_1 \\ a_2 \end{pmatrix} + a_3 \right\}.$$

Therefore, we also have:

$$H^{orth}_{R/T}(x,p) = \sup_{a\in B_3(0,1)} \{[I(x)\begin{pmatrix} a_1 \\ a_2 \end{pmatrix} + 1]\cdot p + I(x)\ a_3 - \gamma\}.$$

Let us note that in this case the control dimension is equal to 3 when the dimension of p is equal to 2.

R31.2 - The above method may be automated through a symbolic computation program such as Maple.

Appendix B

The SFS Hamiltonians and the generic Hamiltonian H_g

B.1 The Hamiltonians H_*^{orth} and H_*^{pers} are special cases of H_g

In this section, we detail the functions $\mu_x, \nu_x, \kappa_x, K_x, \overrightarrow{w_x}, \overrightarrow{v_x}$, and c_x for the SFS Hamiltonians H_*^{orth} and H_*^{pers}.

- For the "Rouy/Tourin Hamiltonian" [39]:
  $H_{R/T}^{orth}(x,p) = I(x)\sqrt{1+|p|^2} + p \cdot \mathbf{l} - \gamma$;

$$\begin{aligned} \mu_x &= 1 & \nu_x &= 1 \\ \kappa_x &= I(x) & K_x &= 1 \\ \overrightarrow{w_x} &= \mathbf{l} & \overrightarrow{v_x} &= 0 \\ c_x &= -\gamma \end{aligned}$$

- For the "Dupuis/Oliensis Hamiltonian" [12]:
  $H_{D/O}^{orth}(x,p) = I(x)\sqrt{|p-\mathbf{l}|^2 + \gamma^2} + p \cdot \mathbf{l} - 1$;

$$\begin{aligned} \mu_x &= 1 & \nu_x &= 1 \\ \kappa_x &= I(x) & K_x &= \gamma \\ \overrightarrow{w_x} &= \mathbf{l} & \overrightarrow{v_x} &= -R_x\mathbf{l} \\ c_x &= -1 \end{aligned}$$

Let us remind the reader that R_x is the rotation

$$R_x = \begin{pmatrix} \frac{x_2}{|x|} & \frac{-x_1}{|x|} \\ \frac{x_1}{|x|} & \frac{x_2}{|x|} \end{pmatrix}.$$

- For the "Eikonal Hamiltonian":
  $H^{orth}_{Eiko}(x,p) = |p| - \sqrt{\frac{1}{I(x)^2} - 1}$;

$$\begin{aligned} \mu_x &= 1 & \nu_x &= 1 \\ \kappa_x &= 1 & K_x &= 0 \\ \overrightarrow{w_x} &= 0 & \overrightarrow{v_x} &= 0 \end{aligned}$$
$$c_x = -\sqrt{\frac{1}{I(x)^2} - 1}$$

Lemma 7 *We have*

$$\left| \begin{pmatrix} f_1 & 0 \\ 0 & \sqrt{f_1^2 + f_2^2|x|^2} \end{pmatrix} R_x p \right|^2 = f_1^2|p|^2 + f_2^2(x \cdot p)^2.$$

Therefore

$$f^2|p|^2 + (p \cdot x)^2 = |D_x R_x p|^2,$$

with $\mu_x = f$ *and* $\nu_x = \sqrt{f^2 + |x|^2}$.

PROOF. Let us denote $x^\perp := \begin{pmatrix} x_2 \\ -x_1 \end{pmatrix}$.

We have

$$R_x p = \frac{1}{|x|} \begin{pmatrix} x^\perp \cdot p \\ x \cdot p \end{pmatrix},$$

therefore

$$\begin{pmatrix} f_1 & 0 \\ 0 & \sqrt{f_1^2 + f_2^2|x|^2} \end{pmatrix} R_x p = \frac{1}{|x|} \begin{pmatrix} f_1 x^\perp \cdot p \\ \sqrt{f_1^2 + f_2^2|x|^2} x \cdot p \end{pmatrix}.$$

Thus the square of the norm of the previous expression is equal to

$$f_1^2 \, (\frac{x^\perp}{|x|} \cdot p)^2 + \; [f_1^2 + f_2^2|x|^2](\frac{x}{|x|} \cdot p)^2.$$

$$= f_1^2 \; [\; (\frac{x^\perp}{|x|} \cdot p)^2 + (\frac{x}{|x|} \cdot p)^2 \;] + f_2^2(x \cdot p)^2.$$

$$= f_1^2|p|^2 + f_2^2(x \cdot p)^2.$$

□

- For the "Perspective SFS" with a point light source located at the focal center:

$$H_F^{pers}(x,p) = I(x)\sqrt{f^2|p|^2 + (p\cdot x)^2 + \frac{f^2}{f^2+|x|^2}} - \sqrt{\frac{f^2}{f^2+|x|^2}},$$

Using lemma 7, we have

$$\begin{aligned} \mu_x &= f & \nu_x &= \sqrt{f^2+|x|^2} \\ \kappa_x &= I(x) & K_x &= \sqrt{\frac{f^2}{f^2+|x|^2}} \\ \overrightarrow{w_x} &= 0 & \overrightarrow{v_x} &= 0 \\ c_x &= -\sqrt{\frac{f^2}{f^2+|x|^2}} & (&= -K_x) \end{aligned}$$

- For the "Perspective SFS" with a point light source at infinity:

$$H_1^{pers}(x,p) = I(x)\sqrt{f^2|p|^2 + (x\cdot p+1)^2} - (f\,1+\gamma x)\cdot p - \gamma,$$

therefore we have

$$\begin{aligned} \mu_x &= f & \nu_x &= \sqrt{f^2+|x|^2} \\ \kappa_x &= I(x) & K_x &= \sqrt{\frac{f^2}{f^2+|x|^2}} \\ \overrightarrow{w_x} &= -(f\,1+\gamma x) & \overrightarrow{v_x} &= D_x^{-1}R_x x = (0, \frac{|x|}{\sqrt{f^2+|x|^2}}) \\ c_x &= -\gamma. \end{aligned}$$

PROOF. By using lemma 7, we have

$$f^2|p|^2 + (x\cdot p+1)^2 = |D_x R_x p|^2 + 2\ x\cdot p + 1$$

with $\mu_x = f$ and $\nu_x = \sqrt{f^2 + |x|^2}$.
If we denote $q := D_x R_x p$, we have

$$\begin{aligned} f^2|p|^2 + (x \cdot p + 1)^2 &= |D_x R_x p|^2 + 2x \cdot (R_x^{-1} D_x^{-1} D_x R_x p) + 1 \\ &= |q|^2 + 2 \left[{}^t(R_x^{-1} D_x^{-1})\ x \right] \cdot q + 1 \\ &= |q|^2 + 2 \left[D_x^{-1} R_x x \right] \cdot q + 1. \end{aligned}$$

Since

$$|q|^2 + 2\mathbf{v} \cdot q = |q + \mathbf{v}|^2 - |\mathbf{v}|^2,$$

then

$$f^2|p|^2 + (x \cdot p + 1)^2 = |D_x R_x p + [D_x^{-1} R_x x]|^2 - |D_x^{-1} R_x x|^2 + 1.$$

Let us note that: $D_x^{-1} R_x x = (0, \frac{|x|}{\sqrt{f^2+|x|^2}})$. □

B.2 HJB formulation of H_g

In this section we show how to compute the HJB formulation of H_g.

$$H_g(x, p) = \tilde{H}_g(x, A_x p + \overrightarrow{v_x}) + \overrightarrow{w_x} \cdot p + c_x, \tag{B.1}$$

with $A_x \in GL^N(\mathbb{R}), \overrightarrow{v_x}, \overrightarrow{w_x} \in \mathbb{R}^2, c_x \in \mathbb{R}$, and $\tilde{H}_g(x, q) : \Omega \times A \to \mathbb{R} : (x, q) \mapsto \tilde{H}_g(x, q)$, convex with respect to q.
We do not use the method presented in the previous section. We have

$$\tilde{H}_g(x, q) = \sup_{a \in Dom(\tilde{H}_g{}^*(x,.))} \{q \cdot a - (\tilde{H}_g)^*(x, a)\}. \tag{B.2}$$

By replacing $\tilde{H}_g$ by the supremum of (B.2) in the identity (B.1), we obtain:

$$H_g(x, p) = \sup_{a \in Dom(\tilde{H}_g{}^*(x,.))} \{ \quad [{}^t A_x a + \overrightarrow{w_x}] \cdot p \quad - \quad [\tilde{H}_g{}^*(x, a) - \overrightarrow{v_x} \cdot a - c_x] \quad \}.$$

Let us emphasize that for computing the HJB formulation of H_g, we do not need to compute the Legendre transform H_g^* of H_g; we only need to compute the Legendre transform $(\tilde{H}_g)^*$ of $\tilde{H}_g$.

Appendix C

Maxi(Mini)mization of various functions

In this section, we details some necessary results for coding the algorithms associated to the implicit and semi-implicit decentered schemes.

C.1 Maximisation of $\delta\sqrt{1-|a|^2}+w\cdot a+c$

Let us consider the function Ψ defined by:

$$\Psi : \overline{B}_2(0,1) \to \mathbb{R} : a \mapsto \delta\sqrt{1-|a|^2}+w\cdot a+c$$

with $w\in\mathbb{R}^2$ and $\delta, c\in\mathbb{R}$, $\delta>0$.

The maximum of Ψ is reached at

$$a_0 = \frac{1}{\sqrt{\delta^2+|w|^2}}w.$$

The value of Ψ at a_0 is:

$$\Psi(a_0) = \sqrt{\delta^2+|w|^2}+c.$$

C.2 Maximisation of $\delta\sqrt{c-br-ar^2}+\mu r+\nu$

Let us consider the function ψ defined by:

$$\psi : I\subset\mathbb{R}\to\mathbb{R} : r\mapsto \delta\sqrt{c-br-ar^2}+\mu r+\nu$$

with $\delta, a, b, c, \mu, \nu\in\mathbb{R}$, $\delta>0$ and $a>0$.

We distinguish two cases:

1. $b^2 + 4ac < 0$:
   The definition set of ψ is the empty set ($I = \emptyset$).
2. $b^2 + 4ac \geq 0$:
   The maximum of ψ is reached at

$$r_0 = \frac{1}{2a} \left[\mu \sqrt{\frac{b^2 + 4ac}{a\delta^2 + \mu^2}} - b \right]$$

   The value of ψ at r_0 is:

$$\psi(r_0) = \frac{1}{2a} \sqrt{a\delta^2 + \mu^2} \sqrt{b^2 + 4ac} - \frac{\mu b}{2a} + \nu.$$

C.3 Minimization $\delta\sqrt{c + br + ar^2} + \mu r + \nu$

Let us consider the function ϕ defined by:

$$\phi : J \subset \mathbb{R} \rightarrow \mathbb{R} : r \mapsto \delta\sqrt{c + br + ar^2} + \mu r + \nu$$

with $\delta, a, b, c, \mu, \nu \in \mathbb{R}$, $\delta > 0$ and $a > 0$.

1. **If $a\delta^2 - \mu^2 \leq 0$, there are no minima.**
   To have a minimum, the function ϕ needs to be coercive.
   We have:
   ϕ is coercive

$$\begin{aligned} \text{iff} \quad & \lim_{r \rightarrow \pm\infty} \delta\sqrt{a}|r| + \mu r = +\infty \\ \text{iff} \quad & \delta\sqrt{a} \geq |\mu| \\ \text{iff} \quad & a\delta^2 - \mu^2 \geq 0. \end{aligned}$$

2. **If $4ac - b^2 \leq 0$, there are no minima.**
   Let us suppose that $a\delta^2 - \mu^2 \geq 0$.
   If $4ac - b^2 \leq 0$, there are no minima in the set of definition of ϕ.
   If $4ac - b^2 \geq 0$, then ϕ reaches his minimum at

$$r_0 = -\frac{b}{2a} - \frac{\mu}{2a} \sqrt{\frac{4ac - b^2}{a\delta^2 - \mu^2}}.$$

   The value of this minimum is:

$$\phi(r_0) = \frac{1}{2a} \sqrt{a\delta^2 - \mu^2} \sqrt{4ac - b^2} - \frac{\mu b}{2a} + \nu.$$

C.4 Solving $\sqrt{c+br+ar^2}+\mu r+\nu=0$ with respect to r

Let us consider the following function φ:

$$\varphi : J \subset \mathbb{R} \to \mathbb{R} : r \mapsto \sqrt{c+br+ar^2}+\mu r+\nu$$

with $a, b, c, \mu, \nu \in \mathbb{R}$, $a > 0$ (φ is the above function ϕ with $\delta = 1$).

We have :

$$\varphi(r) = 0 \qquad \Longleftrightarrow \qquad \left\{ \begin{array}{l} \mu r+\nu \leq 0, \\ c+br+ar^2-(\mu r+\nu)^2 = 0. \end{array} \right.$$

The discriminant of

$$c-\nu^2+(b-2\mu\nu)r+(a-\mu^2)r^2 = 0$$

is:

$$\Delta = (b-2\mu\nu)^2-4(c-\nu^2)(a-\mu^2).$$

- If $\Delta < 0$, then equation

  $$c+br+ar^2-(\mu r+\nu)^2 = 0$$

  has no solutions.

- If $\Delta \geq 0$, then it has two solutions (which can be equal):

  $$r_\pm := \frac{-(b-2\mu\nu) \pm \sqrt{\Delta}}{2(a-\mu^2)}.$$

  Therefore, $\varphi(r) = 0$ can have two solutions: $r_\pm$

  - if $\mu r_+ + \nu \leq 0$, then r_+ is solution,
  - if $\mu r_- + \nu \leq 0$, then r_- is solution.

Appendix D

List of all hypotheses

(H1) *H is convex with respect to p for all x in $\overline{\Omega}$.* *(page 16)*

(H2) *$H(x,p) \to +\infty$ when $|p| \to +\infty$ uniformly with respect to $x \in \overline{\Omega}$.* *(page 16)*

(H3) *$inf_{p\in\mathbb{R}^2} H(x,p) \leq 0$ in $\overline{\Omega}$.* *(page 17)*

(H4) *$H \in C(\overline{\Omega} \times \mathbb{R}^2)$.* *(page 17)*

(H5) *$\forall x, y \in \partial\Omega\ ,\ \varphi(x) - \varphi(y) \leq L(x,y)$.* *(page 17)*

(H6) *A is a compact topological space and Ω is a bounded open subset of $\mathbb{R}^N$.* *(page 20)*

(H6') *A is a compact topological space.* *(page 54)*

(H7) *$f : \overline{\Omega} \times A \to \mathbb{R}^N$ is continuous;*
$l : \overline{\Omega} \times A \to \mathbb{R}$ is continuous and bounded. *(page 20)*

(H7') *$f : A \to \mathbb{R}^N$ is continuous;*
$l : A \to \mathbb{R}$ is continuous and bounded. *(page 54)*

(H8) *f and l are Lipschitz continuous in $x \in \overline{\Omega}$ uniformly in $a \in A$.* *(page 20)*

(H9) *There exists a nondecreasing function ω which goes to zero at zero, such that* $\forall x, y \in \Omega,\ \forall p \in \mathbb{R}^N, \quad |H(x,p) - H(y,p)| \leq \omega(|x-y|(1+|p|))$. *(page 32)*

(H10) *For all x in Ω, $H(x,p)$ is convex with respect to p.* *(page 32)*

(H11) *there exists a strict viscosity subsolution $\underline{u} \in C^1(\Omega) \cap C(\overline{\Omega})$ of (3.27) (i.e. such that $H(x, \nabla\underline{u}(x)) < 0$ for all x in Ω).* *(page 32)*

(H11') *there exist* $\underline{u} \in C^1(\Omega) \cap C(\overline{\Omega})$ *and* $\delta < 0$ *such that for all* x *in* Ω,
$$H(x, \nabla \underline{u}(x)) < \delta. \qquad \textit{(page 35)}$$

(H12) Ω *is a bounded open subset of* $\mathbb{R}^N$ *of class* $W^{2,\infty}$. *(page 35)*

(H13) *There exists a function* ω *which goes to zero at zero, such that*
$$\forall x \in \Gamma,\ \forall p, q \in \mathbb{R}^N,\ |H(x,p) - H(x,q)| \leq \omega(|p-q|). \qquad \textit{(page 35)}$$

(H14) $\forall x \in \Gamma,\ \forall p \in \mathbb{R}^N, \qquad H(x, p + \lambda\eta(x)) \leq 0 \implies \lambda \leq C(1 + |p|).$ *(page 35)*

(H15) $\forall p \in \mathbb{R}^N, \qquad H(x, p - \lambda\eta(x)) \to +\infty$ *uniformly with respect to* x *in* Γ, *when* $\lambda \to +\infty$. *(page 35)*

(H16) *For all* x *fixed in* $\overline{\Omega}$ *and for all fixed* $\rho > 0$, *there exists a* finite *"neighbourhood" noted* $\mathcal{V}_x^\rho$ *of* x *such that* $S_{\rho,x,t}(u) := S(\rho, x, t, u)$ *does not depend on all the values of the function* u *but only on the values it takes at points* $y \in \mathcal{V}_x^\rho$.
In other words, we can rewrite $S(\rho, x, t, u)$ *as* $\breve{S}(\rho, x, t, (u(y))_{y \in \mathcal{V}_x^\rho})$.
(page 48)

(H17) $\forall \rho > 0, x \in \overline{\Omega}, u \in B(\overline{\Omega})$, *the function* $S_{\rho,x,u} : t \mapsto S(\rho, x, t, u)$ *is continuous, nondecreasing and* $lim_{t \to +\infty} S_{\rho,x,u}(t) \geq 0$. *(page 49)*

(H18) *The scheme is monotonous (see definition 8).* *(page 49)*

(H19) $\forall \rho > 0,\ x \in \overline{\Omega}$, *the function* $\breve{S}_{\rho,x}$ *is continuous with respect to* $\left(t, (u(y))_{y \in \mathcal{V}_x^\rho}\right)$
(we denote $\breve{S}_{\rho,x}(.,.) := \breve{S}(\rho, x, ., .)$ *where* $\breve{S}$ *is defined in the hypothesis* (H16)*).*
(page 49)

(H20) $\forall \rho > 0$, *there exists a subsolution of the scheme (4.8).* *(page 49)*

(H21) $\forall \rho > 0$, *there exists* $M^\rho \in \mathbb{R}$ *such that for all subsolutions* v^ρ *of (4.8),* $\forall x \in \overline{\Omega}$, $v^\rho(x) \leq M^\rho$. *(page 49)*

(H22) *There exists* $M \in \mathbb{R}$ *such that for all* $\rho > 0$, *all subsolutions of (4.8) are upper bounded by* M. *(page 51)*

(H23) *For all* $x \in \Omega$, *we have:*
there exists $a_x \in A$ *such that* $f(x, a_x) \neq 0$. *(page 54)*

Bibliography

[1] M. Bardi and I. Capuzzo-Dolcetta. *Optimal control and viscosity solutions of Hamilton-Jacobi-Bellman equations*. Birkhauser, 1997.

[2] G. Barles. *Solutions de Viscosité des Equations de Hamilton–Jacobi*. Springer–Verlag, 1994.

[3] G. Barles and P.E. Souganidis. Convergence of approximation schemes for fully nonlinear second order equations. *Asymptotic Analysis*, 4:271–283, 1991.

[4] M.J. Brooks, W. Chojnacki, and R. Kozera. Shading without shape. *Quarterly of Applied Mathematics*, 50(1):27–38, 1992.

[5] A.R. Bruss. The eikonal equation: Some results applicable to computer vision. *Journal of Mathematical Physics*, 23(5):890–896, May 1982.

[6] F. Camilli and M. Falcone. An approximation scheme for the maximal solution of the shape-from-shading model. *International Conference on Image Processing*, pages 49–52, 1996.

[7] F. Camilli and L. Grune. Numerical approximation of the maximal solutions for a class of degenerate hamilton-jacobi equations. *SIAM Journal of Numerical Analysis*, 38(5):1540–1560, 2000.

[8] F. Camilli and A. Siconolfi. Maximal subsolutions for a class of degenerate hamilton-jacobi problems. *Indiana Univ. Math. J.*, 48(3):1111–1132, 1999.

[9] M.G. Crandall. Viscosity solutions of Hamilton–Jacobi equations. In *Nonlinear Problems: Present and Future, Proc. 1st Los Alamos Conf., 1981*, volume 61, pages 117–125. North-Holland Math. Stud., 1982.

[10] M.G. Crandall, H. Ishii, and P.-L. Lions. User's guide to viscosity solutions of second order partial differential equations. *Bull. Amer. Soc.*, 27:1–67, 1992.

[11] M.G. Crandall and P.-L. Lions. Viscosity solutions of Hamilton–Jacobi equations. *Trans. AMS*, 277:1–43, 1983.

[12] P. Dupuis and J. Oliensis. An optimal control formulation and related numerical methods for a problem in shape reconstruction. *The Annals of Applied Probability*, 4(2):287–346, 1994.

[13] J.-D. Durou and H. Maître. On convergence in the methods of Strat and Smith for shape from shading. *The International Journal of Computer Vision*, 17(3):273–289, 1996.

[14] J.-D. Durou and D. Piau. Ambiguous shape from shading with critical points. *Journal of Mathematical Imaging and Vision*, 12(2):99–108, 2000.

[15] I. Ekeland and R. Temam. *Analyse Convexe et Problèmes Variationnels.* Etudes mathematiques. Dunod; Gauthier-Villars, Paris, Bruxelles, Montreal, 1974.

[16] M. Falcone and M. Sagona. An algorithm for the global solution of the shape-from-shading model. *International Conference on Image Analysis and Processing*, 1:596–603, 1997. LNCS 1310.

[17] M. Falcone, M. Sagona, and A. Seghini. A scheme for the shape-from-shading model with "black shadows". In *Proceedings of ENUMATH 2001*, 2001.

[18] Maurizio Falcone and Charalampos Makridakis, editors. *numerical methods for viscosity solutions and applications*, volume 59 of *Series on advances in mathematics for applied sciences.* World Scientific, 2001.

[19] J.K. Hasegawa and C.L. Tozzi. Shape from shading with perspective projection and camera calibration. *Computers and Graphics*, 20(3):351–364, May 1996.

[20] B.K. Horn and M.J. Brooks, editors. *Shape from Shading.* The MIT Press, 1989.

[21] B.K.P. Horn. Obtaining shape from shading information. In P.H. Winston, editor, *The Psychology of Computer Vision.* McGraw-Hill, New York, 1975.

[22] B.K.P Horn, R.S. Szeliski, and A.L. Yuille. Impossible shaded images. *IEEE Transactions on Pattern Analysis and Machine Intelligence*, 15(2):166–170, 1993.

[23] A. Ishii. A simple, direct proof of uniqueness for solutions of the hamilton-jacobi equations of eikonal type. *Proceedings of the American Mathematical Society*, pages 247–251, 1987.

[24] H. Ishii. Hamilton-Jacobi equations with discontinuous hamiltonians on arbitrary open subsets. *Bull. Fac. Sci. Engrg. Chuo Univ.*, 28:33–77, 1985.

[25] H. Ishii. a boundary value problem of the dirichlet type for hamilton-jacobi equations. *Ann. Sci. Ecole Norm. Sup.*, 4(16):105–135, 1989.

[26] J. Kain and D.N. Ostrov. Numerical shape-from-shading for discontinuous photographic images. *The International Journal of Computer Vision*, 44(3):163–173, 2001.

[27] Reinhard Klette, Ryszard Kozera, and Karsten Schlüns. Shape from shading and photometric stereo methods. Technical Report CITR-TR-20, CITR, University of Auckland, New Zealand, 1998.

[28] R. Kozera. An overview of the shape from shading problem. *Machine Graphics and Vision*, 7(1-2):291–312, 1998.

[29] K.M. Lee and C.C.J. Kuo. Shape from shading with perspective projection. *CVGIP: Image Understanding*, 59(2):202–212, 1994.

[30] P.-L. Lions. *Generalized Solutions of Hamilton–Jacobi Equations.* Number 69 in Research Notes in Mathematics. Pitman Advanced Publishing Program, 1982.

[31] P.-L. Lions, E. Rouy, and A. Tourin. Shape-from-shading, viscosity solutions and edges. *Numer. Math.*, 64:323–353, 1993.

[32] D.N. Ostrov. Extending viscosity solutions to eikonal equations with discontinuous spatial dependence. *Nonlinear Anal.*, 42(4):709–736, 2000.

[33] M.A. Penna. Local and semi-local shape from shading for a single perspective image of a smooth object. *Computer Vision, Graphics, and Image Processing*, 46(3):346–366, 1989.

[34] M.A. Penna. A shape from shading analysis for a single perspective image of a polyhedron. *IEEE Transactions on Pattern Analysis and Machine Intelligence*, 11(6):545–554, June 1989.

[35] E. Prados and O. Faugeras. Une approche du "shape from shading" par solutions de viscosité. Master's thesis, Université de Nice Sophia-Antipolis, France, INRIA Sophia-Antipolis, September 2001.

[36] E. Prados and O. Faugeras. "perspective shape from shading" and viscosity solutions. In *IEEE Proceedings of ICCV'03*, volume 2, pages 826–831, October 2003.

[37] E. Prados, O. Faugeras, and E. Rouy. Shape from shading and viscosity solutions. In *Proceedings of ECCV'02, LNCS*, volume 2351, pages 790–804, May 2002.

[38] E. Prados, O. Faugeras, and E. Rouy. Shape from shading and viscosity solutions. Technical Report 4638, INRIA, November 2002.

[39] E. Rouy and A. Tourin. A Viscosity Solutions Approach to Shape-from-Shading. *SIAM Journal of Numerical Analysis*, 29(3):867–884, June 1992.

[40] P. Soravia. Optimal control with discontinuous running cost: eikonal equation and shape from shading. In *39th IEEE Conference on Decision and Control*, pages 79–84, December 2000.

[41] I. Weiss. A perspective 3D formalism for shape from shading. In *Proceedings of DARPA Image Understanding Workshop*, volume 2, pages 1393–1402, May 1997.

[42] S.M. Yamany and A.A. Farag. A system for human jaw modeling using intra-oral images. In *IEEE-EMBS*, volume 20, pages 563–566, 1998.

[43] R. Zhang, P.-S. Tsai, J.-E. Cryer, and M. Shah. Shape from shading: A survey. *IEEE Transactions on Pattern Analysis and Machine Intelligence*, 21(8):690–706, August 1999.

List of Figures

1.1 The "Shape-from-Shading" problem. 5

2.1 Images arising from an orthogonal (versus perspective) projection. 9
2.2 Perspective projection with a single point light source located at the optical center. 11

3.1 Viscosity solutions for opposite hamiltonians 15
3.2 Example of discontinuous a viscosity solution 20
3.3 A surface with a critical point at the boundary. 39
3.4 Examples of several discontinous viscosity solutions. 40

4.1 Partition of $\overline{\Omega}$ in dimension 2. 52

6.1 Most effective path we have tested. 73
6.2 Solution computed by our and Falcone's algorithms 79

7.1 Results for a synthetic image generated by a paraboloidal surface. 85
7.2 Results for a synthetic image generated by a sinusoidal surface. 86
7.3 Results for a synthetic image generated by a pyramidal surface. 87
7.4 Experimental results obtained with the implicit algorithm starting from a subsolution, for a synthetic image representing Mozart's face 88
7.5 Experimental results obtained with the semi-implicit algorithm starting from a supersolution, for a synthetic image representing Mozart's face 90
7.6 Experimental results obtained with the implicit algorithm starting from a supersolution, for a synthetic image representing Mozart's face 91
7.7 First example of a reconstruction from an image with black shadows. 94
7.8 Second example of a reconstruction from an image with black shadows 95
7.9 Results for a noisy image generated by a sinusoidal surface 96
7.10 Results for a noisy image generated by a pyramidal surface 97
7.11 Sinusoidal surface of figure 7.2 reconstructed with an error on the light parameter. 98

7.12 Pyramidal surface of figure 7.3 reconstructed with an error on the light parameter. 98
7.13 Results with a synthetic image corrupted by a gamma correction 99
7.14 "Perspective SFS" results for an image generated by a smooth surface. 100
7.15 "Perspective SFS" results for an image generated by a pyramidal surface. . . . 101
7.16 "Perspective SFS" results for an image generated by Mozart's face. 102
7.17 Perspective SFS results for a noisy image of Mozart's face 103
7.18 "Perspective SFS" results for Mozart's face with an error on the light parameter 104
7.19 "Perspective SFS" results for Mozart's face reconstructed with an error on the focal length parameter 104

Contents

1 Introduction **5**

2 Mathematical formulations of the Lambertian SFS problem **7**
2.1 The "orthographic SFS" problem 8
2.2 The "perspective SFS" problem 10
2.3 The "Perspective SFS" with a point light source located at the optical center 10

3 Shape from Shading and Viscosity solutions **13**
3.1 Why using viscosity solutions to solve SFS 13
3.2 Viscosity solutions of Hamilton-Jacobi equations 14
3.2.1 Continuous viscosity solutions 14
3.2.2 Discontinuous viscosity solutions 18
3.3 Hamiltonians for the SFS problems and unification of the "perspective" and "orthographic SFS" 21
3.3.1 Basic Hamiltonians for SFS 21
3.3.2 A "generic" Hamiltonian for SFS 22
3.3.3 SFS Hamiltonians such that $H(x,0) \leq 0$ 25
3.4 Existence of viscosity solutions of the SFS problems 27
3.4.1 Existence of continuous viscosity solutions of the SFS problems 27
3.4.2 Existence of discontinuous viscosity solutions of the SFS problems . . 30
3.5 Characterization of viscosity solutions of the SFS problems 31
3.5.1 Uniqueness results for continuous viscosity solutions 31
3.5.2 uniqueness results for discontinuous viscosity solutions 34
3.5.3 Characterization of the viscosity solutions of the SFS problem when the set $\{x \mid I(x) = 1\}$ is not empty 37
3.6 Noise robustness of the viscosity solutions of SFS 41
3.7 SFS with discontinuous images; shadows 42

4 Monotonous approximation schemes of the form $S(\rho, x, u^\rho(x), u^\rho) = 0$; Two examples for HJB equations **43**
4.1 Approximation schemes 43

4.2 Decentered schemes for HJB equations 45
4.2.1 An "implicit" decentered scheme 45
4.2.2 A "Semi implicit" decentered scheme 46
4.3 Stability of the approximation schemes 48
4.3.1 Stability of monotonous schemes 49
4.3.2 Stability of the implicit decentered schemes (4.3) 53
4.4 Convergence of the solutions of the approximation schemes toward the viscosity solutions 59
4.4.1 Consistency of a scheme with an HJB equation and convergence of its solutions towards discontinuous viscosity solutions 59
4.4.2 Application to the decentered schemes 61

5 Decentered schemes for SFS **67**
5.1 Stability of the Decentered schemes for SFS 67
5.2 Convergence toward the viscosity solutions of SFS 69

6 Numerical algorithm associated with a monotonous scheme of the form $S(\rho, x, u^\rho(x), u^\rho) = 0$; Some new SFS algorithms **71**
6.1 Numerical algorithm for monotonous schemes of the form $S(\rho, x, u^\rho(x), u^\rho) = 0$; 71
6.2 New "generic" algorithms for SFS 73
6.2.1 Two "generic" SFS algorithms 73
6.2.2 Comments about initialisation 74
6.2.3 SFS algorithms with discontinuous images and black shadows 79

7 Experimental results **81**
7.1 Experimental results for the general "orthographic SFS" 83
7.1.1 Comparison of the implicit algorithm and the semi-implicit algorithm 83
7.1.2 Robustness to noise 89
7.1.3 Some remarks 92
7.2 Experimental results for "perspective SFS" 93

8 Conclusion **105**

A How to transform a convex Hamiltonian into a HJB Hamiltonian; Legendre Tranform **107**

B The SFS Hamiltonians and the generic Hamiltonian H_g **111**
B.1 The Hamiltonians H_*^{orth} and H_*^{pers} are special cases of H_g 111
B.2 HJB formulation of H_g 114

C Maxi(Mini)mization of various functions **115**
C.1 Maximisation of $\delta\sqrt{1-|a|^2}+w\cdot a+c$ 115
C.2 Maximisation of $\delta\sqrt{c-br-ar^2}+\mu r+\nu$ 115
C.3 Minimization $\delta\sqrt{c+br+ar^2}+\mu r+\nu$ 116
C.4 Solving $\sqrt{c+br+ar^2}+\mu r+\nu=0$ with respect to r 117

D List of all hypotheses **119**

Unité de recherche INRIA Sophia Antipolis
2004, route des Lucioles - BP 93 - 06902 Sophia Antipolis Cedex (France)

Unité de recherche INRIA Futurs : Parc Club Orsay Université - ZAC des Vignes
4, rue Jacques Monod - 91893 ORSAY Cedex (France)
Unité de recherche INRIA Lorraine : LORIA, Technopôle de Nancy-Brabois - Campus scientifique
615, rue du Jardin Botanique - BP 101 - 54602 Villers-lès-Nancy Cedex (France)
Unité de recherche INRIA Rennes : IRISA, Campus universitaire de Beaulieu - 35042 Rennes Cedex (France)
Unité de recherche INRIA Rhône-Alpes : 655, avenue de l'Europe - 38334 Montbonnot Saint-Ismier (France)
Unité de recherche INRIA Rocquencourt : Domaine de Voluceau - Rocquencourt - BP 105 - 78153 Le Chesnay Cedex (France)

Éditeur
INRIA - Domaine de Voluceau - Rocquencourt, BP 105 - 78153 Le Chesnay Cedex (France)
http://www.inria.fr
ISSN 0249-6399